

# **Carbonaceous Aerosols over Indo-Gangetic Plain in India: Spatial and Temporal Variation and Potential Source Regions**

A DISSERTATION

SUBMITTED IN PARTIAL FULFILLMENT OF THE REQUIREMENTS

FOR THE AWARD OF THE DEGREE

OF

**MASTER OF TECHNOLOGY**

IN

**ENVIRONMENTAL ENGINEERING**

Submitted by

**Shailvy Kaushik**

**2K20/ENE/09**

Under the supervision of

Mrs. Lovleen Gupta



**ENVIRONMENTAL ENGINEERING  
DELHI TECHNOLOGICAL UNIVERSITY**

(Formerly, Delhi College of Engineering)

Bawana Road, Delhi-110042

May 2022

DELHI TECHNOLOGICAL UNIVERSITY  
(Formerly Delhi College of Engineering)  
Bawana Road, Delhi-110042

## **CANDIDATE'S DECLARATION**

I, Shailvy, Roll No. 2K20/ENE/09 of MTech (Department of Environmental Engineering), hereby declare that the project Dissertation titled “Carbonaceous Aerosols over Indo-Gangetic Plain in India: Spatial and Temporal Variation and Potential Source Regions” which is submitted by me to the Department of Environmental Engineering, Delhi Technological University, Delhi in partial fulfillment of the requirement for the award of the degree of Master of Technology in Environmental Engineering is original and not copied from any source without proper citation. This work has not previously formed the basis for the award of my Degree, Diploma Associateship, Fellowship, or other similar title or recognition.

Place: Delhi

SHAILVY

Date

ENVIRONMENTAL ENGINEERING  
DELHI TECHNOLOGICAL UNIVERSITY  
(Formerly Delhi College of Engineering)  
Bawana Road, Delhi-110042

## **CERTIFICATE**

I, hereby certify that the project Dissertation titled “Carbonaceous Aerosols over Indo-Gangetic Plain in India: Spatial and Temporal Variation and Potential Source Regions” which is submitted by Shailvy, Roll No. 2K20/ENE/09 (Department of Environmental Engineering), Delhi Technological University, Delhi in partial fulfillment of the requirement for the award of the Degree of Master of Technology, is a record of the project carried out by the student under my supervision. To the best of my knowledge this work has not been submitted in part or full for any degree or diploma to this University or elsewhere.

Place: Delhi

Date

**LOVLEEN GUPTA**

**SUPERVISOR**

## **ACKNOWLEDGEMENT**

I want to express my deepest gratitude to my supervisor Mrs. Lovleen Gupta (Assistant Professor, Environmental Engineering Department, Delhi Technological University, Delhi) for her guidance, help, useful suggestions, and supervision without which this report could not have been possible in showing a proper direction while carrying out the project. I also must acknowledge the unconditional freedom to think, plan, execute and express, that I was given in every step of my project work while keeping faith and confidence in my capabilities.

Above all, I owe it all to my Almighty God for granting me the wisdom health, and strength to undertake this research task and for enabling me to completion.

SHAILVY KAUSHIK

2K20/ENE/09

## ABSTRACT

Indo-Gangetic plain - India's most densely populated area comprises some of the world's most smog-plagued cities. The area witnesses the worst air pollution episodes each year burdened by PM<sub>2.5</sub> of which the major section is carbonaceous aerosols. Hence, in this study, the BC and OC surface mass concentration trends of 6 highly polluted IGP cities are analyzed for temporal variations, and the assertive role of meteorology and long-range transfer of carbonaceous aerosols has been studied. The reanalysis data from Modern-Era Retrospective Analysis for Research and Applications version-2 (MERRA-2), for BC and OC from January 2019 to December 2021 for 6 cities have been investigated for seasonal, monthly, and yearly variations. The 5-day air back trajectory has been studied using the Hybrid Single-Particle Lagrangian Integrated Trajectory Model (HYSPLIT) backward trajectory clustering and concentration-weighted trajectory (CWT) analysis for identifying the regional transport of aerosols. Correlation analysis was performed for carbonaceous species (BC & OC), PM<sub>2.5</sub>, gaseous air pollutants, and meteorological conditions for the study areas. The annual average BC and OC were found to be highest for Muzaffarpur, Bihar. The monthly means for BC, OC, and OC/BC for IGP ranged between 0.94 to 10.05  $\mu\text{g m}^{-3}$ , 3.49 to 48.74  $\mu\text{g m}^{-3}$ , and 3.56 and 11.11 respectively. The concentrations were observed to peak in the winter months followed by post-monsoon and summers with the least values exhibited in monsoon throughout the IGP except for Guwahati. Guwahati displayed a peculiar pattern with a peak observed in March of every year. OC/BC ratio above 4 was reported for all locations indicating the burning of fossil fuels, biomass, dust storms, transportation, and industrial activities as the major polluters. For all locations, OC and BC were positively and significantly correlated (>0.95) indicating common emission sources. Carbonaceous aerosols displayed a moderate to strong correlation with PM<sub>2.5</sub> and an inverse correlation with Wind Speed, Relative Humidity, and Ambient Temperature.

Based on the cluster and CWT analysis, IGP itself was identified as a major contributor to BC and OC loads. Long-range transportation of aerosols from Myanmar; Bangladesh; Tibet; Yunnan China; the Arabian Sea, Laccadive Sea, and the Bay of Bengal was observed for most of the locations during the monsoon season. Moreover, the Sindh and Punjab regions of Pakistan were also contributing.

Keywords: Carbonaceous Aerosols, Indo-Gangetic Plains, Cluster Analysis, Source Identification, Backward Trajectories, CWT

# CONTENTS

CANDIDATE'S DECLARATION	i
CERTIFICATE	ii
ACKNOWLEDGEMENT	iii
ABSTRACT	iv
CONTENTS	vi
LIST OF FIGURES	viii
LIST OF TABLES	xi
LIST OF SYMBOLS AND ABBREVIATIONS	xii
Chapter 1 Introduction	1
1.1 Air Pollution in India	1
1.2 Carbonaceous Aerosols	2
1.3 Why Studying BC and OC is important?	3
1.4 Why Indo-Gangetic Plain's Pollution is a Matter of Concern?	4
Chapter 2 Literature Review	6
Chapter 3 Methodology	13
3.1 Study Area	13
3.2 Data Collection and Analysis	15
3.2.1 MERRA-2 Reanalysis Dataset	15
3.2.2 Meteorological Data Collection	16
3.2.3 HYSPLIT Data, Cluster Analysis and CWT Method	18
3.2.3.1 Backward-Trajectory Cluster Analysis	18
3.2.3.2 CWT	18

Chapter 4	Results and Discussion	20
4.1	Monthly Temporal Variations in BC and OC Mass Concentrations	20
4.2	Seasonal Variations in BC and OC Mass Concentrations	26
4.3	Interannual Variations in BC and OC Mass Concentrations	29
4.4	Analyzing OC/BC Ratio	32
4.4.1	Seasonal variations observed in OC/BC	34
4.4.2	Yearly variations observed in OC/BC	36
4.5	Correlation of Carbonaceous Aerosols with Meteorological Conditions and Gaseous Pollutants	37
4.6	Backward Trajectory Cluster and CWT Analysis of Carbonaceous Species	42
Chapter 5	Conclusion	54
Chapter 6	Limitations	55
References		56



## LIST OF FIGURES

Fig 1.1: Map representing the annual average concentration of PM <sub>2.5</sub> globally (Source: IQAir: World Air Quality Report 2021)	1
Fig 1.2: Graph representing the top 10 polluted Indian Cities based on US AQI as per IQAir	4
Fig 3.1: Indian map representing study locations	14
3.2. Step 1 Shows the steps followed for downloading the MERRA-2 reanalysis data for carbonaceous aerosols (BC and OC) and the planetary boundary layer height data for the selected locations.	16
3.3. Step 2 Shows the steps followed for downloading the MERRA-2 reanalysis data for carbonaceous aerosols (BC and OC) and the planetary boundary layer height data for the selected locations.	16
3.4. Step 3 Shows the steps followed for downloading the MERRA-2 reanalysis data for carbonaceous aerosols (BC and OC) and the planetary boundary layer height data for the selected locations.	17
Figure 3.5: Central Pollution Control Board's website used for downloading the continuous ambient air quality monitoring data for meteorological parameters for the study area.	17
Figure 3.6: READY National Oceanic and Atmospheric Administration (NOAA) Air Resource Laboratory's website used for downloading the Trajectory endpoint data for the chosen locations.	18
Fig 4.1 Time variation plot representing BC, OC, and OC/BC monthly mean ( $\mu\text{gm}^{-3}$ ) for locations starting from (a.) Muzaffarpur, (b.) Delhi, (c.) Guwahati, (d.) Hisar, (e.) Kanpur and (f.) Kolkata for 2019	21
Fig 4.2 Time variation plot representing BC, OC, and OC/BC monthly mean ( $\mu\text{gm}^{-3}$ ) for locations starting from (a.) Muzaffarpur, (b.) Delhi, (c.) Guwahati, (d.) Hisar, (e.) Kanpur and (f.) Kolkata for 2020	22

Fig 4.3 Time variation plot representing BC, OC, and OC/BC monthly mean ( $\mu\text{gm}^{-3}$ ) for locations starting from (a.) Muzaffarpur, (b.) Delhi, (c.) Guwahati, (d.) Hisar, (e.) Kanpur and (f.) Kolkata for 2021	22
Fig 4.4 Raincloud plot representing BC monthly means ( $\mu\text{gm}^{-3}$ ) dispersion across all locations for 3 years	23
Fig 4.5 Raincloud plot representing OC monthly means ( $\mu\text{gm}^{-3}$ ) dispersion across all locations for 3 years	24
Fig 4.6: Smoke from crop fires in northern India on 11 November 2021 (Source: NASA)	25
Figure 4.7: Seasonal variations in BC mass concentrations ( $\mu\text{gm}^{-3}$ ) from 2019-21	27
Figure 4.8: Seasonal variations in OC mass concentrations ( $\mu\text{gm}^{-3}$ ) from 2019-21	27
Fig 4.9: Interannual variations in BC mass concentrations ( $\mu\text{gm}^{-3}$ ) from 2019-21	30
Fig 4.10: Interannual variations in OC mass concentrations ( $\mu\text{gm}^{-3}$ ) from 2019-21	31
Fig 4.11: Raincloud plot representing OC/BC monthly means dispersion across all locations for 3 years	34
Fig 4.12: Seasonal variations in OC/BC ratio	35
Fig 4.13: Interannual variations in OC/BC values from 2019-21	36
Fig 4.14: Correlation among carbonaceous aerosols, local meteorology, and air pollutants for Hisar	38
Fig 4.15: Correlation among carbonaceous aerosols, local meteorology, and air pollutants for Delhi	39
Fig 4.16: Correlation among carbonaceous aerosols, local meteorology, and air pollutants for Kanpur	39
Fig 4.17: Correlation among carbonaceous aerosols, local meteorology, and air pollutants for Muzaffarpur	40
Fig 4.18: Correlation among carbonaceous aerosols, local meteorology, and air pollutants for Kolkata	40

Fig 4.19: Correlation among carbonaceous aerosols, local meteorology, and air pollutants for Guwahati	41
Fig 4.20: 5-day Backward Trajectory Clusters for Hisar for the study period	43
Fig 4.21: 5-day Backward Trajectory Clusters for Delhi for the study period	44
Fig 4.22: 5-day Backward Trajectory Clusters for Kanpur for the study period	45
Fig 4.23: 5-day Backward Trajectory Clusters for Muzaffarpur for the study period	45
Fig 4.24: 5-day Backward Trajectory Clusters for Kolkata for the study period	46
Fig 4.25: 5-day Backward Trajectory Clusters for Guwahati for the study period	46
Fig 4.26: CWT analysis for BC mass concentrations ( $\mu\text{gm}^{-3}$ ) in Hisar	48
Fig 4.27: CWT analysis for OC mass concentrations ( $\mu\text{gm}^{-3}$ ) in Hisar	48
Fig 4.28: CWT analysis for BC mass concentrations ( $\mu\text{gm}^{-3}$ ) in Delhi	49
Fig 4.29: CWT analysis for OC mass concentrations ( $\mu\text{gm}^{-3}$ ) in Delhi	49
Fig 4.30: CWT analysis for BC mass concentrations ( $\mu\text{gm}^{-3}$ ) in Kanpur	50
Fig 4.31: CWT analysis for OC mass concentrations ( $\mu\text{gm}^{-3}$ ) in Kanpur	50
Fig 4.32: CWT analysis for BC mass concentrations ( $\mu\text{gm}^{-3}$ ) in Muzaffarpur	51
Fig 4.33: CWT analysis for OC mass concentrations ( $\mu\text{gm}^{-3}$ ) in Muzaffarpur	51
Fig 4.34: CWT analysis for BC mass concentrations ( $\mu\text{gm}^{-3}$ ) in Kolkata	52
Fig 4.35: CWT analysis for OC mass concentrations ( $\mu\text{gm}^{-3}$ ) in Kolkata	52
Fig 4.36: CWT analysis for BC mass concentrations ( $\mu\text{gm}^{-3}$ ) in Guwahati	53
Fig 4.37: CWT analysis for OC mass concentrations ( $\mu\text{gm}^{-3}$ ) in Guwahati	53

## LIST OF TABLES

Table 4.1: Seasonal (mean $\pm$ $\sigma$ ) BC mass concentrations ( $\mu\text{gm}^{-3}$ )	29
Table 4.2: Seasonal (mean $\pm$ $\sigma$ ) OC mass concentrations ( $\mu\text{gm}^{-3}$ )	29
Table 4.3: Annual mean for BC, OC, and OC/BC mass concentrations ( $\mu\text{gm}^{-3}$ )	31
Table 4.4: Seasonal (mean $\pm$ $\sigma$ ) OC/BC mass concentrations ( $\mu\text{gm}^{-3}$ )	33
Table 4.5: R-value (correlation coefficients) established between various meteorological parameters, air pollutants, and carbonaceous species	37

## SYMBOLS AND ABBREVIATIONS

BC	Black Carbon
OC	Organic Carbon
EC	Elemental Carbon
BCSMASS	Black Carbon Surface Mass Concentrations
OCSMASS	Organic Carbon Surface Mass Concentrations
$\mu\text{gm}^{-3}$	Microgram per meter cube
CPCB	Central Pollution Control Board
PM <sub>2.5</sub>	Particulate Matter less than 2.5-micron size
PM <sub>10</sub>	Particulate Matter less than 10-micron size
GHGs	Green House Gases
IGP	Indo-Gangetic Plain
ABL	Atmospheric Boundary Layer
PSCF	Potential source contribution function
RH	Relative Humidity
WS	Wind Speed
AT	Ambient Temperature
CWT	Concentration weighted trajectory
SOC	Secondary Organic Carbon
MSL	Mean Sea Level
HYSPLIT	Hybrid Single-Particle Lagrangian Integrated Trajectory
$\sigma$	Standard Deviation
NAAQS	National Ambient Air Quality Standards

# CHAPTER 1

## INTRODUCTION

### 1.1 AIR POLLUTION IN INDIA

Ambient air pollution has been a topic of research and concern around the globe. A world bank report states that as many as 5 million people died prematurely globally in 2017 due to air pollution, which is more than the combined deaths from tuberculosis, malaria, and HIV/AIDS. While almost all developing countries are facing air pollution episodes that come hand in hand with developmental activities, many Indian cities are leading in the list of the world's most polluted cities. India is ranked 5<sup>th</sup> most polluted country in the world after Bangladesh, Chad, Pakistan, and Tajikistan, as cited in IQAir's World Air Quality Report 2021. The report also highlighted New Delhi as the most polluted capital city in the world for 4<sup>th</sup> year in a row. Moreover, in 2021 the pollution levels in most Indian cities exceeded the NAAQS established by the CPCB. With a burgeoning population, the air pollution level in India is also increasing alarmingly and is a great menace to the country's economy and public health. More than 90% of India's population is exposed to unhealthy air. As per (Nagpure et al., 2016), ambient air pollution is a matter of grave concern for global health. According to a report by Health Effects Institute (HEI 2019), particulate matter (PM) was considered the 3<sup>rd</sup> important cause of death globally in 2017 and this rate was highest in India. In 2019, around 1.7 million Indians lost their lives to air pollution, as per a report by the journal Lancet Planetary Health.

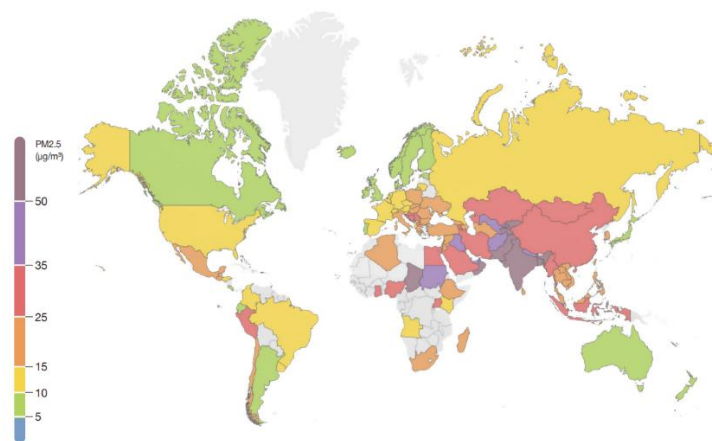


Fig 1.1: Map representing the annual average concentration of PM<sub>2.5</sub> globally (Source: IQAir: World Air Quality Report 2021)

## 1.2 CARBONACEOUS AEROSOLS

Generally, 20–50% of the fine suspended particulate pollution (PM<sub>2.5</sub>) is comprised of carbonaceous aerosols. The carbonaceous section of the total aerosol mass has received huge scientific attention as only little is known of the large number of species responsible for genesis of these aerosols. Carbonaceous aerosol contains many organic species, but most have not yet been established. However, the presence of conventional toxicants such as oxy and nitro-polycyclic aromatic hydrocarbons and polychlorinated dibenzodioxins/furans have been reported. However, what causes aerosol toxicity in the environment is still a topic of huge research potential. Carbonaceous aerosols are the carbon-containing fractions of PM comprising a number of complex organic species but importantly Organic Carbon (OC) and Black Carbon (BC often used interchangeably with Elemental Carbon-EC). OC acquires almost 10-15% of the total PM<sub>2.5</sub> mass while BC forms 2-10%.

BC or EC is the light-absorbing fraction of carbonaceous aerosols differentiated based on the mode of quantification. It is referred to as EC when measured using thermal optical methods and called Black Carbon when evaluated optically. BC is released into the atmosphere from primary sources such as incomplete combustion of fossil fuels, wood-burning, biomass burning, industrial emissions, etc. Other than anthropogenic sources, it is also released from natural forest fires. BC is climatically significant because of its ability to strongly absorb radiations in visible and infrared segments leading to a large positive radiative forcing (heating). According to IPCC, it is estimated that the human-induced BC on snow cover has a positive global and annual mean radiative forcing of + 0.04 Wm<sup>-2</sup>. When incorporated into cloud droplets, they reduce cloud albedo (reflection). Unlike other GHGs, BC has a relatively shorter life spanning from 1 to 2 weeks, and thus stresses more on regional effects than global. Additionally, BC has adverse health effects like respiratory illness, cancer, premature deaths, etc. on the exposed demography. Though BC itself may not have direct toxic adverse health impacts, but it may act as a carrier for much harmful OC hampering human health. As per a report published by (McDonald et al., 2004) fossil fuel related emissions (gasoline and diesel) can be linked directly to the emission of complex respirable organic species like hopanes and steranes, which reportedly causes lung toxicity. Thus, regulating the short-lived BC aerosols can help mitigate the climate and health impacts of atmospheric aerosols.

OC is a fraction of carbonaceous aerosols having both primary and secondary origins. The section of aerosols is emitted either from the primary sources of fossil fuel combustion or formed in the atmosphere

due to condensation of gas-phase organic compounds. After emission, the gas-phase oxidants like  $\text{NO}_3$ , OH, Ozone, etc. chemically changes the hygroscopic, chemical, and optical properties of the OC particles (Kanakidou et al., 2005). Lately, a light-absorbing organic segment of OC i.e., Brown Carbon has been identified which also absorbs in the ultraviolet range. OC when forming a coating on BC can enhance the absorbing capacity of composite aerosol by 2-4 times. As stated by (Kirchstetter et al., 2004), the organic aerosols from low-temperature activities like biomass burning are relatively more absorbing than those emitted out of high-temperature combustion processes (fossil fuels). OC and BC, which make up a large portion of soot, can operate as a natural carbon catalyst, speeding up the oxidation of  $\text{SO}_2$  to sulfate in low-relative-humidity circumstances at night. As a result, carbonaceous aerosols play an important role in particulate matter (PM) pollution, particularly during periods of high pollution.

### **1.3 WHY STUDYING BC AND OC IS IMPORTANT?**

Fine atmospheric aerosols play an important role in maintaining the earth's energy budget both at the regional and global levels (Babu & Moorthy, 2002). Of the major aerosols, Black Carbon (BC) is considered as the 2nd most potent climate forcing agent with a direct radiative forcing of  $+1.1$  ( $+0.17$ - $2.1$ )  $\text{Wm}^{-2}$  (Bond et al., 2013). BC aerosols are short-lived with an average lifetime of 4–12 days in the lower atmosphere (Cape et al., 2012) unlike  $\text{CO}_2$  which stays in the atmosphere for centuries and thus can ferry long distances. BC is a section of soot produced by incomplete combustion of carbon-based (fossil) fuels, biofuels, and biomass. OC, on the other hand, is one of the most significant contributors to PM mass concentrations, and it comes from both anthropogenic (combustion processes) and natural (sea-spray and biogenic emissions) sources. Anthropogenic activities like cooking using bio-fuels like cow dung, wood, and crop residue contribute to indoor aerosol pollution while in an outdoor environment, the use of diesel and coal for vehicular & industrial purposes and stubble burning leads to BC emissions. As estimated by (Ramanathan & Carmichael, 2008), in the year 1996, biofuels, fossil fuels, and open mass burning contributed 20%, 40%, and 40% respectively to the annual emissions of BC worldwide. (Bond et al., 2013), stated that India is the 2nd largest emitter of BC globally. India and China, all alone gauge for 25-35% of BC emissions globally (Ramanathan & Carmichael, 2008).

Because of their minute size, the carbonaceous aerosols more specifically BC can easily infiltrate the human respiratory system and can pose health effects like cardiovascular problems, cancer, and even congenital disorders. The annual number of premature deaths caused by pulmonary and cardiovascular disorders as a result of exposure to ambient air particulate matter (PM) is estimated to be over 800, 000



(World Health Organization (WHO), 2002). Epidemiological studies have recently found a statistical link between carbonaceous aerosol exposure and cardiovascular emergency room visits.

#### 1.4 WHY INDO GANGETIC PLAIN'S POLLUTION IS A MATTER OF CONCERN?

The Indo-Gangetic plain (IGP) is a hotspot of pollution due to its dense population (houses one-seventh of the world's and 40% of India's total population), rapid urbanization, and substantial industrial exploitation, and agricultural activities. Central Pollution Control Board (CPCB) in 2020 reported that out of 54 cities of IGP almost half had poor/very poor air quality. IQAir, a Swiss company working on air quality technology, releases Air quality and pollution city ranking each year. As per its 2021 ranking, IGP cities - Delhi and Kolkata were among the top 10 most polluted cities worldwide (Figure 1.2). Other cities like Noida, Kanpur, Varanasi, Muzaffarpur, Faridabad, and Hisar routinely find themselves leading in the list of most polluted cities nationally and globally with Air Quality Index (AQI) ranging in the poor to severe categories (CPCB, IQAir). IGP is severely impacted by high aerosol concentrations with significant repercussions on regional and global climate cycles and human health. The area's aerosol loading is majorly dominated by BC aerosols (Ramachandran et al., 2020).

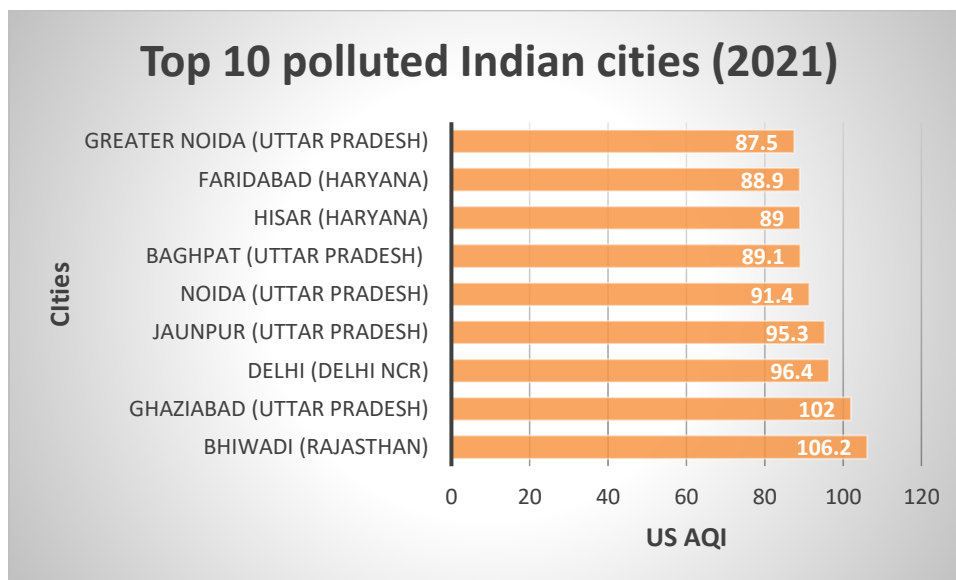


Fig 1.2: Graph representing the top 10 polluted Indian Cities based on US AQI as per IQAir

Air pollution in IGP has become a recurring problem for years and has been extensively studied for PM<sub>2.5</sub> and BC irregularities. The IGP has experienced severe pollution episodes over years especially during the post-monsoon season (October-early December) due to static meteorological conditions and higher emissions of pollutants. Though the Government of India is framing policies and implementing strategies, the pollution episodes are incessant. It is a burgeoning problem to improve the air quality in IGP. Thus, understanding the spatial & temporal variations and trajectories of carbonaceous aerosols across the IGP and their health effects is important for addressing air pollution problems.

## CHAPTER 2

### LITERATURE REVIEW

Ramachandran et al., 2021, measured the Black carbon (BC) aerosols at Ahmedabad (urban source site) and Guru Shikhar (high-altitude background site) region. The study pioneered in determining the influence of ABL on BC mass concentrations diurnally and identified the prospective source regions using PSCF analysis. In the Physical Research Laboratory in Ahmedabad and at Guru Shikhar in Mount Abu, BC mass concentrations were measured using an aethalometer. Ahmedabad's BC mass was substantially higher than Guru Shikhar's (2 to 5 times). When ABL was shallow and anthropogenic emissions were substantial, it peaked in Ahmedabad during the morning and evening hours. During the winter, when Guru Shikhar is within ABL, BC emissions were higher in the afternoon due to a fully formed ABL and upward movement of pollutants from the valley/foothills. During the afternoon hours, when ABL was completely evolved and anthropogenic sources were insignificant over Ahmedabad,  $BC_{max}$  over Guru Shikhar was close to  $BC_{min}$  over Ahmedabad. Long-range transport from North-Western India and the Indo-Gangetic Plain (IGP) is the probable source regions (agricultural waste and biomass burning) to the BC over the high-altitude site during post-monsoon and winter, according to a potential source contribution function (PSCF) analysis. In addition, pre-monsoon PSCF research revealed regional transmission of BC released from Ahmedabad's metropolitan regions to high-altitude Guru Shikhar. When ground-based data were compared to BC mass concentrations simulated by two models, MERRA-2 (fine resolution) and ECHAM6 (coarse resolution), it was discovered that modeled concentrations were greatly underestimated (2-10 times) throughout the source region of Ahmedabad. While the models do a good job of simulating BC mass over Guru Shikhar's background.

Ambade et al., 2021, measured BC mass concentrations using a 7-wavelength Aethalometer (AE-33) and  $PM_{2.5}$  aerosols using a fine particulate sampler (Envirotech APM 550 Mini, India) at Jamshedpur, Jharkhand to provide insight into the transport and impact of carbonaceous aerosols over the region. Apart from describing BC's atmospheric impacts, the health risk assessment of BC during various seasons over Jamshedpur city was also illustrated. The study finds BC mass concentration was lowest in monsoon and peaked in the winters. BC constituted around 6.92% of total  $PM_{2.5}$  concentration in winter, 5.09% in summer, 3.79% in monsoon, and 5.25% in the post-monsoon season. Backward Trajectories analysis

indicated Iran, Afghanistan, Pakistan, Nepal, Myanmar, and Central India as the sources of origin of winter aerosol concentrations. While in the pre-monsoon period, the sources were mainly from the Arabian Sea, Middle East, and IGP. Similar air trajectories were observed for the post-monsoon and monsoon seasons. The study found a strong correlation with  $r = 0.89$ , and  $r^2 = 0.80$  for  $PM_{2.5}$  and BC though a strong negative correlation was reported for BC and temperature, wind speed, precipitation, and humidity with R values of  $-0.92$ ,  $-0.61$ ,  $-0.60$  and  $-0.52$  respectively. Health risk of BC aerosols exposure was evaluated in terms of passively smoked cigarettes considering 4 health risks i.e., Cardiovascular mortality, Lung cancer, Low birth weight, Percentage lung function decrement of school-aged children, and was found to be equivalent to 10.38, 21.12, 18.59, and 42.41 in the winter season and 2.39, 4.86, 4.28, and 9.76 in the summer season, respectively.

Meena et al., 2021, took BC mass concentration observations using Aethalometer (AE-33) at an urban site in Pune and at a high-altitude forest site in Mahabaleshwar from April 2018 to February 2019. Daily, seasonal and diurnal variations of BC over these two different environments were compared. The effect of meteorological parameters on the BC was also evaluated. Source apportionment studies for sources like biomass burning and fossil fuel, along with Cluster analysis and concentration weighted trajectory (CWT) analysis were also performed to visualize the importance of regional transport for both the locations. Results displayed that the annual average BC mass concentration in Pune was 2.8 times more than that observed at Mahabaleshwar. The daytime BC concentrations were effectively diluted by high wind speed and the planetary boundary layer's action at Pune. High RH leads to low dispersion of BC aerosols. The source apportionment studies suggested almost 72-75% of BC loading at Mahabaleshwar was contributed by traffic emissions while it was reckoned to be 82-94% at Pune indicating biomass burning as a major contributor at Mahabaleshwar. Cluster analysis revealed 35-56% and 38-68% regional contribution of BC at Mahabaleshwar and Pune respectively majorly originating from central India and Bombay.

Prabhu et al., 2020, monitored the BC mass concentration and BC generated from biomass burning at Doon Valley from October 2017 to September 2018 using Aethalometer (AE-33). The study also included reanalysis and satellite data from MERRA-2 and CAMS and correlated the data with ground-based observations. The author performed CBPF and CWT analysis for studying the potential emission sources and long-range transportation of aerosol mass. Upon analysis of the BC mass concentrations, seasonally, the order discovered was: winter ( $9.45 \pm 2.65 \mu\text{gm}^{-3}$ ) > post-monsoon ( $6.94 \pm 1.52 \mu\text{gm}^{-3}$ ) > pre-monsoon ( $5.35 \pm 1.46 \mu\text{gm}^{-3}$ ) > monsoon ( $3.36 \pm 0.62 \mu\text{gm}^{-3}$ ). High BC (biomass burning) was observed in November and May owing to the long-range circulation of emissions from regions of high

agricultural activities while in January it was dominated by local emissions from cooking and residential heating. Backward trajectory cluster analysis revealed, the contribution of local sources in winter with a part originating from IGP. While in the pre-monsoon season western IGP dominated with 57.4% contribution followed by South-West Asian and Arabian sea region. Monsoon saw 63.3% of aerosol mass coming from North-Western IGP, 13.3% from Thar desert, and the rest from the North-East IGP border. The MERRA-2 and CAMS data showed positive and moderate to strong correlation with the primary dataset with R-values of 0.52 and 0.74 respectively. The author concluded that the correlation of ground-based data with satellite data improves when monthly means are considered. Aerosols CALIPSO profiles indicated smoke prevalence over IGP and in the Himalayan highland area up to the height of 5 km above ground level for May, November, and January.

Devi et al., 2020 collected samples for PM<sub>2.5</sub> and PM<sub>10</sub> from 7 locations (Delhi, Kanpur, Kolkata, Varanasi, Patna, Prayagraj, and Bhagalpur) across IGP from May to June 2017 to analyze the chemical composition of particulates and identify potential sources. The outcomes of this study suggested that suburban cities were proportionately more polluted than metropolitan cities like Kolkata and Delhi. The carbonaceous aerosols were reported to constitute a major portion of the particulate fraction with OC being 3-5 times the EC. The study states that high particulate pollution in Varanasi and Bhagalpur despite having no significant pollution sources is due to biomass combustion, poor traffic management, traffic emissions, and a thermal power plant operating in the vicinity. Also, the PM level in Varanasi is affected by a large number of crematories besides Ganga Ghats. Around 51-62 % of PM<sub>10</sub> is PM<sub>2.5</sub> in IGP. In this study, the highest EC and OC levels were observed for Patna and Delhi which suggested the highest anthropogenic emissions. OC/EC ratio from this study concludes combined emissions from stubble burning, traffic exhaust, and biomass burning. The backward air trajectories at sampled locations indicate the dominance of continental and marine air mass.

Zhao et al., 2021 investigated the characteristics of BC aerosol and identified potential source regions and associated health risks of BC in Tianjin, China. The author, monitored the BC using an Aethalometer (AE- 33) for the year 2019. MERRA-2 reanalysis data was also used for analysis alongside the ground-based observations. For both the ground-based data and MERRA-2 data, higher BC concentrations appeared in the winter and on the weekends for the entire duration. In all four seasons, the daily variation of BC concentration revealed two maxima. Human actions and meteorological factors caused one peak to appear at 6:00 to 8:00 Hrs and the other at 22:00 to 2:00 Hrs. Coastal cities in China exhibited lower BC concentrations than inland cities. Wind speed and temperature inversion had a significant impact on BC

mass concentration. PSCF analysis was also performed in this study. According to the PSCF findings, pollution sources were majorly found to be from the South-West of Tianjin, including Northern Henan, Beijing, and Southern Hebei (Qi et al., 2018). Cancer risk to adults and children was evaluated in this study. It was found to be higher than US EPA's recommended risk levels which may result in beyond 3.78 cases of cancer per 10,000 adults and 1.55 cases per 10,000 children, respectively. It was observed that the winter season had the largest relative risk of BC exposure on mortality, while summer had the lowest with BC-related respiratory mortality having the highest risk. The study proposed that due of BC exposure in Tianjin, adults were more likely than children to acquire cancer.

Chatterjee et al., 2021, investigated the impact of nationwide COVID-19 lockdown on carbonaceous aerosol concentration in Darjeeling, Eastern Himalayas. PM<sub>2.5</sub> cyclone inlet was used to collect samples of air and a semi-continuous OC - EC Carbon Aerosol Analyzer was used for analyzing OC and EC for April 2020 i.e., the lockdown period and distinguished with April 2019 (the normal period). During the lockdown, even though maximum anthropogenic activities were on halt, OC, EC, and TCA (Total Carbonaceous Aerosols) increased and were much higher than the normal period. Even the OC/EC value for lockdown (5.7) was more than the previous year (4.2). Very low NO levels were observed due to reduced vehicular movement and this reduced NO enhanced the ozone concentrations. As observed in this study, the SOC was 2 times higher for the lockdown period which may have been promoted by high levels of ozone by accelerating the photochemical oxidation of biogenic volatile organic compounds (BVOCs) emanating from the coniferous forest cover. CWT analysis for identification of sources of carbonaceous aerosols was also performed and indicated long-range transport of aerosols from human activities in Nepal and forest fires in North East India. However, at the time of lockdown, Darjeeling received aerosol loading more from the local sources.

Liu et al., 2022, investigated the spatial-temporal variations of organic carbon (OC), elemental carbon (EC), and secondary organic carbon (SOC) in January, July, and October 2015 and April 2016 in Wuhai and its surrounding areas. The industrial sites of resource-based cities were majorly polluted by primary carbonaceous aerosols while residential sites see significant SOC contribution. Due to meteorology, winters were reported to carry maximum carbonaceous aerosol concentrations. This author also plotted backward-trajectory and performed CWT analysis which suggested the role of local sources and transport of aerosols from nearby areas. A low OC/EC value was observed for Wuhai attributed to reduced energy efficiency and increased consumption of coal. The study states that OC/BC ratio for metropolitan cities is

more than the resource-based cities. Cities rich in resources experience high concentrations of primary OC aerosols while more SOC is observed for cities with high energy efficiency.

Sonwani et al., 2021, sampled PM<sub>10</sub> at Okhla Industrial Area, Delhi from July to September 2016 (Summer months) and November 2016-February 2017 (Winter Months) using an Envirotech Respirable Dust Sampler. The sample was then analyzed for OC and EC fractions for the characterization of carbonaceous aerosols and their seasonal distribution. The collected samples were subjected to morphological observations and were found to constitute soot particles, iron, and calcium sulfate particles. Winter aerosol fractions were dominated by soot/char particles. OC/EC for the study location varied between 0.7 to 11.3 (average =  $3 \pm 3.7$ ) with the December peak attributed to biomass burning and the July peak depicting long-range transport of aerosols. The morphological study suggested the dominance of carbonaceous aerosols derived from coal combustion in coal power plants, industries, and emissions from vehicles. Mineral dust along with soot particles observed indicated aged soot particles and crustal resuspension. Wind speed, relative humidity, temperature, and precipitation had a significant impact on OC than EC.

R. Singh et al., 2016 sampled the aerosol samples using a low volume sampler at New Delhi (an urban site) and Nurpur Village near Gurugram (a rural site) for June 2012 to May 2013. The samples were analyzed specifically for OC and EC with mean values of 25.6 and 13.7  $\mu\text{gm}^{-3}$  for Delhi and 29.6 and 12.8  $\mu\text{gm}^{-3}$  at Nurpur village respectively. Peak was observed in November owing to the large-scale agricultural waste burning post-harvesting. Minimum values were observed in the monsoon. OC and EC were strongly correlated exhibiting common emission sources. For Delhi, the OC/EC ratio ranged from 1 to 4 suggesting traffic emissions as a major source while for the rural site the ratio was more than 4 which indicated wood and biomass emissions. CWT analysis was performed in this study suggesting Punjab and Haryana as local sources along with Pakistan for OC in post-monsoon. Europe and Middle East Countries were also responsible for some OC and EC concentrations in the region.

Pipal et al., 2014 collected PM<sub>2.5</sub> samples at 2 IGP locations Delhi and Agra for the winter months of November 2011 – February 2012 using a medium air volume sampler and subsequently analyzed the collected sample for OC and EC. A 27% higher PM<sub>2.5</sub> concentration was observed in Delhi ( $211.67 \pm 41.94 \mu\text{gm}^{-3}$ ) than in Agra ( $165.42 \pm 119.46 \mu\text{gm}^{-3}$ ). Delhi reported 10.60  $\mu\text{gm}^{-3}$  BC mass concentration averaged over the study period. Though the EC values were higher for Delhi, Agra witnessed more OC

concentration than Delhi. OC/EC ratio was evaluated for Delhi and Agra (5.45 and 13.75 respectively). The ratio is more for Agra indicating the presence of secondary organic carbon at Agra due to emissions from extensive biomass burning as a part of rural livelihood which was confirmed with Agra reporting 42% more SOA than Delhi. The PM<sub>2.5</sub> mass was reported to constitute 32 % and 12% SOA in Agra and Delhi's samples. Cluster analysis was also performed using 7-day air mass backward trajectories for both locations indicating that aerosol mass traveled from neighboring countries like Turkmenistan, Pakistan, Afghanistan, and Iran along with South Indian regions covering the Thar desert before setting foot in Agra. Whereas in November local sources and Northern India were seen to contribute more.

Ram & Sarin, 2015 worked on the identification of emission sources of carbonaceous aerosols, their chemical characterization, and optical properties. The author used high-volume samplers for sampling particulate-laden air from 3 urban sites of IGP i.e., Hisar, Kanpur, Allahabad, and Manora Peak, a high-altitude site affected by transported pollutants from IGP. The study indicated a higher concentration of OC, EC, and WSOC in urban locations with relatively higher loading observed in winter and post-monsoon season and lower in summer. The concentrations were higher than the high altitude Manora peak which showed a similar pattern in seasonal variability. Lower summer concentrations were attributed to a decrease in the strength of sources like biomass burning and due to wet removal by precipitation. The OC/EC values exhibited large temporal variability at all locations and were around 6-8 attributed to the agricultural residue and biomass burning in IGP. Such a high OC/EC ratio suggested the dominance of OC in particulate fractions and common emission sources. The study identifies biomass burning emissions as a substantial source based on chemical tracers such as K<sup>+</sup>/OC and OC/EC ratios. WSOC concentrations were found to be lower at high-altitude sites and higher in urban cities.

(Srivastava et al., 2014), measured the mass concentrations of carbonaceous species, OC, and EC simultaneously using a semicontinuous thermo-optical EC-OC analyzer and BC using an Aethalometer from January 2011 to May 2012 in the Ganga basin. OC, EC, and BC concentrations varied seasonally, with winter concentrations being 2 times greater (OC -  $38.1 \pm 17.9 \mu\text{g m}^{-3}$ , EC -  $15.8 \pm 7.3 \mu\text{g m}^{-3}$ , and BC -  $10.1 \pm 5.3 \mu\text{g m}^{-3}$ ) than summer concentrations (OC  $14.1 \pm 4.3 \mu\text{g m}^{-3}$ , EC  $7.5 \pm 1.5 \mu\text{g m}^{-3}$ , and BC  $4.9 \pm 1.5 \mu\text{g m}^{-3}$ ). A strong and positive association between OC and EC (R=0.95) indicated that they share similar emission sources, with a lower OC/EC ratio (ranging between 1 to 3.6) indicating fossil fuel emissions. A low value of ratio suggested the dominance of EC over OC unlike other locations of the Ganga basin. During the study period, the average concentration of EC was evaluated to be 38% greater than BC. A high association was observed between the measured aerosol absorption coefficient ( $b_{\text{abs}}$ ) and



EC, implying that EC is a key absorbing species in Delhi's ambient aerosols. Winter high concentrations of 3 species were attributed to higher emission strength, reduced planetary boundary layer height, and stagnant meteorology. However, low summer values were due to higher mixing height, decreased strength of sources, and unstable atmosphere.

Patiala, a North-Western IGP city was sampled for particulate matter from October 2012 to September 2013 for characterizing the carbonaceous aerosols based on size ( $PM_{0.95}$ ,  $PM_{0.95-1.5}$ ,  $PM_{1.5-3.0}$ ,  $PM_{3.0-7.2}$ , and  $PM_{>7.2}$ ) (A. Singh et al., 2016). The samples were analyzed for OC, EC, and water-soluble OC (WSOC). Total suspended particulates (TSP) concentration was observed varying between 88–387  $\mu\text{gm}^{-3}$ . Peak observed in autumn ( $267 \pm 69 \mu\text{gm}^{-3}$ ) and lowest mass concentration in monsoon ( $130 \pm 62 \mu\text{gm}^{-3}$ ). Similar behavior was observed for EC, highest during paddy season and minimum in wet season ranging from 2.4 – 6.7  $\mu\text{gm}^{-3}$ . For submicron particulates, OC was observed to cover the major fraction with 75% mass indicating OC from combustion emissions and secondary sources. The study mentions high OC/EC ratio observations which indicated biomass burning as a major contributor. Carbonaceous aerosols accounted for 10-59% of  $PM_{0.95}$  concentration.

## CHAPTER 3

### METHODOLOGY

#### 3.1 STUDY AREA

The Indo-Gangetic Plain (IGP) lies in the Indian subcontinent running parallel to the Himalayas, stretching 2400 Km from the West to the East encompassing an area of around 7 lakh km<sup>2</sup> covering Northern Pakistan, Northern, and Eastern India, Bangladesh, and Nepal. It drains most of Northern and Eastern India, stretching from Jammu and Kashmir in the West to Assam in the East. The IGP is a hotspot of pollution due to its dense population (houses one-seventh of the world's and 40% of India's total population), rapid urbanization, substantial industrial exploitation, and extensive agricultural activities. The region is India's most densely populated owing to its highly fertile alluvial soil formed by the deposition of silt by the 3 major rivers i.e., the Indus, the Ganga, and the Brahmaputra. Within India, which is home to 14 of the world's most polluted cities, PM<sub>2.5</sub> emissions in the densely populated Indo Gangetic Plain (IGP) are responsible for nearly half (46%) of the country's premature deaths. The aerosol pollution in IGP cities has been widely studied but distinctly. In this study, we extend the focus on analyzing the carbonaceous aerosol surface mass concentrations over 6 IGP major cities namely Hisar, Haryana; NCT of Delhi; Kanpur, Uttar Pradesh; Muzaffarpur, Bihar; Kolkata, West Bengal and Guwahati, Assam; spanning over the entire IGP. Hisar, the city of steel, is one of the most developed cities of Haryana located at 29° N, 75.625° E with an average elevation of 215 m above MSL. The region has been facing poor to severe air quality due to extensive agricultural burning, vehicular emissions, and emissions from brick kilns and industries.

Delhi, the world's most polluted capital city, is located in Northern India at 28.5° N, 77.5° E with an average elevation of 216 m above MSL. The capital encounters severe air pollution episodes every winter attributed to the weather patterns, burning of crackers on Diwali, and stubble burning emissions from adjoining states. Kanpur, renowned for its huge leather industry, is located at 26.5° N, 80.625° E at an elevation of 126 m above MSL, is the biggest city and industrial & commercial capital of Uttar Pradesh. The region has been extensively studied for its worsening air quality due to high traffic density and industrial emissions. Muzaffarpur is a city in Bihar located at 25° N, 85.625° E 60 m above MSL and famous for its Shahi litchi among other agricultural produces'. It has a highly polluted air dominated by PM<sub>2.5</sub>, PM<sub>10</sub>, and NO<sub>2</sub> mainly from road dust, vehicular emissions, stubble burning, open burning of

waste, fuel burning, and industrial activities. Kolkata lies in the Eastern state of West Bengal in India on the bank of Hooghly River with coordinates 22.5° N, 88.125° E, and 9.14 m elevation above MSL. It is the meteorological conditions, heavy usage of diesel vehicles (also known as the diesel capital of India), industrial sources, dust, and traffic congestion that leads to high pollution loads in the city (Haque & Singh, 2017). Guwahati is a resource-rich metropolis in the North-Eastern state of Assam lying in between the Shillong plateau and the Brahmaputra River. It lies at 26° N, 91.875° E, and 55 m above the MSL. The pollution trends in North-East India are gradually increasing with Guwahati being the most polluted North-Eastern city due to rapid urbanization, open burning of waste, increase in private vehicles thereby vehicular emissions and dust. Guwahati experiences one of the highest BC contaminations around the globe.

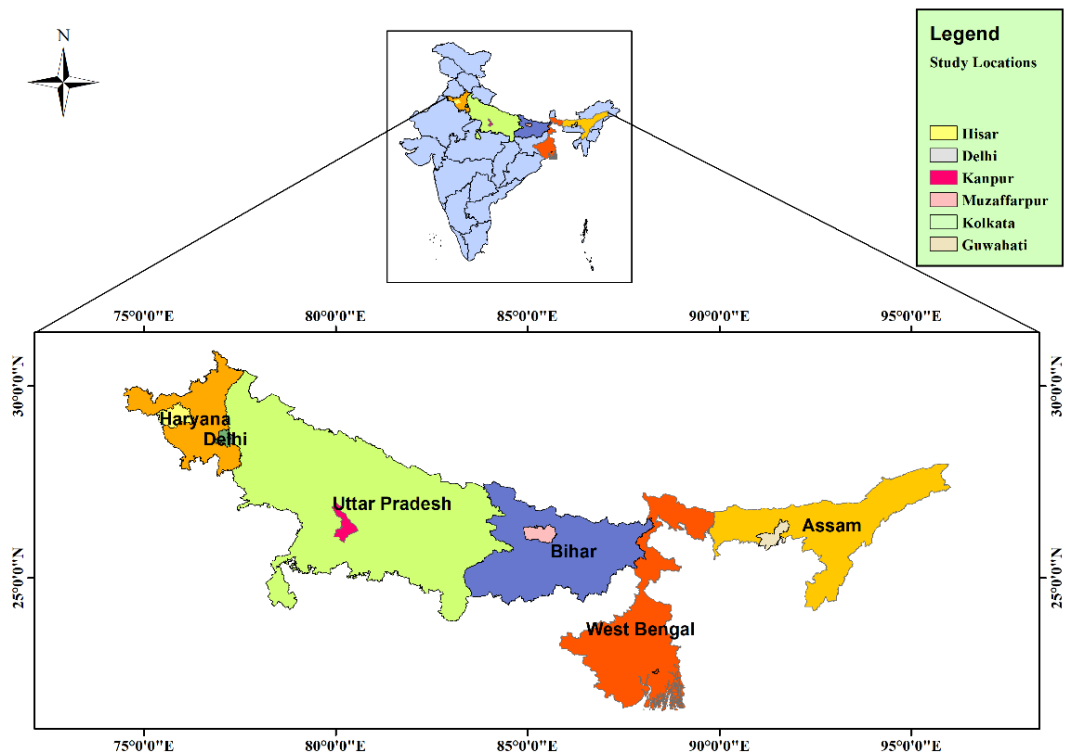


Fig 3.1: Indian map representing study locations

The study locations have been the most polluted cities in the respective states as stated in different reports and articles published from time to time. With this study, we propose to work on these 6 distinct locations of IGP and try to study the pattern of BC and OC over the entire region.

## 3.2 DATA COLLECTION AND ANALYSIS

### 3.2.1 MERRA-2 Reanalysis Dataset

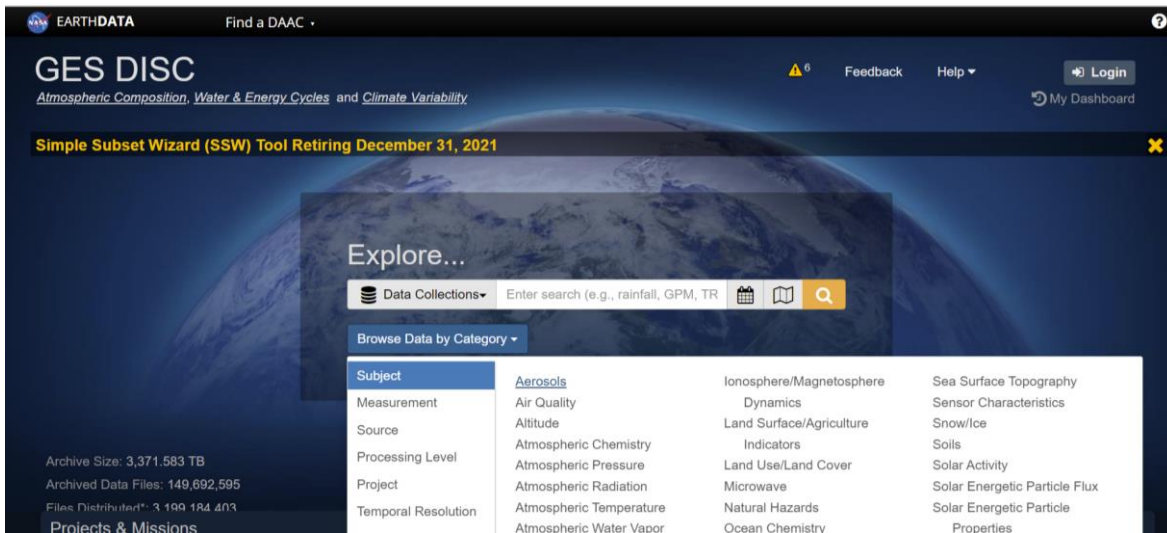
The Modern-Era Retrospective Analysis for Research and Application Version-2 (MERRA-2) is a global atmospheric reanalysis data product from the NASA Global Modeling and Assimilation Office using the 5.12.4 version of the Goddard Earth Observing System Model (GEOS). It provides regularly gridded aerosol reanalysis data from 1980 onwards made available through the NASA Goddard Earth Sciences Data and Information Services Center (GES DISC) (<https://disc.gsfc.nasa.gov/datasets?project=MERRA-2>). The product consists of 1h, 3h, and monthly assimilated aerosol data on surface mass concentration, total extinction, column mass density, and scattering of the aerosol optical thickness (AOT) for aerosol components like BC, OC, dust, sulfate, and sea salt. It offers a high spatial resolution of  $0.5^\circ \times 0.625^\circ$  and 72-hybrid-eta levels up to 0.01 mbar. MERRA-2 system derives the aerosol observations from ground-based Aerosol Robotic Network (AERONET), AOD from Moderate Resolution Imaging Spectroradiometer (MODIS) aboard Terra and Aqua satellites, Advanced Very High-Resolution Radiometer (AVHRR), Multiangle Imaging Spectro-Radiometer (MISR) (Buchard et al., n.d.; Randles et al., 2017a, 2017b).

As per (Randles et al., 2017a), the carbonaceous aerosols are mainly sourced from natural and anthropogenic activities like biomass burning and plant matters. (Buchard et al., n.d.), found that MERRA-2 simulated the aerosol mass concentrations well with a correlation value above 0.69 with ground-based surface mass concentrations. A study by (Prabhu et al., 2020) suggests a positive correlation (0.52) of MERRA-2 BC observations with ground-based daily mean BC concentrations. However, the MERRA-2 data correlated even better with the monthly data with a correlation of 0.80. Similar results were stated by (Qin et al., 2019), that the correlation of MERRA-2 with observed values improves when the averaging time is increased from hourly to 12-hourly. So, it is suggested by (Prabhu et al., 2020), that in the paucity of ground-based observations, the monthly mean of MERRA-2 BC data can be used.

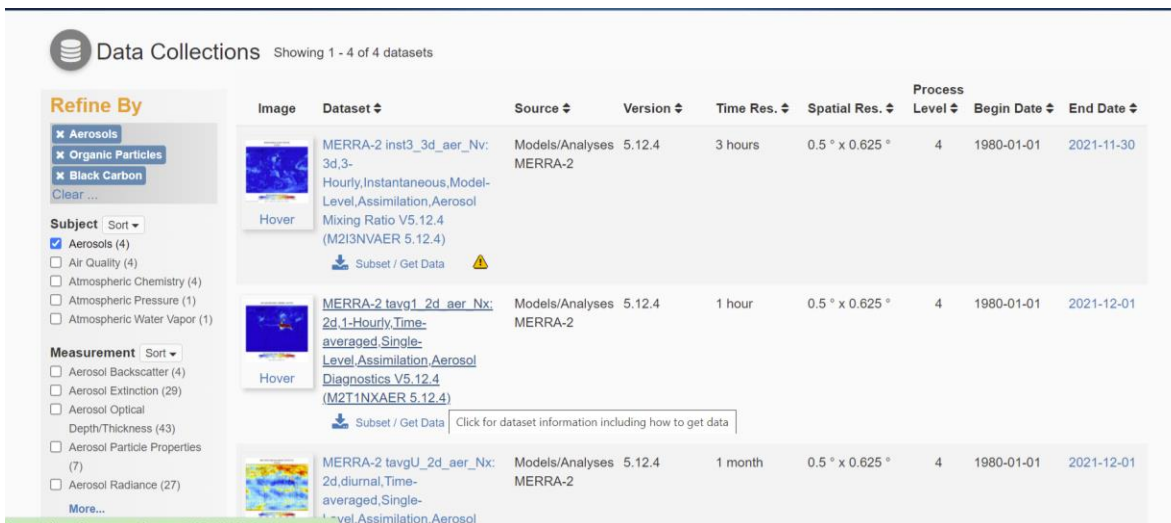
In the absence of the aethalometers and amid COVID-19 restrictions, in this study, we have used MERRA-2's 1- hourly time-averaged 2-dimensional data for black carbon surface mass concentration (BCSMASS) and Organic carbon surface mass concentration (OCSMASS) for the study locations for 3 years starting January 2019 till December 2021.

### 3.2.2 Meteorological Data Collection


The hourly concentrations of air pollutants - PM<sub>2.5</sub>, NO<sub>2</sub>, SO<sub>2</sub>, CO, Ozone and data for meteorological parameters - Relative Humidity (RH), Wind Speed (WS), Ambient Temperature (AT) were downloaded from the Central Pollution Control Board's website (<https://app.cpcbcr.com/ccr/#/caaqm-dashboard-all/caaqm-landing/data>). CPCB has an established network of 340 monitoring stations i.e., Continuous ambient air quality monitoring system (CAAQMS) across India which records real-time ambient air quality parameters.

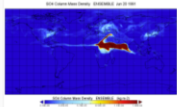


3.2. Step 1



3.3. Step 2

MERRA-2 tavg1\_2d\_aer\_Nx: 2d,1-Hourly,Time-averaged,Single-Level,Assimilation,Aerosol Diagnostics V5.12.4 (M2T1NXAER) 



[View Full-size Image](#)

M2T1NXAER (or tavg1\_2d\_aer\_Nx) is an hourly time-averaged 2-dimensional data collection in Modern-Era Retrospective analysis for Research and Applications version 2 (MERRA-2). This collection consists of assimilated aerosol diagnostics, such as column mass density of aerosol components (black carbon, dust, sea salt, sulfate, and organic carbon), surface mass concentration of aerosol components, and total extinction (and scattering) aerosol optical thickness (AOT) at 550 nm. The total PM1.0, PM2.5, and PM10 may be derived with the formula described in the FAQs under the Documentation tab of this page. The data field is time-stamped with the central time of an hour starting from 00:30 UTC, e.g.: 00:30, 01:30, ..., 23:30 UTC.

MERRA-2 is the latest version of global atmospheric reanalysis for the satellite era produced by NASA Global Mod ...more

**Data Access**

[Online Archive](#)

[Earthdata Search](#)

[Giovanni](#)

[Web Services](#)

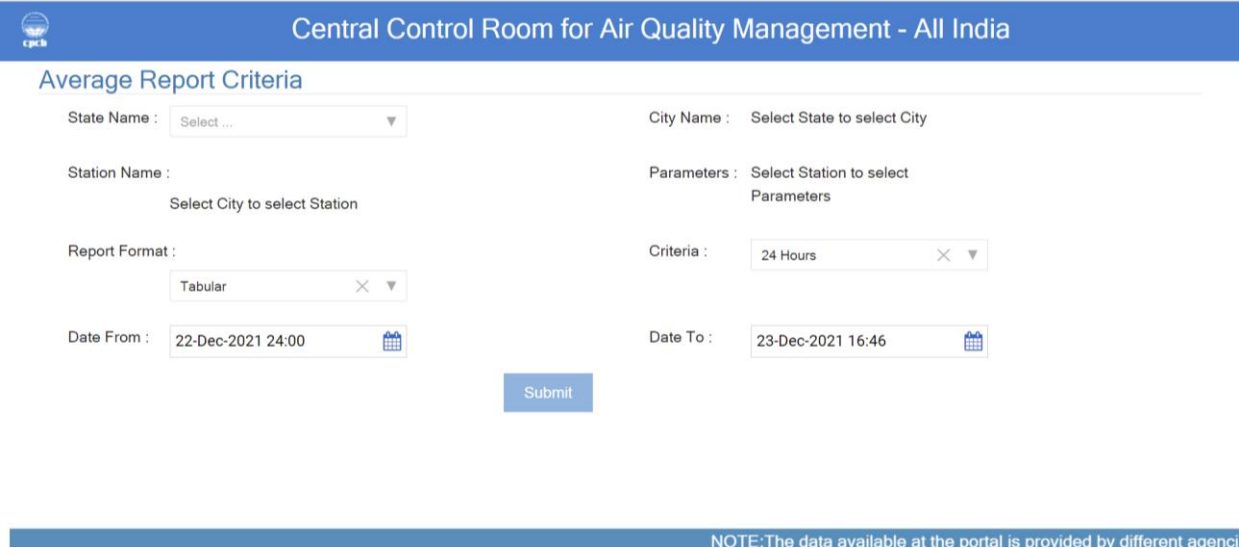
[Subset / Get Data](#)

[Product Summary](#) | [Data Citation](#) | [Documentation](#) | [References](#)

**Shortname:** M2T1NXAER  
**Longname:** MERRA-2 tavg1\_2d\_aer\_Nx: 2d,1-Hourly,Time-averaged,Single-Level,Assimilation,Aerosol Diagnostics V5.12.4  
**DOI:** 10.5067/KLICTZ8EM9D  
**Version:** 5.12.4  
**Format:** netCDF  
**Spatial Coverage:** -180.0,-90.0,180.0,90.0  
**Temporal Coverage:** 1980-01-01 to 2021-12-01

### 3.4. Step 3

Figure 3.2, 3.3, 3.4: Shows steps followed for downloading the MERRA-2 reanalysis data for carbonaceous aerosols (BC and OC) and the planetary boundary layer height data for the selected locations. Available at: [https://disc.gsfc.nasa.gov/datasets/M2T1NXAER\\_5.12.4/summary](https://disc.gsfc.nasa.gov/datasets/M2T1NXAER_5.12.4/summary)



**Central Control Room for Air Quality Management - All India**

**Average Report Criteria**

State Name :

Station Name :

Report Format :

Date From :

City Name :

Parameters :

Criteria :

Date To :

[Submit](#)

NOTE: The data available at the portal is provided by different agency

Figure 3.5: Central Pollution Control Board's website used for downloading the continuous ambient air quality monitoring data for meteorological parameters for the study area. Available at: <https://app.cpcbcr.com/ccr/#/caaqm-dashboard-all/caaqm-landing>



Figure 3.6: READY National Oceanic and Atmospheric Administration (NOAA) Air Resource Laboratory’s website used for downloading the Trajectory end point data for the chosen locations. Available at: [https://www.ready.noaa.gov/HYSPLIT\\_traj.php](https://www.ready.noaa.gov/HYSPLIT_traj.php)

### 3.2.3 HYSPLIT Data, Cluster Analysis and CWT Method

#### 3.2.3.1 Backward-Trajectory Cluster Analysis:

For investigating the transport pathways of carbonaceous aerosol species and influence of large-scale atmospheric circulations on their movement, the 5-day backward trajectories were created for the study locations using Air Resource Laboratory (ARL), National Oceanic and Atmospheric Administration’s (NOAA’s) Hybrid Single Particle Lagrangian Integrated Trajectory (HYSPLIT) model. The NCEP/NCAR Reanalysis daily meteorological data was used for HYSPLIT trajectory generation having resolution 2.5 degree (<ftp://ftp.arl.noaa.gov/pub/archives/reanalysis> ). The 3-dimensional 5-day air mass backward trajectory at a height of 500 m above the ground level were worked out at 00, 06, 12, and 18 UTC each day for each location for 2019-2021. The cluster analysis was done using Openair package in R programming which is provides open-source tools for analyzing air pollution data. The purpose of cluster analysis is to group trajectories based on geographic origins.

#### 3.2.3.2 CWT:

Concentration weighted trajectory analysis is a qualitative approach to identify the potential source regions of air pollutants. In this method, the study area is divided into grids of  $1^{\circ} \times 1^{\circ}$  and each grid is assigned a weighted average concentration evaluated a function of pollutant concentration and its

residence time in each grid (Chen et al., 2019; Liu et al., 2022; Meena et al., 2021; Pipal et al., 2014). The CWT formula is:

$$CWT_{i,j} = \frac{\sum_{l=1}^L C_l \tau_{i,j,l}}{\sum_{l=1}^L \tau_{i,j,l}} \quad \text{Eq.3.1}$$

Where,  $CWT_{i,j}$  is CWT value of grid  $i,j$ ;  $C_l$  is receptor concentration of trajectory  $l$  when it passes through grid  $i,j$ .  $L$  is total number of back trajectories and  $\tau_{i,j,l}$  refers to duration for which trajectory  $l$  stays in grid  $i,j$ . A high value of  $CWT_{i,j}$  indicates that the air parcels passing over the grid  $i,j$  would contribute more to high pollutant concentration at the study area. Openair package in R programming was used to perform CWT analysis.



## CHAPTER 4

### RESULTS AND DISCUSSION

#### 4.1 MONTHLY TEMPORAL VARIATIONS IN BC AND OC MASS CONCENTRATIONS

The monthly mean BC and OC concentrations over IGP varied from 0.94 to 10.05  $\mu\text{gm}^{-3}$  and 3.49  $\mu\text{gm}^{-3}$  to 48.74  $\mu\text{gm}^{-3}$  respectively in different months. The highest monthly mean BC concentrations observed for 2019 are: Kolkata (January - 8.12  $\mu\text{gm}^{-3}$ ) > Kanpur (January - 7.17  $\mu\text{gm}^{-3}$ ) > Muzaffarpur (January - 7.08  $\mu\text{gm}^{-3}$ ) > Delhi (December - 5.72  $\mu\text{gm}^{-3}$ ) > Hisar (December - 5.13  $\mu\text{gm}^{-3}$ ) > Guwahati (March - 3.22  $\mu\text{gm}^{-3}$ ). For 2020, an almost similar pattern was observed with Muzaffarpur recording the maximum BC mass concentration in December (10.05  $\mu\text{gm}^{-3}$ ) followed by Kolkata (December - 9.71  $\mu\text{gm}^{-3}$ ) > Kanpur (November - 6.88  $\mu\text{gm}^{-3}$ ) > Delhi (December - 5.94  $\mu\text{gm}^{-3}$ ) > Hisar (November - 5.47  $\mu\text{gm}^{-3}$ ) > Guwahati (February - 4.09  $\mu\text{gm}^{-3}$ ). Unlikely, in 2021, Delhi encountered a maximum BC mass concentration among all locations in November (8.25  $\mu\text{gm}^{-3}$ ). For other locations the values are Hisar (November - 7.94  $\mu\text{gm}^{-3}$ ) > Kanpur (November - 7.36  $\mu\text{gm}^{-3}$ ) > Muzaffarpur (November - 7.36  $\mu\text{gm}^{-3}$ ) > Kolkata (January - 7.17  $\mu\text{gm}^{-3}$ ) and Guwahati (February - 3.7  $\mu\text{gm}^{-3}$ ).

A similar pattern was observed in monthly mean OC mass concentrations with OC peaking for respective states in 2019 in the order: Guwahati (March - 35.84  $\mu\text{gm}^{-3}$ ) > Kolkata (32.63  $\mu\text{gm}^{-3}$ ) > Muzaffarpur (November - 30.56  $\mu\text{gm}^{-3}$ ) > Kanpur (January - 28.58  $\mu\text{gm}^{-3}$ ) > Delhi (December - 22.54  $\mu\text{gm}^{-3}$ ) > Hisar (December - 19.79  $\mu\text{gm}^{-3}$ ). An extremely high OC was observed for Muzaffarpur in December 2020 (41.35  $\mu\text{gm}^{-3}$ ) followed by Kolkata (November - 39.63  $\mu\text{gm}^{-3}$ ) > Kanpur (November - 35.73  $\mu\text{gm}^{-3}$ ) > Guwahati (March - 30.51  $\mu\text{gm}^{-3}$ ) > Delhi (November - 30.12  $\mu\text{gm}^{-3}$ ) > Hisar (November - 28.11  $\mu\text{gm}^{-3}$ ). Overall, for 2020, the maximum OC for all locations increased by 20-40% except Guwahati which shows a decrease in maximum value. In 2021, Hisar and Delhi which showed the lowest maximum OC for 2019 and 2020, surprisingly, experienced highest maximum OC value of 48.74  $\mu\text{gm}^{-3}$  and November - 44.74  $\mu\text{gm}^{-3}$  respectively among all locations with OC peaking in November 2021. These were followed by Guwahati (March - 38.93  $\mu\text{gm}^{-3}$ ) > Kanpur (November - 38.53  $\mu\text{gm}^{-3}$ ) > Muzaffarpur (November - 37.30  $\mu\text{gm}^{-3}$ ) > Kolkata (January - 30.00  $\mu\text{gm}^{-3}$ ). Kolkata observed a decrease in maximum OC concentration from 2020 to 2021.

Delhi saw minimum monthly mean BC and OC mass concentrations of  $1.48 \mu\text{gm}^{-3}$  and  $5.65 \mu\text{gm}^{-3}$ , respectively in June 2019. Similarly, for all the study locations, the lowest BC and OC monthly means were observed in June or July of every year, with Hisar witnessing the lowest BC concentration at  $0.94 \mu\text{gm}^{-3}$  and OC at  $3.49 \mu\text{gm}^{-3}$  among all locations. June, July, and August recorded the lowest values for all locations and are homogenous throughout all years, attributed to the washout of pollutants due to precipitation. 2020 saw a decrease in the usual uprise in BC and OC mass concentrations for all locations. The concentrations for the two variables increased by the end of 2020 and were lower as compared to the other years. A possible reason might be the imposition of lockdown throughout the country due to COVID-19. Figures (4.1, 4.2, 4.3) also gives us the 95% confidence intervals, at which point we can surely say that an observation lying in that interval has a 0.95 probability of actually having that observation.

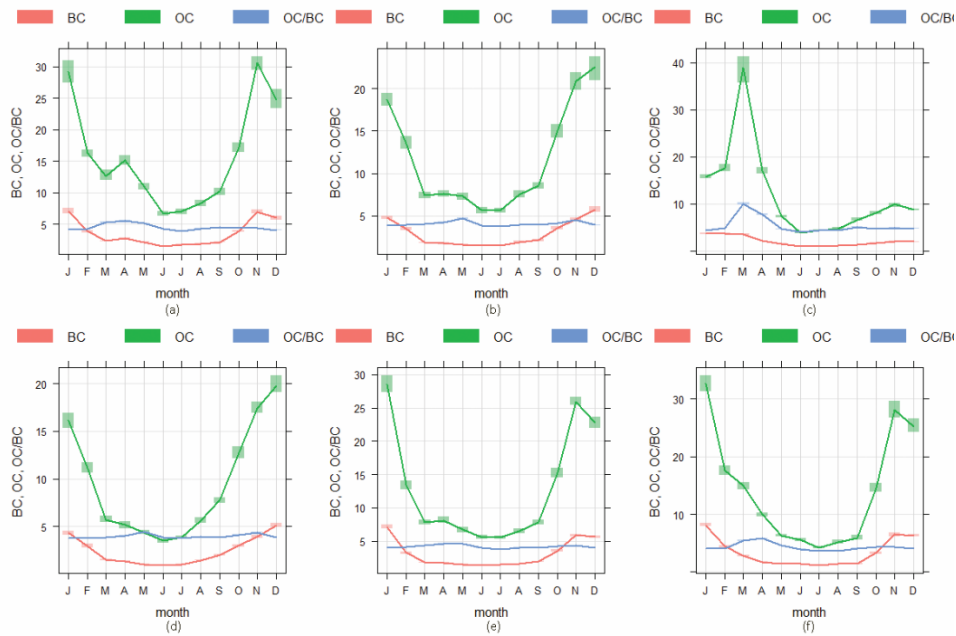


Fig 4.1 Time variation plot representing BC, OC ( $\mu\text{gm}^{-3}$ ), and OC/BC monthly mean for locations starting from (a.) Muzaffarpur, (b.) Delhi, (c.) Guwahati, (d.) Hisar, (e.) Kanpur and (f.) Kolkata for 2019

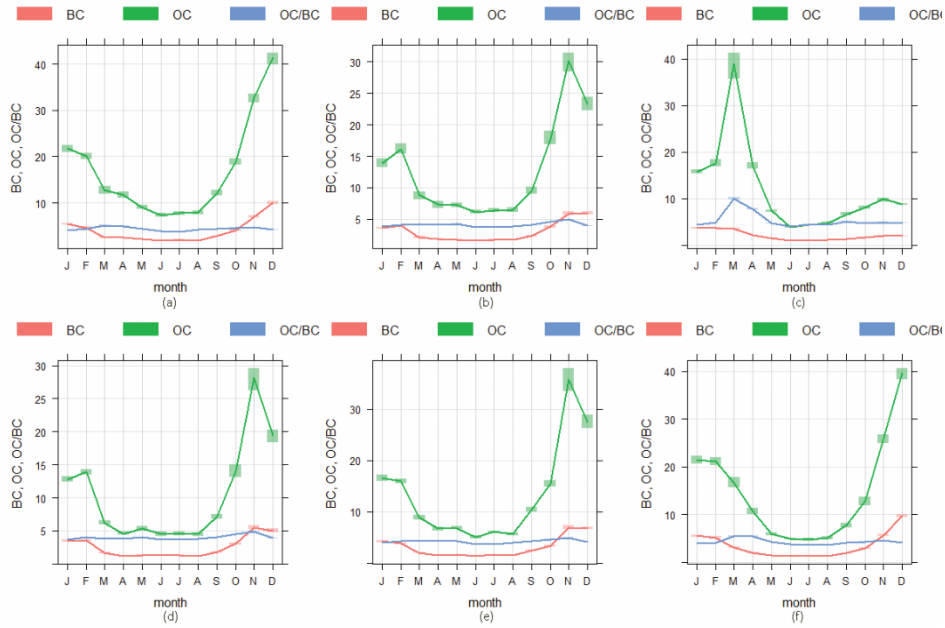


Fig 4.2 Time variation plot representing BC, OC ( $\mu\text{g m}^{-3}$ ), and OC/BC monthly mean for locations starting from (a.) Muzaffarpur, (b.) Delhi, (c.) Guwahati, (d.) Hisar, (e.) Kanpur and (f.) Kolkata for 2020

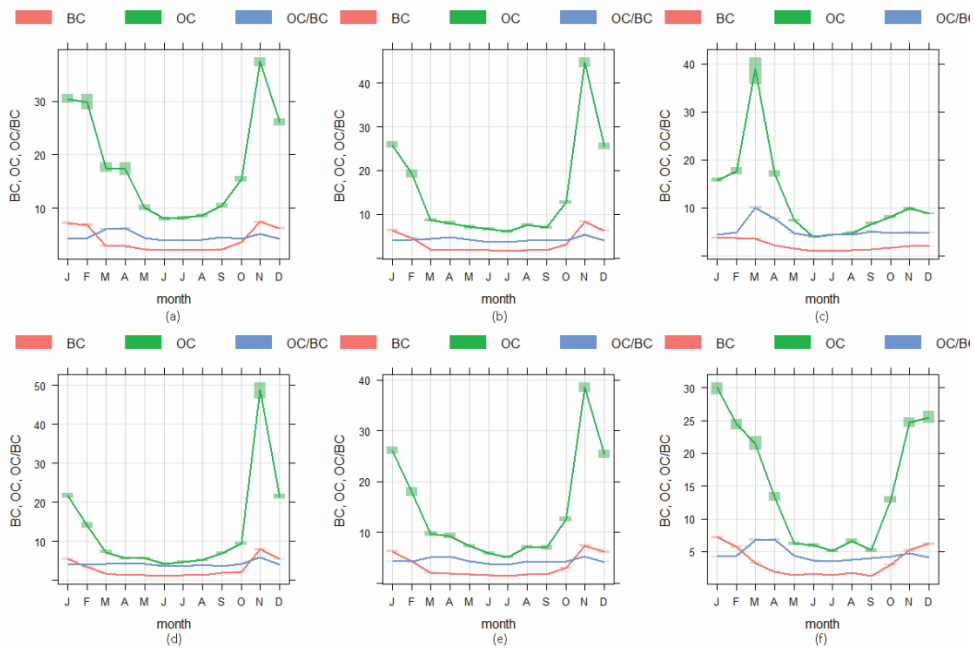


Fig 4.3 Time variation plot representing BC, OC ( $\mu\text{g m}^{-3}$ ), and OC/BC monthly mean for locations starting from (a.) Muzaffarpur, (b.) Delhi, (c.) Guwahati, (d.) Hisar, (e.) Kanpur and (f.) Kolkata for 2021

The raincloud, figure 4.4 & 4.5 gives us an overall idea of the density spread and distribution of the values of carbonaceous aerosols. For BC mass concentration, we see that Kolkata has the highest spread, followed by Muzaffarpur, Kanpur, and then Delhi and Hisar. Guwahati has the least spread of density among all the locations. Similarly, for OC mass concentration, we have a similar order. All of the locations seem to have a negatively skewed distribution for both BC and OC mass concentrations, with Delhi, Hisar, and Kanpur being the most skewed. Kolkata, Muzaffarpur, and Guwahati are more symmetrical in terms of distribution, with Guwahati being the most symmetrical. The pattern followed by monthly mean BC and OC concentrations during the study period is in line with previous research.

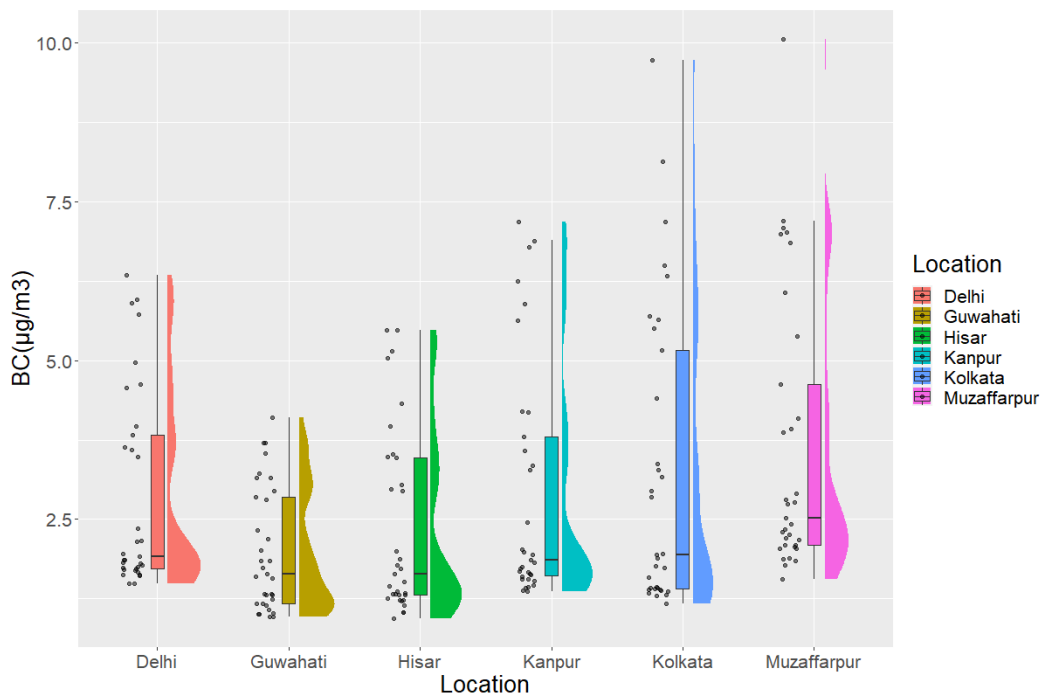


Fig 4.4 Raincloud plot representing BC monthly means dispersion across all locations for 3 years

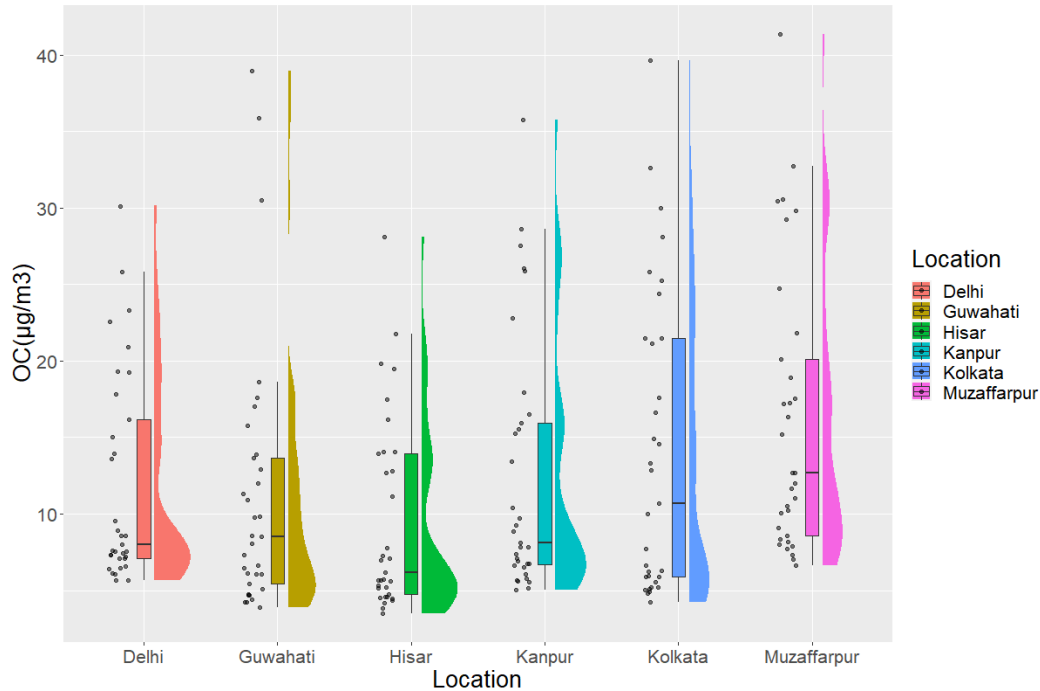


Fig 4.5 Raincloud plot representing OC monthly means dispersion across all locations for 3 years

The patterns observed for BC and OC monthly means indicate that Delhi and Hisar’s air saw a massive increase in carbonaceous aerosols loading at the end of 2021, which was more than other locations, unlike 2020, and 2019 when they experienced the lowest concentrations. In 2021, Delhi experienced the worst November since 2015, reporting more than 11 days of severe air quality (BBC,2021) owing to the burning of crackers at Diwali (Figure 4.6) and crop stubble burning in neighboring states, pushed to November due to prolonged monsoon. As per a CEEW (Council on Energy, Environment and Water) report, 2021 saw the highest number of crop residue burning incidents reported in 5 years for Uttar Pradesh, Haryana, and Punjab alone. Delhi’s air quality is deteriorated by the biomass burning from North-Western states and fossil fuel burning, escalated by the unfavorable wind direction, speed and dipping atmospheric temperature during winter months (Srivastava et al., 2014).

Hisar has similar precursors of poor air quality as Delhi mostly affected by natural dusty winds, stubble burning, and combustion of fossil fuel for vehicles and industrial works (D. Singh et al., 2022).

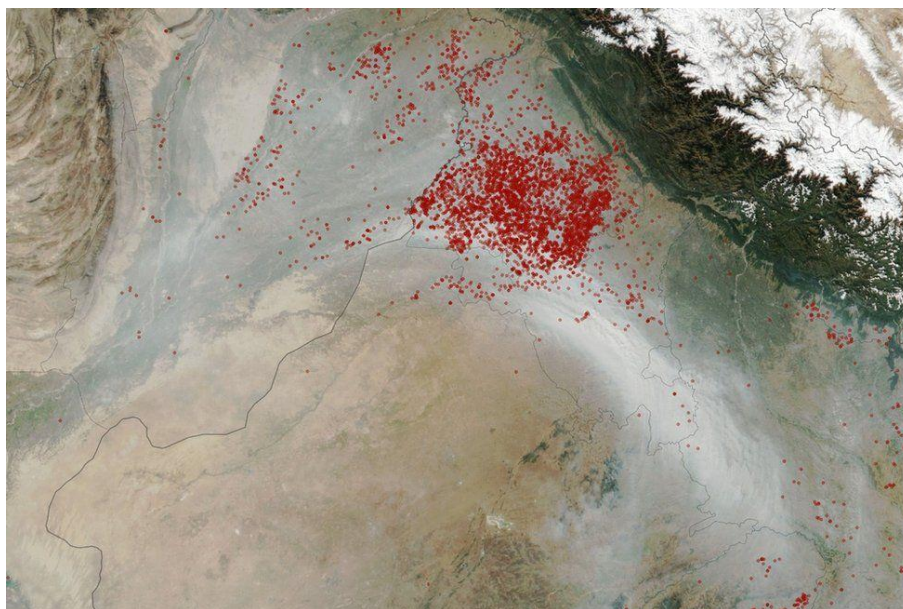


Fig 4.6: Smoke from crop fires in Northern India on 11 November 2021 (Source: NASA)

High levels of BC concentrations were observed in Kanpur during the winter months ranging from  $6.88$  to  $7.36 \mu\text{gm}^{-3}$ . The city's air is significantly loaded with particulate matter, predominantly carbonaceous aerosols, due to the freshly emitted vehicular emissions, mainly from heavy-duty diesel vehicles like trucks (Ram et al., 2014). Peak OC levels in Kanpur ranged from  $28.58$  to  $38.53 \mu\text{gm}^{-3}$  observed during the latter part of the year. High levels of OC were also observed by per Ram et al., 2010, who suggested that Kanpur owes its poor air quality to biomass burning.

Guwahati has high concentrations of BC (relatively lower) and OC because of its rapid urbanization, infrastructure development, poorly managed industrial emissions, and biomass burning activities. Another primary reason for Guwahati's high BC concentration is extensive open burning of solid waste and an unplanned transportation system with a rapidly increasing number of private vehicles leading to high fuel consumption in the city. Moreover, Guwahati shows a moderate inverse correlation between OC and relative humidity ( $r = -0.53$ ), which confirms the fact that high OC levels in the March are a result of highly humid climatic conditions and hot and dry summers.

High BC mass concentrations (ranging from  $7.08$ - $10.05 \mu\text{gm}^{-3}$ ) and OC mass concentrations (ranging from  $31.56$ - $41.35 \mu\text{gm}^{-3}$ ) as observed for Muzaffarpur are sourced from incomplete combustion of coal in a huge number of brick kilns operating in the area along with unbridled infrastructure development activities, burning of biofuels for domestic purposes, industrial emissions and resuspension of dust. The city, which otherwise ranked 3<sup>rd</sup> or 4<sup>th</sup> among all locations, showed BC and OC mass concentrations of

10.05 and 41.35  $\mu\text{gm}^{-3}$  in December 2020, which may be due to heavy industrial activities after eased covid restrictions.

Kolkata is highly polluted, with BC and OC comprising a major fraction of particulate pollution. It observed peaks for BC and OC for 3 years ranging from 7.17 - 9.71  $\mu\text{gm}^{-3}$  and 30 - 39.63  $\mu\text{gm}^{-3}$ , respectively. Kolkata saw a decrease of around 25% in usual rise in carbonaceous aerosol concentration in 2021, which was the lowest in 3 years. The high levels of particulate pollution in Kolkata are because of the vast number of large industrial units such as minerals, steel, jute, and food processing industries established here, road dust, construction activities, and coal used in thermal power plants, residential use of biofuels and burning of waste. The major contributor to Kolkata's poor air quality and high levels of BC and OC is transportation and thereby, the combustion of fossil fuel for transportation. According to a recent study, almost 49% of vehicles plying in Kolkata are older than 15 years which is the reason for incomplete and inefficient consumption of diesel and gasoline.

## 4.2 SEASONAL VARIATIONS IN BC AND OC MASS CONCENTRATIONS

As observed, the average BC and OC concentrations were the highest for each location in the winter (December – January - February) and lowest in the monsoon season (June–July-August-September) (except Guwahati). The concentrations of BC follow the order: Winter (DJF) > Post-Monsoon (ON) > Summer (MAM) > Monsoon (JJAS) ranging from  $3.08 \pm 0.69 \mu\text{gm}^{-3}$  to  $6.47 \pm 1.63 \mu\text{gm}^{-3}$ ,  $1.83 \pm 0.16 \mu\text{gm}^{-3}$  to  $5.48 \pm 1.80 \mu\text{gm}^{-3}$ ,  $1.38 \pm 0.21 \mu\text{gm}^{-3}$  to  $2.47 \pm 0.29 \mu\text{gm}^{-3}$  and  $1.11 \pm 0.12 \mu\text{gm}^{-3}$  to  $2.03 \pm 0.30 \mu\text{gm}^{-3}$  respectively. Kolkata recorded the highest BC mass concentration at  $6.47 \pm 1.63 \mu\text{gm}^{-3}$ . While, Muzaffarpur recorded the highest OC mass concentration at  $26.66 \pm 7.28 (\mu\text{gm}^{-3})$  in Winter among all the other locations. Minimum BC and OC mass concentrations were observed in the monsoon, with Guwahati reporting the lowest compared to other locations at  $1.11 \pm 0.12 \mu\text{gm}^{-3}$  and  $5.02 \pm 0.87 \mu\text{gm}^{-3}$ , respectively. BC mass concentrations in the Winter season were as high as 3 times the monsoon season average for all locations except Kolkata, for which the winter average was 4.5 times the monsoon average. A similar pattern was submitted by (Krishna et al., 2019) who studied the radiative forcing of particulate matter ( $\text{PM}_{2.5}$  and BC) over Delhi and Pune.

The seasonal variation for each location can be showcased in the plots below (Figures 4.7 and 4.8):

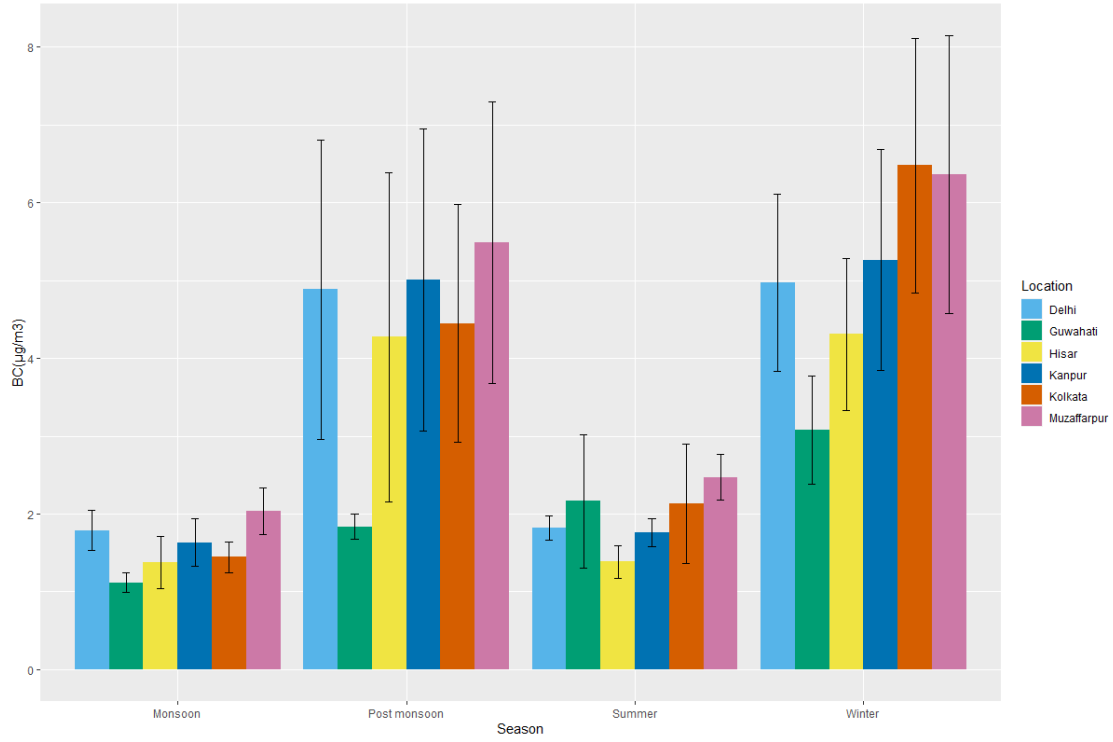


Figure 4.7: Seasonal variations in BC mass concentrations ( $\mu\text{g}\cdot\text{m}^{-3}$ ) from 2019-21

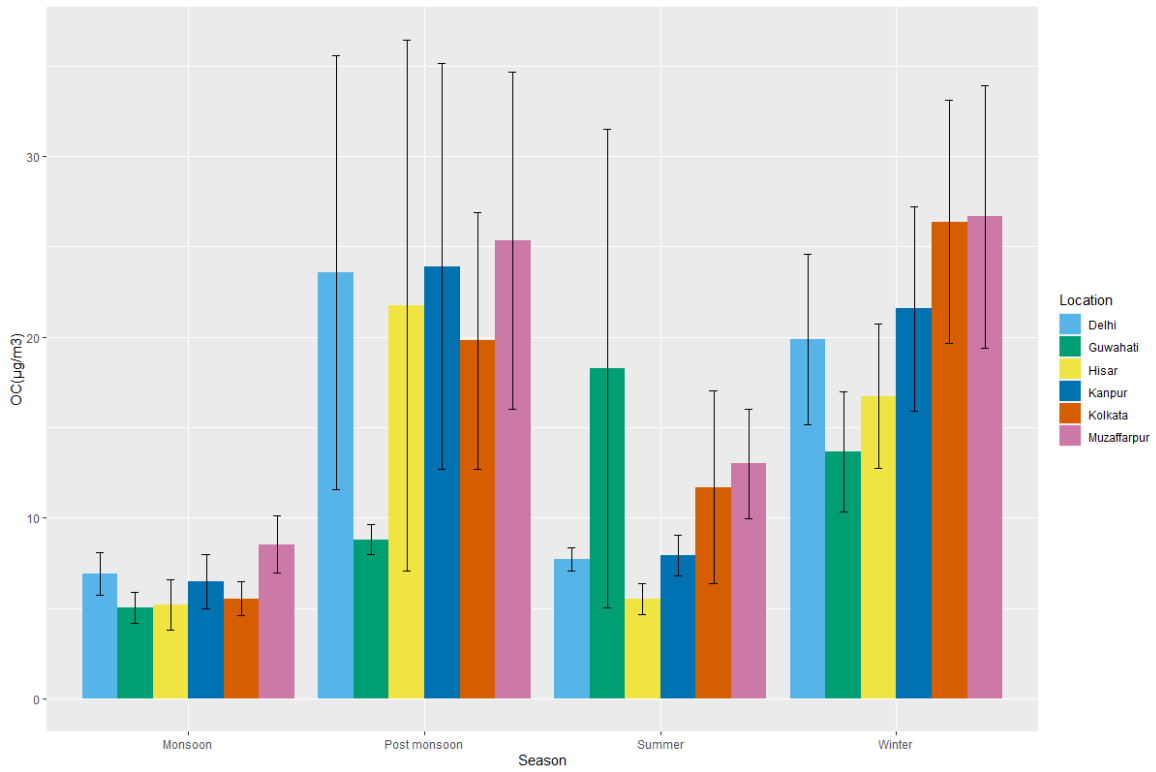


Figure 4.8: Seasonal variations in OC mass concentrations ( $\mu\text{g}\cdot\text{m}^{-3}$ ) from 2019-21



The concentrations of OC follow the same order as that of BC as observed, i.e., Winter (DJF) > Post-Monsoon (ON) > Summer (MAM) > Monsoon (JJAS) for Muzaffarpur and Kolkata with values ranging between  $8.53 \pm 1.58 \mu\text{gm}^{-3}$  to  $26.66 \pm 7.28 \mu\text{gm}^{-3}$  and  $5.52 \pm 0.93 \mu\text{gm}^{-3}$  to  $26.38 \pm 6.73 \mu\text{gm}^{-3}$  respectively. For Hisar, Delhi, and Kanpur, the OC concentrations were highest in post-monsoon, followed by winter, then summer, and minimum in monsoon. Whereas for Guwahati, the OC concentrations peaked in summers with an average of  $18.25 \pm 13.22 \mu\text{gm}^{-3}$ . The results are in line with previous research, which reported that IGP's air is dominated by soaring levels of secondary aerosols during the winter season (Rengarajan et al., 2007).

The high concentrations of carbonaceous aerosols observed in winter are due to the presence of unfavorable meteorological conditions such as low wind speed, low temperature, high relative humidity, and low mixing height, leading to frequent incidences of atmospheric inversions inhibiting the movement of aerosols and therefore high aerosol concentrations at surface. The pollutants in the Gangetic plains get trapped due to above mentioned calm weather conditions leading to severe pollution episodes. The lowest aerosol concentrations in monsoon can be attributed to the washout of particulates with precipitation (Sharma et al., 2016). Moreover, the high wind speed during monsoon diffuses the aerosol particles rapidly, and hence monsoon manifests the lowest pollutant concentrations of all seasons. The effect of meteorological parameters on aerosol concentrations has been discussed later in section 4.5. In summer, the contribution to aerosol loading may be from the long-range transport of mineral dust from South Asian countries and the Thar desert in the western part of India (Ram et al., 2010).

There is an anomaly in Guwahati's OC variations which were maximum in summers i.e., March. The summer season in Assam is arid and highly humid; starting in March, it sees a rise in temperature and increased incidents of dust storms in western Assam. Moreover, during summer in Guwahati, the wind speed is relatively higher, which leads to the resuspension of dust in the atmosphere. It may also be attributed to excessive use of biomass and solid fuel, traffic congestion, increased motorization, and escalated infrastructure development generating dust in this hilly region.

The average BC and OC concentrations, seasonally, for all the locations are given in the table below:

Table 4.1: Seasonal mean  $\pm \sigma$  BC mass concentrations ( $\mu\text{gm}^{-3}$ )

S. No.	Cities	Season			
		Winter	Summer	Monsoon	Post-Monsoon
1	Hisar	4.311 $\pm$ 0.97	1.38 $\pm$ 0.21	1.37 $\pm$ 0.33	4.27 $\pm$ 2.11
2	Delhi	4.97 $\pm$ 1.13	1.82 $\pm$ 0.16	1.78 $\pm$ 0.25	4.88 $\pm$ 1.92
3	Kanpur	5.26 $\pm$ 1.42	1.76 $\pm$ 0.17	1.63 $\pm$ 0.30	5 $\pm$ 1.94
4	Muzaffarpur	6.36 $\pm$ 1.78	2.47 $\pm$ 0.29	2.03 $\pm$ 0.30	5.48 $\pm$ 1.80
5	Kolkata	6.47 $\pm$ 1.63	2.12 $\pm$ 0.76	1.44 $\pm$ 0.19	4.44 $\pm$ 1.52
6	Guwahati	3.08 $\pm$ 0.69	2.16 $\pm$ 0.85	1.11 $\pm$ 0.12	1.83 $\pm$ 0.16

Table 4.2: Seasonal mean  $\pm \sigma$  OC mass concentrations ( $\mu\text{gm}^{-3}$ )

S. No.	Cities	Season			
		Winter	Summer	Monsoon	Post-Monsoon
1	Hisar	16.73 $\pm$ 3.98	5.53 $\pm$ 0.85	5.20 $\pm$ 1.38	21.76 $\pm$ 14.68
2	Delhi	19.86 $\pm$ 4.70	7.71 $\pm$ 0.63	6.92 $\pm$ 1.19	23.57 $\pm$ 12.00
3	Kanpur	21.57 $\pm$ 5.67	7.92 $\pm$ 1.14	6.46 $\pm$ 1.5	23.91 $\pm$ 11.23
4	Muzaffarpur	26.66 $\pm$ 7.28	13.01 $\pm$ 3.03	8.53 $\pm$ 1.58	25.33 $\pm$ 9.31
5	Kolkata	26.38 $\pm$ 6.73	11.70 $\pm$ 5.35	5.52 $\pm$ 0.93	19.81 $\pm$ 7.09
6	Guwahati	13.66 $\pm$ 3.29	18.25 $\pm$ 13.22	5.02 $\pm$ 0.87	8.81 $\pm$ 0.84

### 4.3 INTERANNUAL VARIATIONS IN BC AND OC MASS CONCENTRATIONS

The annual mean concentrations ( $\pm \sigma$ ) of BC and OC at 6 locations are summarized in Fig. 4.9 & 4.10 and Table 4.3). The annual average for BC and OC over the study area ranged between 1.91 to 4.26  $\mu\text{gm}^{-3}$  and 9.38 to 19.61  $\mu\text{gm}^{-3}$ , respectively. We see for Inter-annual plots, for BC and OC, Muzaffarpur has the highest BC and OC mean values for all 3 years. Whereas the minimum annual average BC values were reported in Guwahati and for OC Hisar experienced the lowest for 2019 & 2020 and Guwahati for 2021. The order for BC mass concentration is Kolkata > Muzaffarpur > Kanpur > Delhi > Hisar > Guwahati for the year 2019 and Muzaffarpur > Kolkata > Delhi > Kanpur > Hisar > Guwahati for 2020. For 2021, the order is more or less the same except Delhi has the second highest BC mass concentration.

Muzaffarpur reported highest BC yearly average mass concentration among all locations because of heavy dust load from re-suspension of road side dust, open burning of waste, poor control on industrial emissions etc. Muzaffarpur is surrounded by brick kilns which are also responsible increased levels of aerosol concentration. Moreover, use of diesel for D.G. sets and plying of commercial diesel driven

vehicles which are more than 15 years old leads to emission of particulates in Muzaffarpur (Action Plan, Bihar SPCB). Second to Muzaffarpur is Kolkata which remains one of the highly polluted cities of West Bengal. Kolkata poorly-managed transportation (51.4%) with old vehicles, traffic congestion and high fuel consumption emits large amounts of particulates in air (Haque & Singh, 2017). Additionally, the coal based nuclear power plants, small-scale industries (24.5%) and dust (21.1%) are responsible for such high values of carbonaceous aerosols.

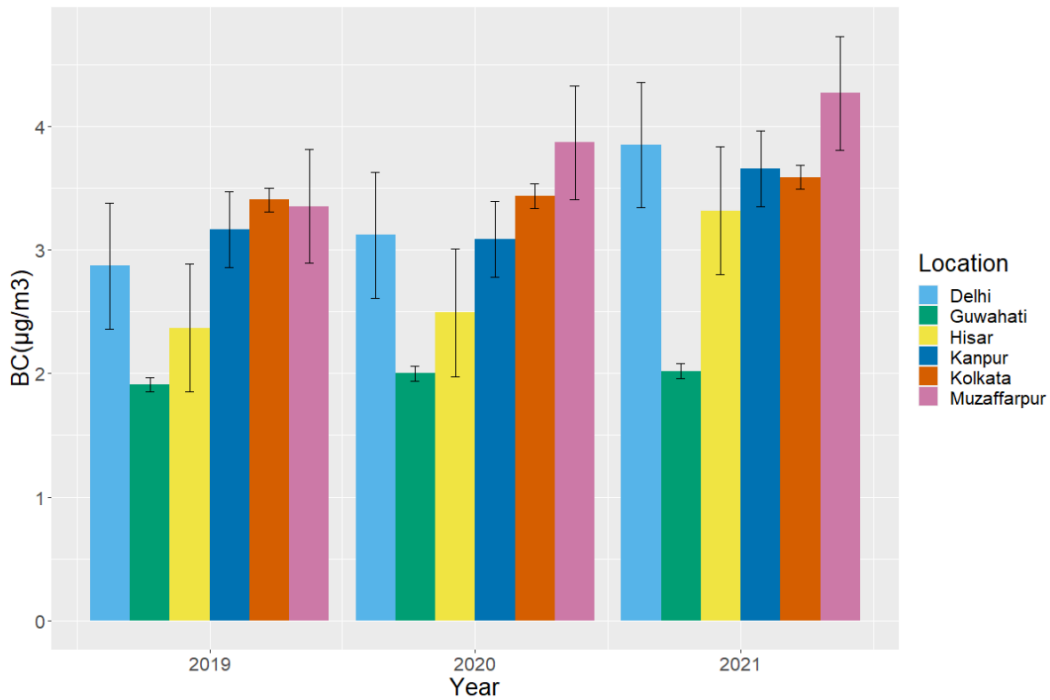


Fig 4.9: Interannual variations in BC mass concentrations from 2019-21

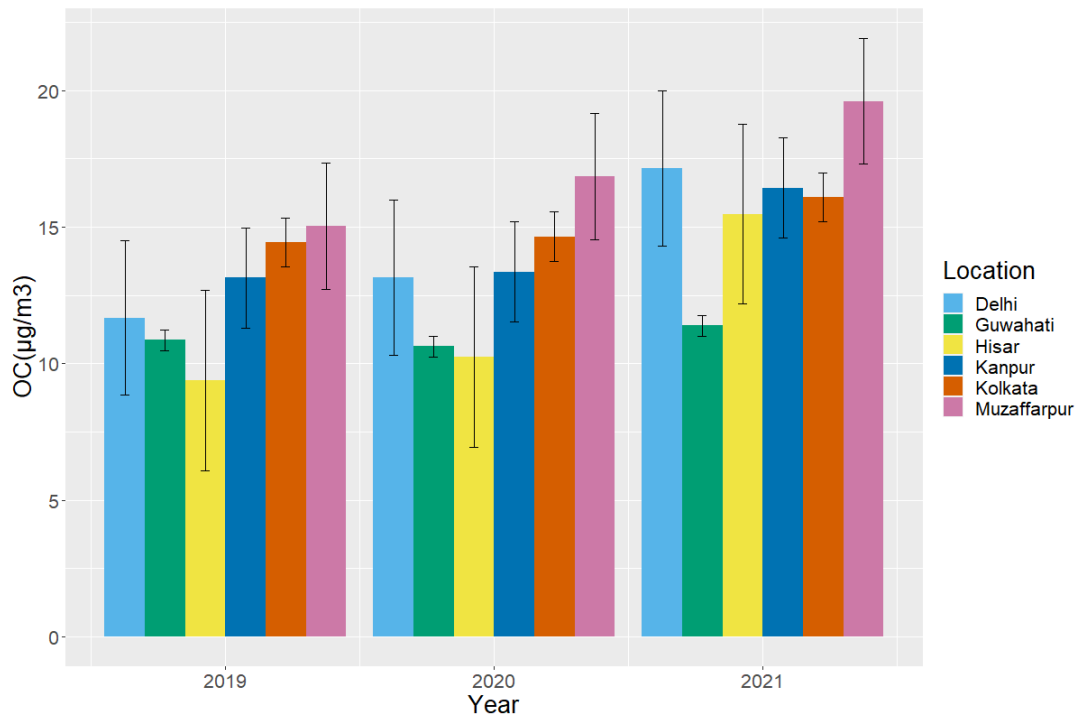


Fig 4.10: Interannual variations in OC mass concentrations from 2019-21

Table 4.3: Annual mean for BC, OC and OC/BC mass concentrations ( $\mu\text{gm}^{-3}$ )

S. No.	Location	Year								
		BC			OC			OC/BC		
		2019	2020	2021	2019	2020	2021	2019	2020	2021
1	Hisar	2.36 ± 1.45	2.49 ± 1.55	3.31 ± 2.22	9.38 ± 5.81	10.24 ± 7.5	15.47 ± 12.88	3.96 ± 0.23	3.96 ± 0.45	4.26 ± 0.65
2	Delhi	2.86 ± 1.5	3.12 ± 1.61	3.84 ± 1.34	11.67 ± 6.18	13.15 ± 7.75	17.16 ± 11.9	4.06 ± 0.25	4.10 ± 0.39	4.27 ± 0.45
3	Kanpur	3.16 ± 2.04	3.08 ± 1.99	3.65 ± 2.17	13.14 ± 8.4	13.36 ± 9.63	16.42 ± 10.53	4.17 ± 0.23	4.18 ± 0.41	4.37 ± 0.47
4	Muzaffarpur	3.35 ± 2.05	3.86 ± 2.53	4.26 ± 2.22	15.03 ± 8.32	16.85 ± 10.77	19.61 ± 10.2	4.55 ± 0.52	4.37 ± 0.36	4.59 ± 0.76
5	Kolkata	3.40 ± 2.43	3.43 ± 2.59	3.58 ± 2.15	14.43 ± 9.87	14.65 ± 10.73	16.08 ± 9.47	4.33 ± 0.6	4.25 ± 0.58	4.50 ± 1.05
6	Guwahati	1.91 ± 0.8	1.99 ± 1	2.02 ± 1.03	10.85 ± 8.53	10.63 ± 7.54	11.38 ± 9.79	5.23 ± 1.92	5.05 ± 1.77	5.22 ± 2.02

Besides, the interannual fluctuations were noticed for BC and OC mean for all the locations, and the values increased by following percentage: Hisar (BC 5% (2019-20) 32% (2020-21), OC 9% (2019-20) 51% (2020-21), Delhi (BC 9% (2019-20) 23.3% (2020-21), OC 12.12% (2019-20) 30.5% (2020-21)), Kanpur (BC -2.5% (2019-20) 18.5% (2020-21), OC 1% (2019-20) 22.9% (2020-21)), Muzaffarpur (BC 15% (2019-20) 10.3% (2020-21), OC 12% (2019-20) 16.3% (2020-21)), Kolkata (BC 0.9% (2019-20) 4.4% (2020-21), OC 1.5% (2019-20) 9.7% (2020-21)) and Guwahati (BC 4.6% (2019-20) 1.5% (2020-

21), OC -2% (2019-20) 7% (2020-21)). The concentrations increased every year for all locations at a different rate depending upon the strength of the emission sources and local meteorology of the study locations. Nonetheless, Kanpur noticed a reduction in BC concentration in 2020 as compared to 2019 and only 1% increase in OC concentration for the said period. Guwahati also experienced a 2% decrease in OC mass concentration from 2019 to 2020 unlike other locations and years where an increase in aerosol concentrations were observed throughout. Hisar and Delhi encountered a huge upsurge in the pollutant concentrations in 2021 contrary to other locations which may be attributed to escalated economic activities after stringent covid incited restrictions.

In the correlation analysis section, we have seen that BC and OC have an extremely high correlation. It can be proved with the yearly OC mass concentrations per location as we see, the orders match up. That is, locations that had high BC mass concentrations also has high OC mass concentrations.

We also observe from the summary table given below that the maximum extremities were observed in Kanpur, followed by Kolkata and Muzaffarpur for BC and Guwahati, followed by Hisar and then Delhi for OC. However, the Mean for BC and OC both remains highest for Muzaffarpur. The highest median for BC and OC was also observed for Muzaffarpur, the values respectively being 3.015 and 13.535. This implies Muzaffarpur has the highest percentile of mass concentrations for both BC and OC.

#### **4.4 ANALYSING OC/BC RATIO**

OC/BC ratio is a significant indicator to identify if the carbonaceous species are of primary or secondary origin and to check for long-range transport of these species. As per (R. Singh et al., 2016) and other researchers, OC/EC ratio more than 2.0 suggests the dominance of secondary organic carbon (SOC), a value of 2.2 corresponds to petrol combustion, biomass burning and burning of coal for domestic heating stipulates OC/EC ratio of 2.5 – 10.5. Whereas, larger OC/EC values strongly indicates the long-range transport of aerosols (Saarikoski et al., 2008). Moreover, biomass burning emits higher amount of OC than BC leading to higher OC/BC ratios unlike emissions from combustion of fossil fuels used in vehicles and industries.

The OC/BC ratio variability was discerned for IGP and found varying between 3.56 and 11.11, with average ratio for entire IGP being  $4.42 \pm 0.98$ . Based on the average OC/BC ratios over 3 years (Figure 4.11) the cities can be ordered as: Guwahati ( $5.27 \pm 1.85$ ) > Muzaffarpur ( $4.5 \pm 0.56$ ) > Kolkata ( $4.36 \pm 0.76$ ) > Kanpur ( $4.23 \pm 0.38$ ) > Delhi ( $4.12 \pm 0.37$ ) > Hisar ( $4.02 \pm 0.47$ ). Pipal et al., 2014; Ram & Sarin,

2015; Srivastava et al., 2014 have reported similar results stating that the OC/EC ratio in Northern states of India is much lower than the Eastern and Central states of IGP.

Table 4.4: Seasonal mean  $\pm \sigma$  OC/BC ratio

S. No.	Cities	Season			
		Winter	Summer	Monsoon	Post-Monsoon
1	Hisar	$3.87 \pm 0.12$	$3.99 \pm 0.21$	$3.76 \pm 0.13$	$4.8 \pm 0.72$
2	Delhi	$3.98 \pm 0.12$	$4.24 \pm 0.21$	$3.86 \pm 0.12$	$4.67 \pm 0.50$
3	Kanpur	$4.10 \pm 0.1$	$4.48 \pm 0.28$	$3.93 \pm 0.21$	$4.66 \pm 0.44$
4	Muzaffarpur	$5.19 \pm 0.11$	$5.2 \pm 0.63$	$4.17 \pm 0.28$	$4.57 \pm 0.28$
5	Kolkata	$4.07 \pm 0.11$	$5.34 \pm 0.91$	$3.8 \pm 0.19$	$4.43 \pm 0.18$
6	Guwahati	$4.42 \pm 0.24$	$7.5 \pm 2.71$	$4.48 \pm 0.33$	$4.79 \pm 0.16$

In fig. 4.11, we observe that Kanpur has the most skewed distribution (positively) amongst other locations indicating that the density cloud of OC/BC values is mainly around the mean observation i.e., 4.23. Other locations have a more or less symmetric distribution albeit a high number of outliers that might undermine the fact the distribution is not skewed. We also observe, the spread for OC/BC is highest for Guwahati courtesy of the peaks detected for the location. Guwahati reported OC/BC ratio of 11.11, 10.36 and 11.01 for March 2019, 2020 and 2021 respectively which was highest in respective years followed by 6.51, 6.66 and 7.78 for April 2019, 2020 and 2021 respectively. Such high values of OC/BC indicate biomass burning and long-range transport of carbonaceous aerosols as the major sources of OC and BC (Bhuyan et al., 2018). While the minimum ratio was observed for Hisar as 3.71, 3.62 and 3.61 for June 2019, June 2020 and July 2021 respectively.

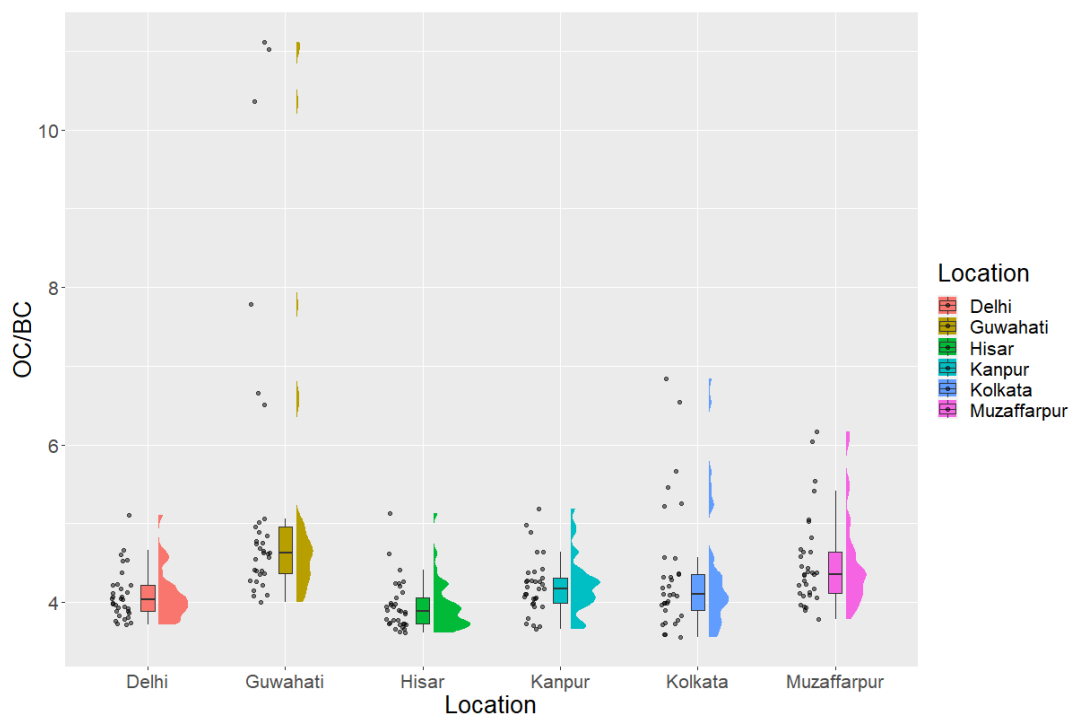


Fig 4.11: Raincloud plot representing OC/BC monthly means dispersion across all locations for 3 years

#### 4.4.1 Seasonal variations observed in OC/BC

For OC/BC ratio, as observed Guwahati has the highest mean across all seasons followed by Muzaffarpur, albeit with a larger variance. The order is: Guwahati > Muzaffarpur > Kolkata > Kanpur > Delhi > Hisar. For Hisar, Delhi and Kanpur the maximum OC/BC ratio was observed during post-monsoon season with average value of  $4.8 \pm 0.72$ ,  $4.6 \pm 0.50$  and  $4.66 \pm 0.44$  respectively because OC concentration was maximum in post-monsoon season for Hisar, Delhi and Kanpur while BC was lower. Whereas, for Eastern cities i.e., Muzaffarpur, Kolkata and Guwahati the maximum OC/BC ratio was  $5.2 \pm 0.63$ ,  $5.34 \pm 0.91$  and  $7.5 \pm 2.71$  respectively observed in summer season owing to low levels of BC reported in summer season unlike post-monsoon season where both OC and BC were higher for these locations. Rajput et al., 2014; Ram & Sarin, 2015, have studied OC/EC at Hisar, Kanpur and Allahabad - 3 major cities of IGP and concluded that since these locations are surrounded by rural communities thereby leading to increased emissions from agricultural waste burning and use of biomass for domestic heating and cooking (Sembhi et al., 2020).

In this study, for all locations the average OC/BC ratio is above and around 4 specifying dominance of diesel and gasoline vehicular emissions, biomass burning and coal combustion (power plants) as the

major sources of carbonaceous aerosols throughout IGP. High levels of OC reported in post-monsoon season for North-Western locations of IGP i.e., Delhi, Hisar and Kanpur may be attributed to local meteorological conditions and crop residue burning while peaks observed during summer in central and Eastern part of IGP suggests long-range transport (Bangar et al., 2021). Another reason for high OC/BC reported for post-monsoon season could be the increased combustion of coal for meeting the demand of electricity for heating during winters. Relatively lower OC/BC during winter season may be indicating the fresh and abundant emissions of BC from increased use of fuel for vehicles and residential heating. The lower OC/BC value during monsoon season suggests clean air with rain washing out the atmospheric aerosols (Sonwani et al., 2021).

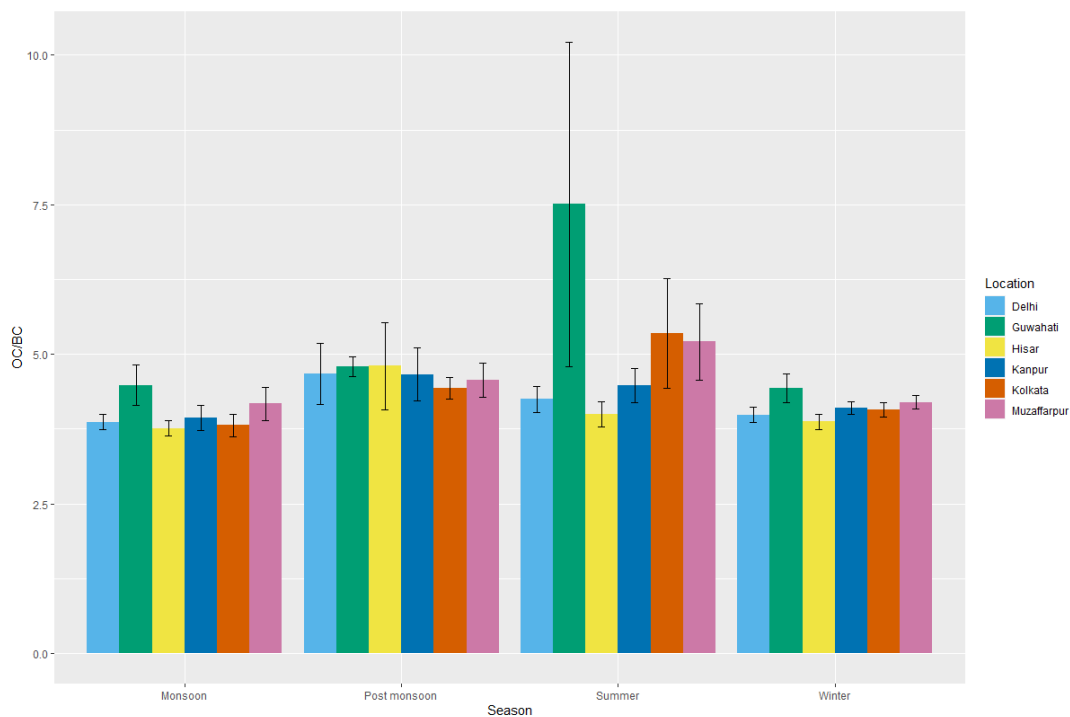


Fig 4.12: Seasonal variations in OC/BC ratio



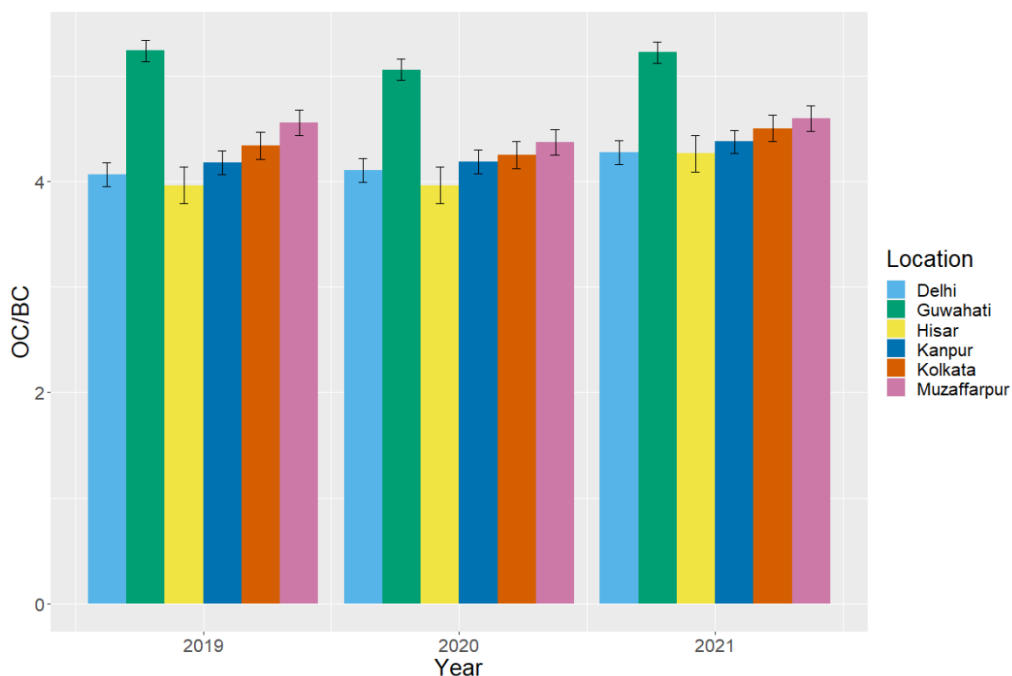


Fig 4.13: Interannual variations in OC/BC values from 2019-21

#### 4.4.2 Yearly variations observed in OC/BC

Unsurprisingly, the OC/BC ratio is the highest for Guwahati and lowest for Hisar across 3 years (Figure 4.13). The OC/BC ratio for 2019 and 2020 were almost similar for Hisar, Delhi and Kanpur while it decreased by 1-3% for Muzaffarpur, Kolkata and Guwahati. OC/BC ratio saw an increase from 2020 to 2021 due to the usual increasing trend observed in both BC and OC values over the years. Covid-19 had not much effect on the OC/BC ratio over the studied location. According to Ram et al, 2010a and Tiwari et al. 2013b, the higher value of OC/BC reported in IGP is mainly due to the transfer of carbonaceous species emitted out of excessive biomass and agricultural burning from Gangetic basin and NW parts of the country (Srivastava et al., 2014). The ratio varied from 3.71 to 5.41, 3.61 to 6.13, 4.0 to 11.11, 3.55 to 6.83, 3.66 to 5.22 and 3.79 to 6.16 for Delhi, Hisar, Guwahati, Kolkata, Kanpur and Muzaffarpur respectively. Fig. 4.10 shows Hisar, Delhi and Kanpur have almost consistent value for OC/BC while maximum variations can be seen for Guwahati, Kolkata and Muzaffarpur which may be due to large fluctuations in the OC levels at these locations. These results are consistent with the results obtained by Tiwari et al, 2016 who reported OC/EC ratio of  $5.0 \pm 2$  for Delhi; Ram et al, 2010 who reported  $6.2 \pm 3.7$  for Kanpur (Pipal et al., 2014).

#### 4.5 CORRELATION OF CARBONACEOUS AEROSOLS WITH METEOROLOGICAL CONDITIONS AND GASEOUS POLLUTANTS

The relationship of aerosol species under study was analyzed with meteorological parameters and other gaseous pollutants (Figure 4.13 to 4.18). A very strong positive correlation ( $>0.95$ ) with a significant level of  $p \leq 0.001$  is observed between OC and BC for all locations indicating common sources of emission (Table 4.5). Apart from BC, OC has a strong positive correlation with  $PM_{2.5}$  for all locations except Guwahati for which it is weak, indicating additional sources of particulate emission. OC shows weak correlation coefficient with CO for Muzaffarpur (0.21), Guwahati (0.34) and Kanpur (0.2) while a strong correlation was observed for Hisar (0.62) and moderate for Delhi (0.51) and Kolkata (0.57). OC and BC were found to be moderately to strongly correlated with  $NO_2$  for all sites except Muzaffarpur which showed a weak negative correlation (-0.1). The correlation coefficients have a significant value of  $p \leq 0.001$  for all the pollutants. Furthermore, there seems to be a strong positive correlation in between the solid particulates, namely, BC, OC and  $PM_{2.5}$  except for Guwahati for which these are moderately correlated. The relationship between the solid particulates is also pretty much homogenous for all locations. 5 out of 6 locations show a very high positive correlation between BC and OC, with the values being between 0.95 to 0.97. The only exception is Guwahati, where the correlation coefficient between BC and OC is 0.75, which is still high.

Table 4.5: R value (correlation coefficients) established between various meteorological parameters, air pollutants and carbonaceous species

Locations	Variables								
		$PM_{2.5}$	$NO_2$	$SO_2$	CO	$O_3$	RH	WS	AT
Hisar	BC	0.73	0.51	-0.25	0.65	-0.35	0.2	-0.48	NA
	OC	0.72	0.46	-0.23	0.62	-0.29	0.06	-0.43	NA
Delhi	BC	0.83	0.38	-0.02	0.55	-0.27	0.33	-0.13	-0.57
	OC	0.82	0.35	-0.1	0.51	-0.25	0.25	-0.15	-0.5
Kanpur	BC	0.7	0.7	0.36	0.23	-0.38	-0.01	-0.58	-0.64
	OC	0.7	0.68	0.39	0.2	-0.38	-0.1	-0.6	-0.58
Muzaffarpur	BC	0.83	-0.1	-0.09	0.27	-0.12	0.1	-0.37	-0.65
	OC	0.79	-0.1	-0.1	0.21	-0.13	0	-0.34	-0.58
Kolkata	BC	0.85	0.67	0.46	0.64	0.12	-0.33	-0.48	-0.79
	OC	0.83	0.63	0.5	0.57	0.2	-0.41	-0.51	-0.72
Guwahati	BC	0.53	0.48	0	0.58	0	-0.37	0	-0.18
	OC	0.35	0.51	0.1	0.34	0.12	-0.53	0	-0.18

Both BC and OC are moderately negatively correlated with AT, negative and weakly correlated with SO<sub>2</sub>, O<sub>3</sub> and WS except Guwahati. The correlation coefficients have significant levels of 0.001, with the exception of SO<sub>2</sub> which has a significant level of 0.01. The correlation coefficients of BC and OC between the air pollutants and meteorological conditions more or less remain homogenous throughout the locations. Delhi and Kolkata show a positive and strong correlation of 0.70 and 0.73 respectively between CO and NO<sub>2</sub> indicating emissions from combustion of coal (Mor et al., 2021). RH for a weak positive correlation was observed for Hisar, Delhi and Muzaffarpur while it inversely correlated with BC and OC for Kanpur, Kolkata and Guwahati.

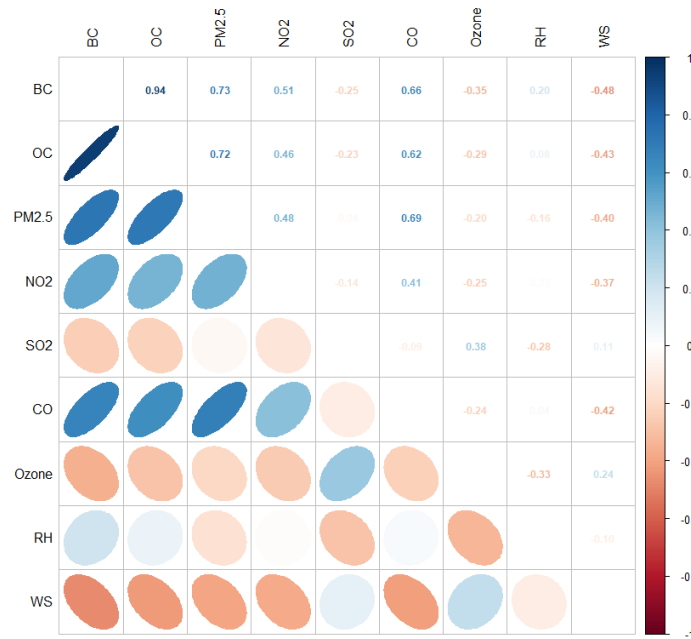


Fig 4.14: Correlation among carbonaceous aerosols, local meteorology and air pollutants for Hisar

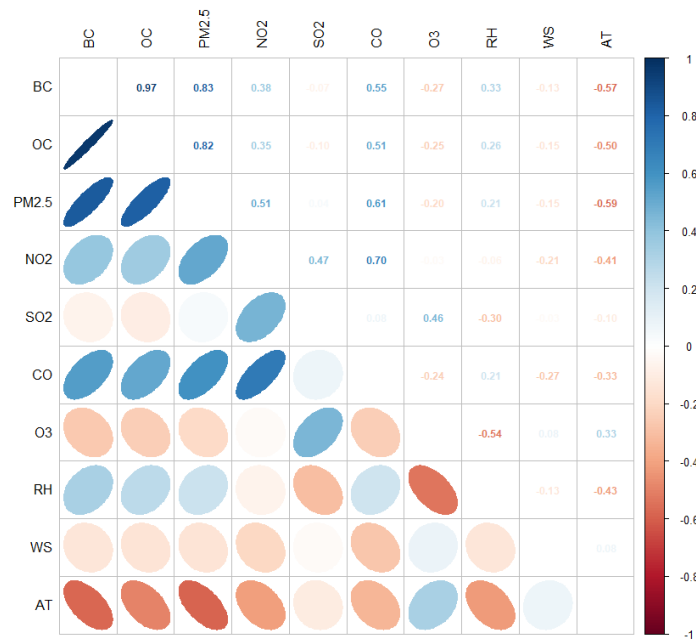


Fig 4.15: Correlation among carbonaceous aerosols, local meteorology and air pollutants for Delhi

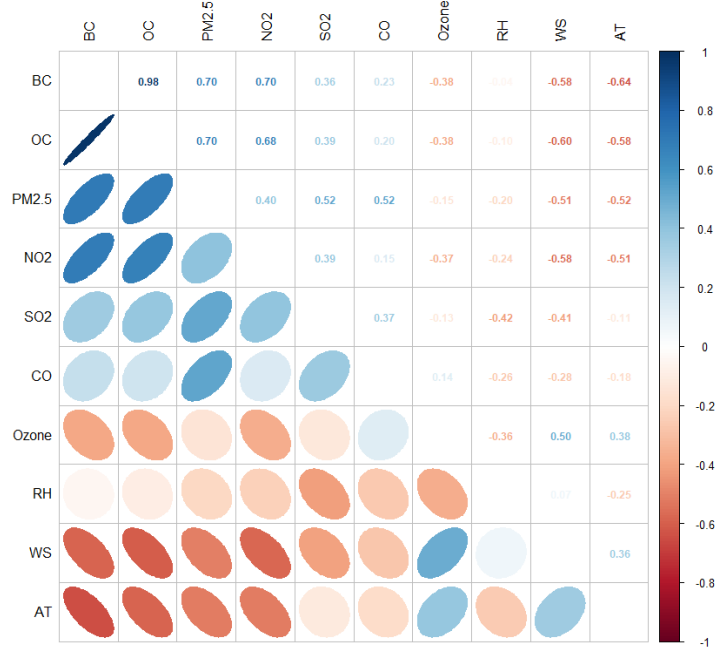


Fig 4.16: Correlation among carbonaceous aerosols, local meteorology and air pollutants for Kanpur

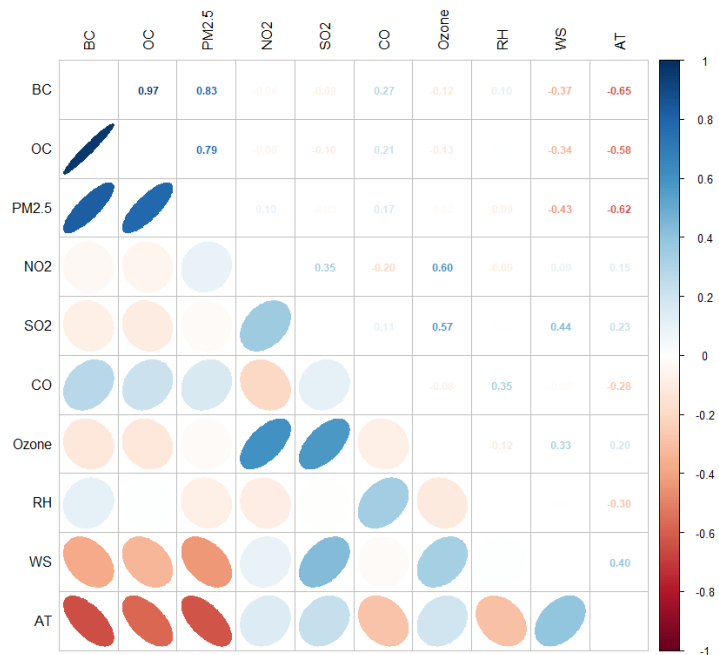


Fig 4.17: Correlation among carbonaceous aerosols, local meteorology and air pollutants for Muzaffarpur

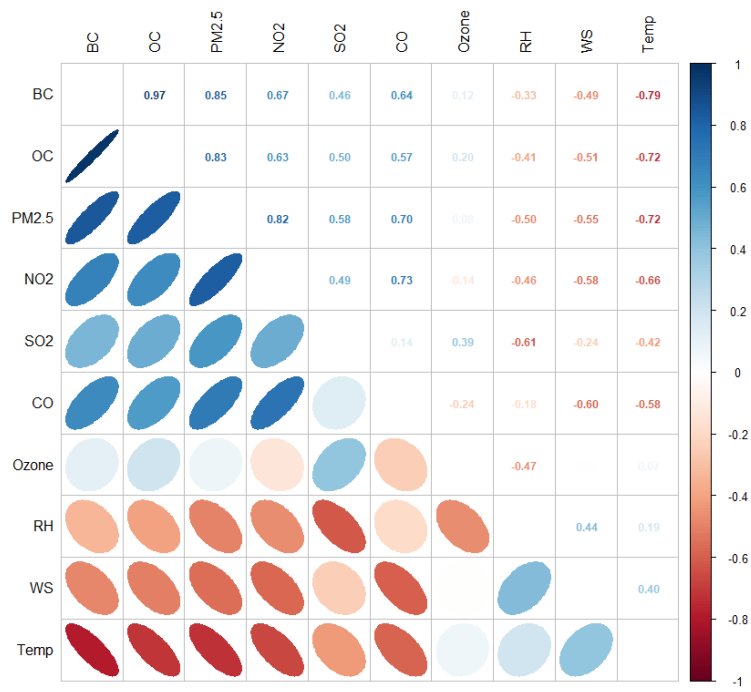


Fig 4.18: Correlation among carbonaceous aerosols, local meteorology and air pollutants for Kolkata

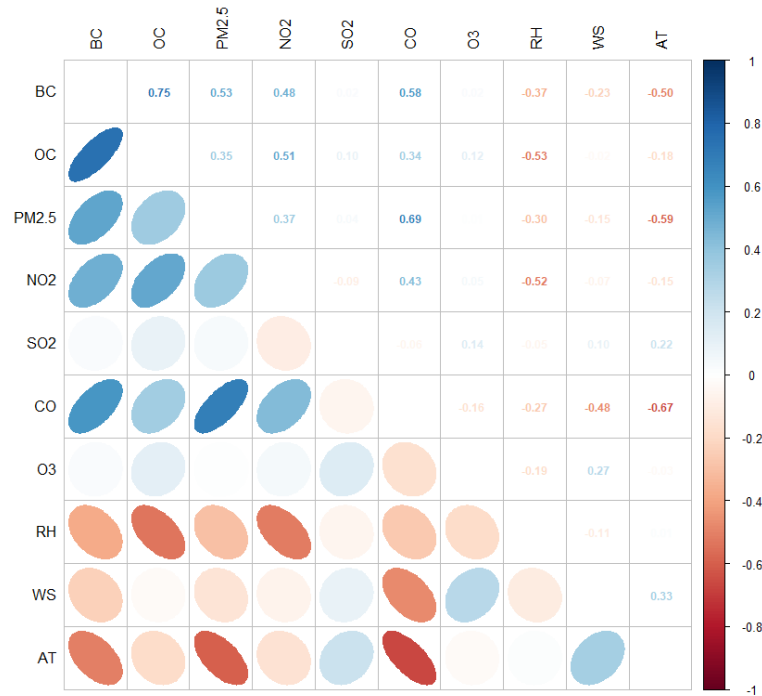


Fig 4.19: Correlation among carbonaceous aerosols, local meteorology and air pollutants for Guwahati

Overall, BC and OC have negative relationships with the meteorological conditions (RH, WS and AT) and low to moderate coefficients for the gaseous (air) pollutants. A moderate to strong negative correlation of carbonaceous aerosols with atmospheric temperature for all locations (except Guwahati) is due to increased consumption of coal and other fossil fuels for power generation, heating and starting the vehicles during winters. Low temperatures during winters and relatively lower boundary layer height leads to accumulation of pollutants near surface. A weak to moderate negative correlation of OC and BC with wind speed reassures the importance of wind in dispersing and eliminating the air pollutants.

For Guwahati, the carbonaceous aerosols showed a weak inverse correlation with atmospheric temperature (-0.18) which means temperature has only a slight role in governing their concentrations. Moreover, the aerosols were found to have zero correlation with wind speed for Guwahati and a strong inverse correlation was observed for relative humidity (-0.53). The particulate matter unlike, other locations of IGP, exhibited a moderate positive correlation with BC (0.53) and weak with OC (0.35) which means BC and PM<sub>2.5</sub> have somewhat similar sources but Guwahati has different sources of emissions for OC (Liu et al., 2022).

#### **4.6 BACKWARD TRAJECTORY CLUSTER AND CWT ANALYSIS OF CARBONACEOUS SPECIES**

Seasonal variations in backward air mass trajectories and CWT analysis for all the 6 locations have been studied and depicted in Figures 4.20 to 4.37. For cluster analysis, 5 air mass trajectories have been used numbered C1 to C5 for each location.

For the winter season, for all locations, the clusters originated mostly from the upper IGP. For Hisar, Delhi, and Kanpur, more than half of the trajectories were from Nepal and Uttarakhand regions. Clusters observed from Uttarakhand where the temperature dips to negative during winter indicate a contribution from biomass and coal burning for domestic heating purposes. Cluster C2 (42.7%) for Hisar originated from Punjab (Pakistan) while for Delhi C2 (41.3%) and C3 (23.5%) for Kanpur were observed from Punjab (India). Muzaffarpur received 84.9% of the trajectories from Uttarakhand and Western Nepal region and C2 (10.9%) and C3 (4.2%) from eastern Nepal and Kolkata respectively and the trajectories observed were rather straight covering the whole of Uttar Pradesh. Kolkata received 92.2% of the trajectories from the western parts of Uttar Pradesh. A cluster C2 (7.8%) from Central Bangladesh also reached Kolkata. The trajectories observed for Guwahati were different from other locations. Cluster C3 (38.5%) and C4 (22.9%) emerged from the western province of Nepal and West Bengal respectively and C3 covered the entire Nepal before reaching the location. C1 (27.1%) stemmed from North Myanmar.

For the summer season, Hisar, Delhi, and Kanpur experienced similar trajectories with their origin from Uttarakhand, Punjab, and the coast of the Arabian Sea near Pakistan. Cluster C2 (23.5%) and C3 (14.4%) reached Hisar from Upper IGP i.e., Punjab and Sindh provinces of Pakistan respectively. C4 (25.9%) reached Delhi from Punjab (Pakistan). 53.6% of the trajectories arriving at Muzaffarpur were from the Himalayan region (C1), a part also from Central India and the West Bengal coastline. Kolkata received aerosol-loaded air masses from Tamil Nadu (C4 – 43.6%) and Andhra Pradesh (C1 – 15.3%). The state also received trajectories from North India. While for Guwahati, 37% of the total air mass received was from Western Nepal (C1). The three locations, Muzaffarpur, Kolkata, and Guwahati also received a substantial number of trajectories from the Bay of Bengal.

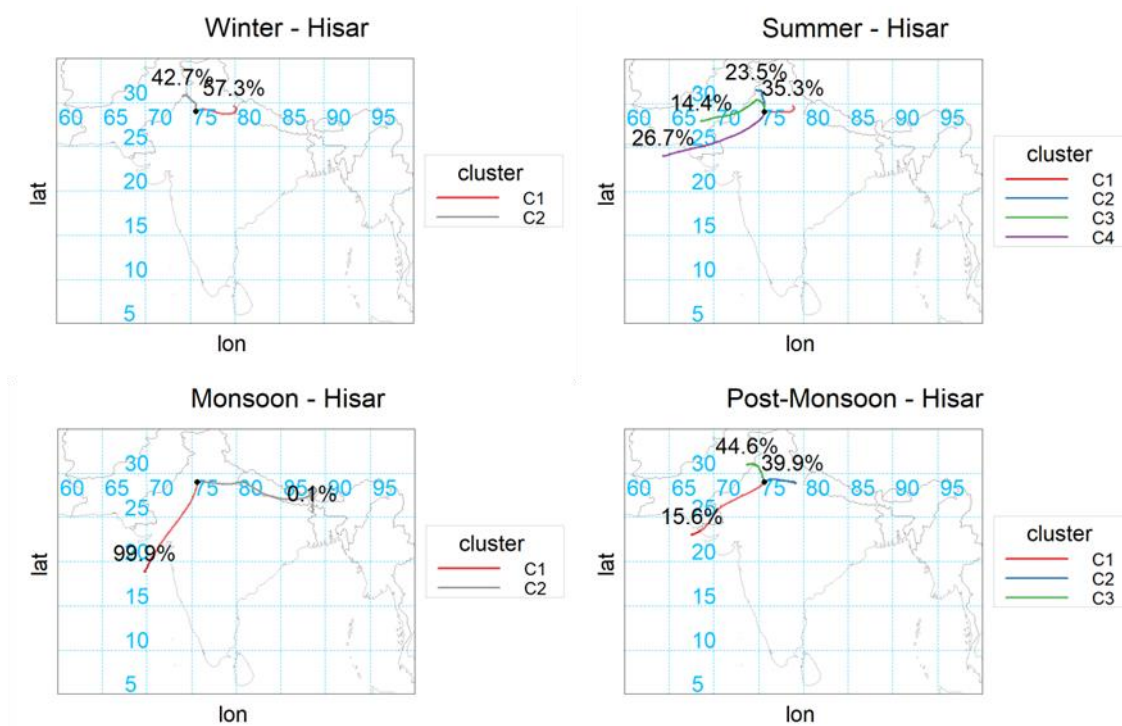


Fig 4.20: 5-day Backward Trajectory Clusters for Hisar for the study period

Monsoon in Hisar shows cluster C1 accumulated 99.9% of the trajectories emanating from the Arabian Sea. Cluster C1(38.4%) and C2(43.2%) of Delhi and Kanpur respectively show long-range transport from the Arabian Sea and traversing the Thar Desert before merging at Delhi. Delhi's monsoon also saw air masses falling in from Eastern and Northern India. Cluster C4 (33.5%) of Kanpur originated in West Bengal and a C3 (14.3%) was observed from the west coast. Similarly, Guwahati's clusters were from the Palk Strait (48%) and the Bay of Bengal (35.4%). Long-range travel of air mass from the Arabian Sea was observed for almost all clusters in Kolkata except cluster C2 (13.7%) from Tamil Nadu. C1 (27.1%) and C4(20.4%) for Muzaffarpur originated from Maharashtra and Karnataka respectively and Clusters C2 (26.9%) and C3 (25.6%) from Myanmar and the Bay of Bengal respectively.



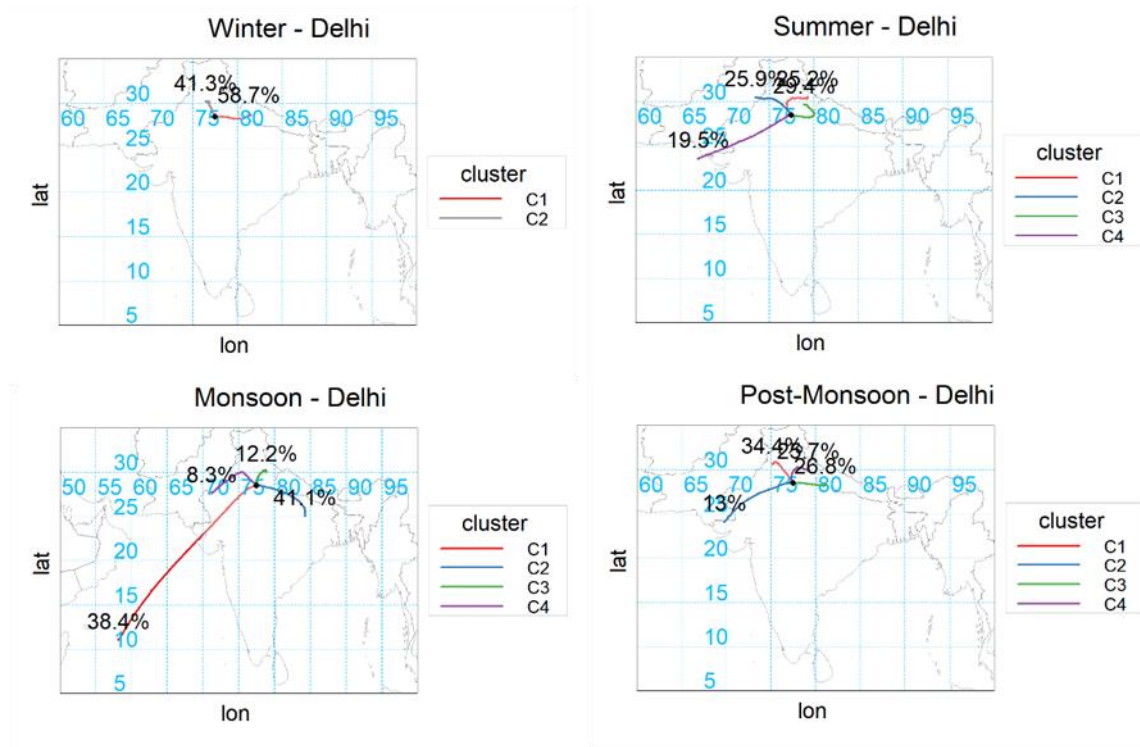


Fig 4.21: 5-day Backward Trajectory Clusters for Delhi for study period

Post-Monsoon clusters for Hisar, Delhi, and Kolkata were similar to summer clusters while a small proportion was received from western India (Gujarat and its coast). Muzaffarpur received clusters from Nepal, North and East-Central India covering Eastern India. Unlike other locations, post-monsoon clusters for Kolkata were different from summer clusters with the dominance of Cluster C2 (43.8%) originating from Uttar Pradesh. Cluster C4 (20.5%) and C3 (12.6%) of Kolkata were sourced from central Bangladesh and Myanmar. It also received clusters from the Deccan region. Post-Monsoon clusters for Guwahati were mainly from local areas and short-range transport from North East India and Kolkata. Cluster C1 (19.7%) for Guwahati sprouted from Yunnan Province of China crossing over Myanmar. Cluster C2 (23.1%) arrived from the Bay of Bengal.

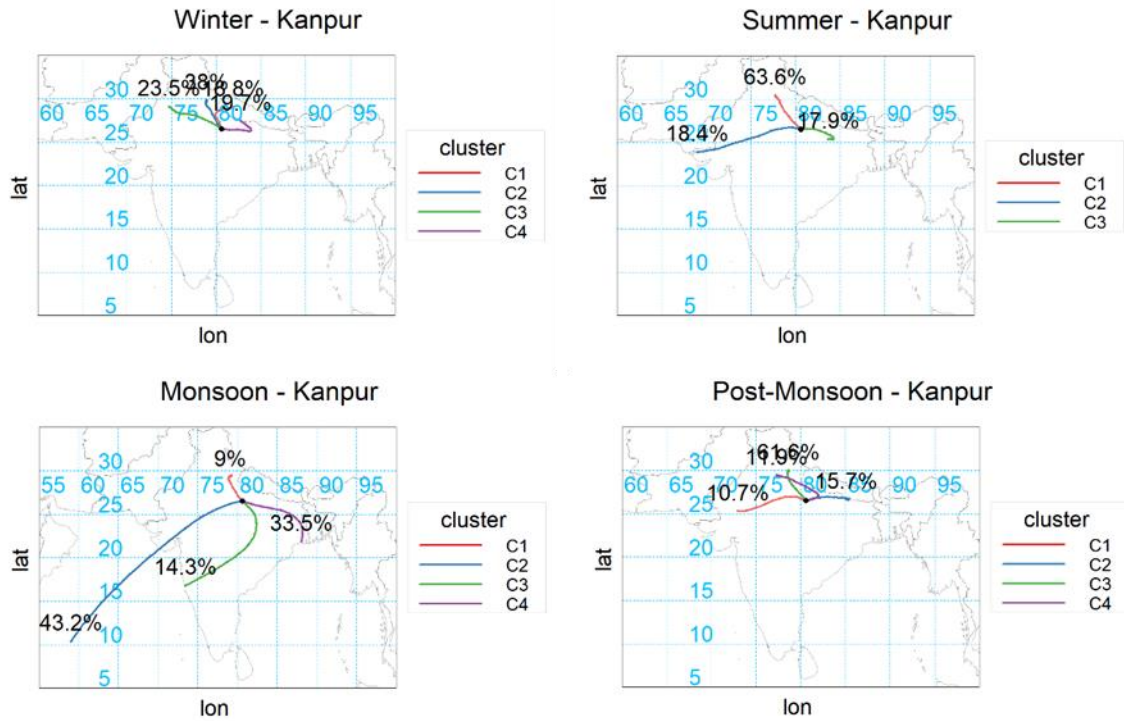


Fig 4.22: 5-day Backward Trajectory Clusters for Kanpur for the study period

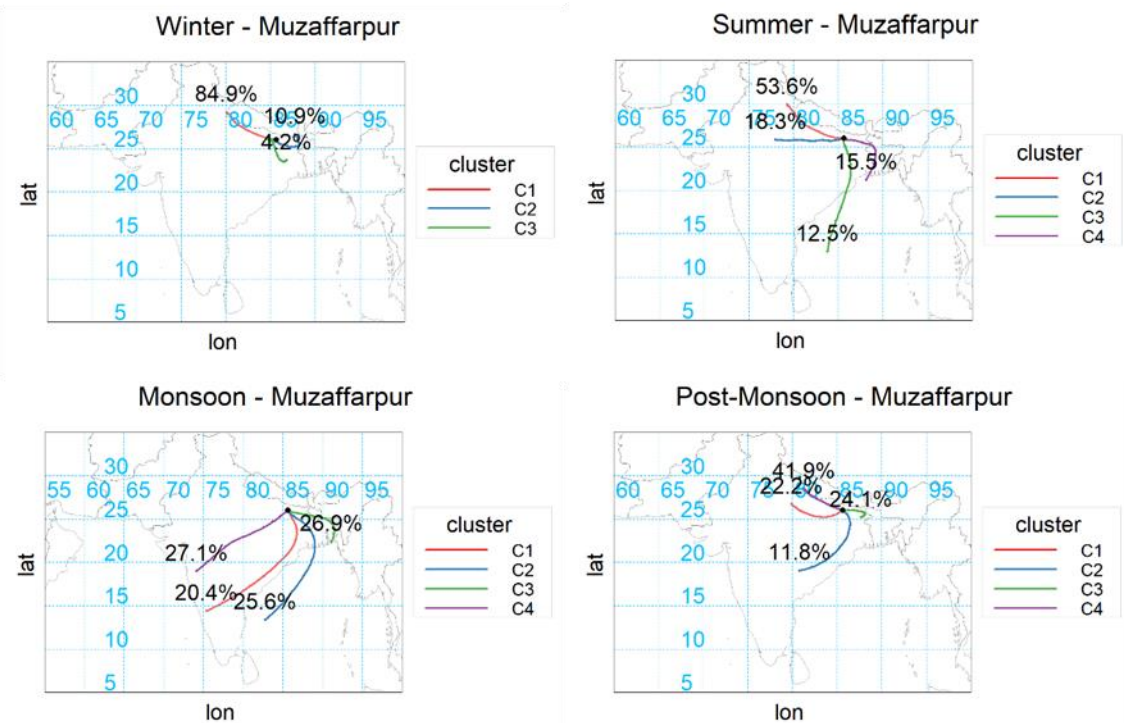


Fig 4.23: 5-day Backward Trajectory Clusters for Muzaffarpur for the study period

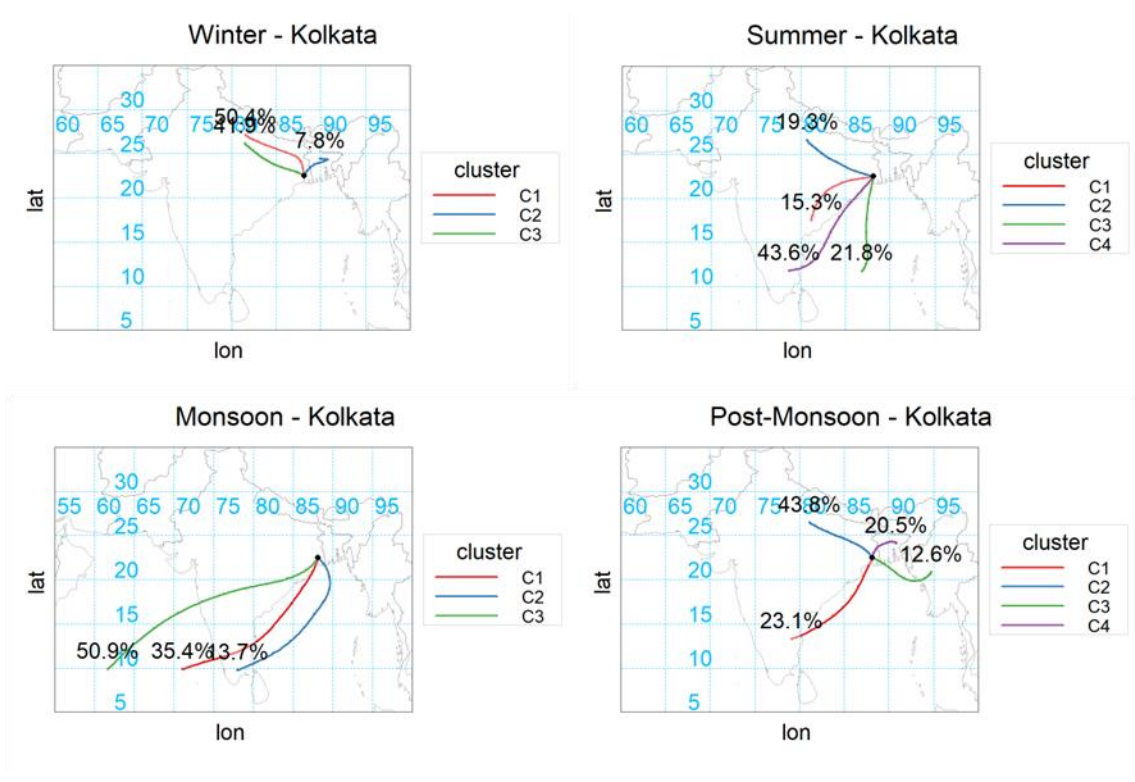


Fig 4.24: 5-day Backward Trajectory Clusters for Kolkata for the study period

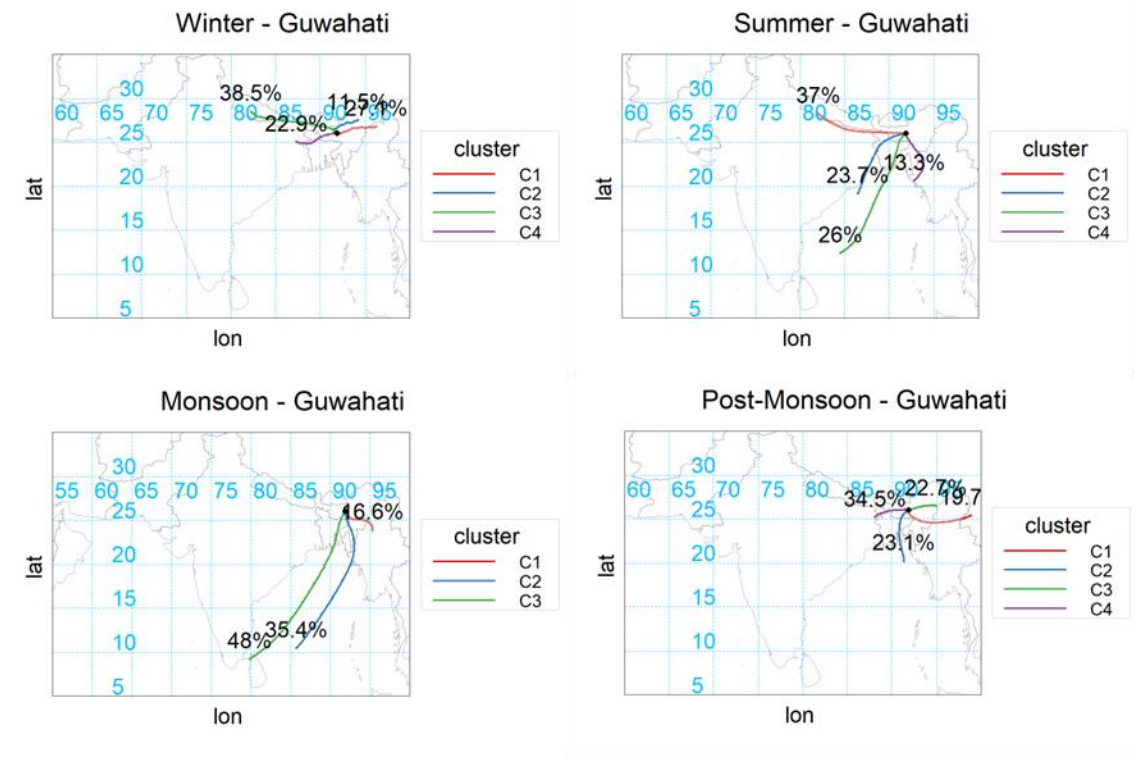


Fig 4.25: 5-day Backward Trajectory Clusters for Guwahati for the study period

Cluster analysis gave an idea about the trajectory of the air masses received at the 6 receptor locations but it is not sufficient to identify the potential and significant source regions for the carbonaceous aerosols. Thus, to identify the sources for BC and OC aerosols, CWT analysis was performed and results are depicted in Figure 4.26 to 4.37. As observed, the CWT analysis for BC and OC aerosols gave similar results which hints at the common source areas for these pollutants. At Hisar, the carbonaceous aerosols were contributed by local sources and Upper to Central IGP with Uttar Pradesh contributing the most. The major and strong contributors to summer aerosols load was from Himalayan region, western Uttar Pradesh and moderately from Western India. For post-monsoon, Upper IGP states i.e., Pakistan Punjab, Punjab and Haryana were potential contributors due to the post-harvesting crop residue burning in these agriculture intensive states. For monsoon, the major sources were entire IGP and moderately from Arabian Sea. Similar sources were observed for Delhi and Kanpur for all seasons. Additionally, during summer season, Delhi saw major contributions from Tibet and Kanpur from Bihar. Winter and Post-Monsoon sources for Muzaffarpur and Kolkata were similar and majorly from central IGP. In summers, Muzaffarpur received aerosols from Haryana, Uttar Pradesh, Kolkata and Bay of Bengal. While in monsoon, local sources along with long range transport from Arabian Sea and Bay of Bengal were major contributors. Summers in Kolkata witnessed neighboring states of Jharkhand, Bihar and Odisha as the major contributors while Bay of Bengal contributed moderately. Totally different sources were identified for monsoon season in Kolkata wherein Maharashtra, Chhattisgarh, Odisha houses significant sources along with long range transport of aerosols from Arabian Sea, Eastern and Western Coast of India and parts of Sri Lanka. For Guwahati, post-monsoon season saw localised sources and major proportion of aerosols from West Bengal and western Bangladesh. Summers in Guwahati were dominated by contributions from the whole IGP and to some extent from the Bay of Bengal. Whereas, in winters, Himalayan region from North India and Nepal; Bihar, West Bengal and Bangladesh added majorly to the BC and OC concentrations. Disparately, for monsoon in Guwahati, Myanmar, North East states of Nagaland, Manipur, Mizoram and Tripura; and long-range transportation of aerosols load from Laccadive Sea and Bay of Bengal were observed to be contributing the most.

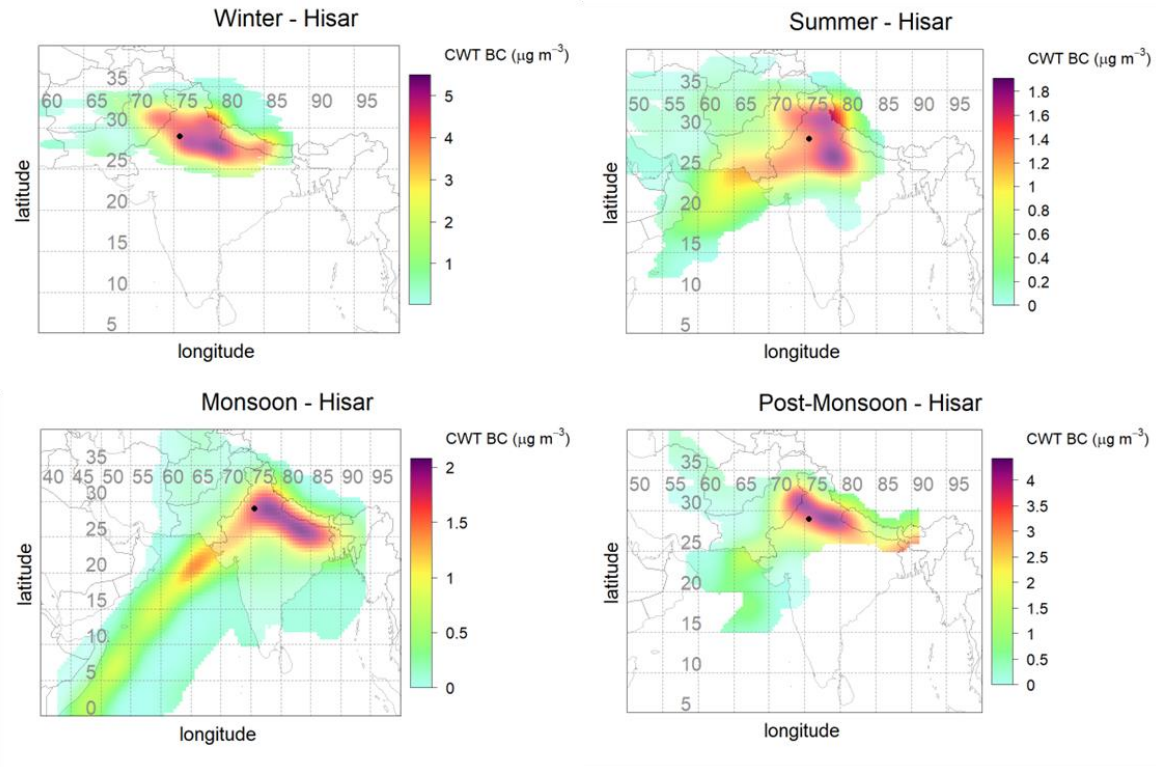


Fig 4.26: CWT analysis for BC mass concentrations ( $\mu\text{g m}^{-3}$ ) in Hisar

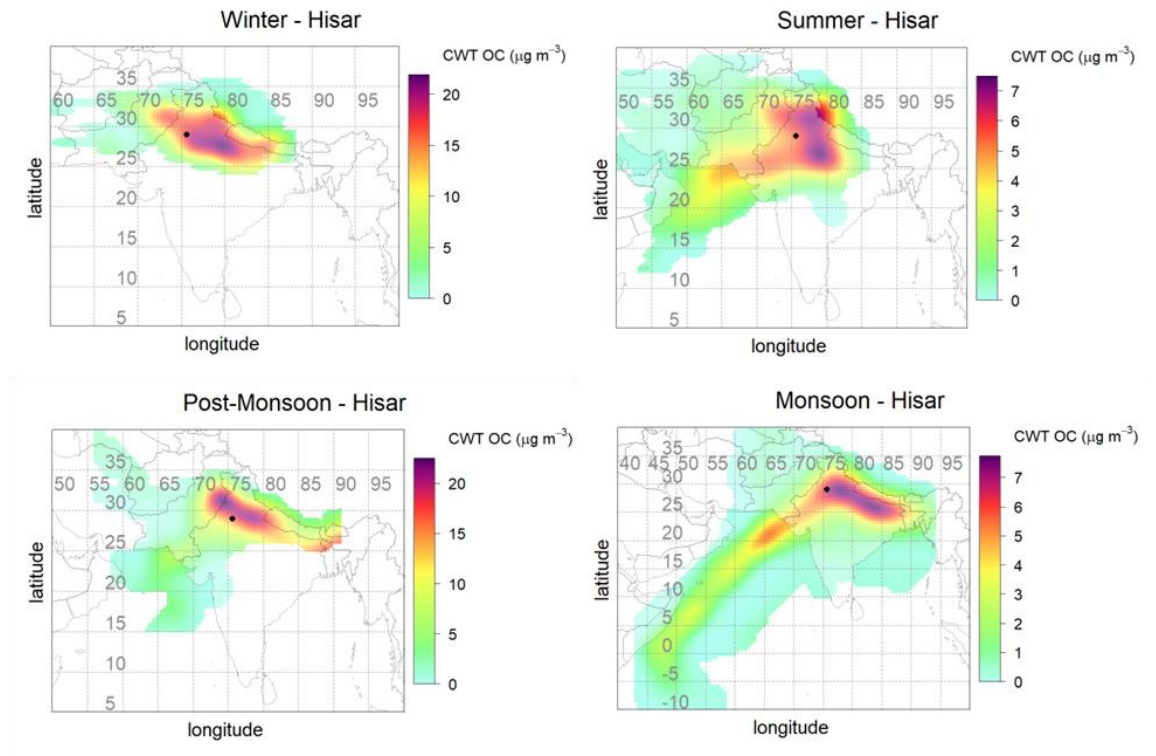


Fig 4.27: CWT analysis for OC mass concentrations ( $\mu\text{g m}^{-3}$ ) in Hisar

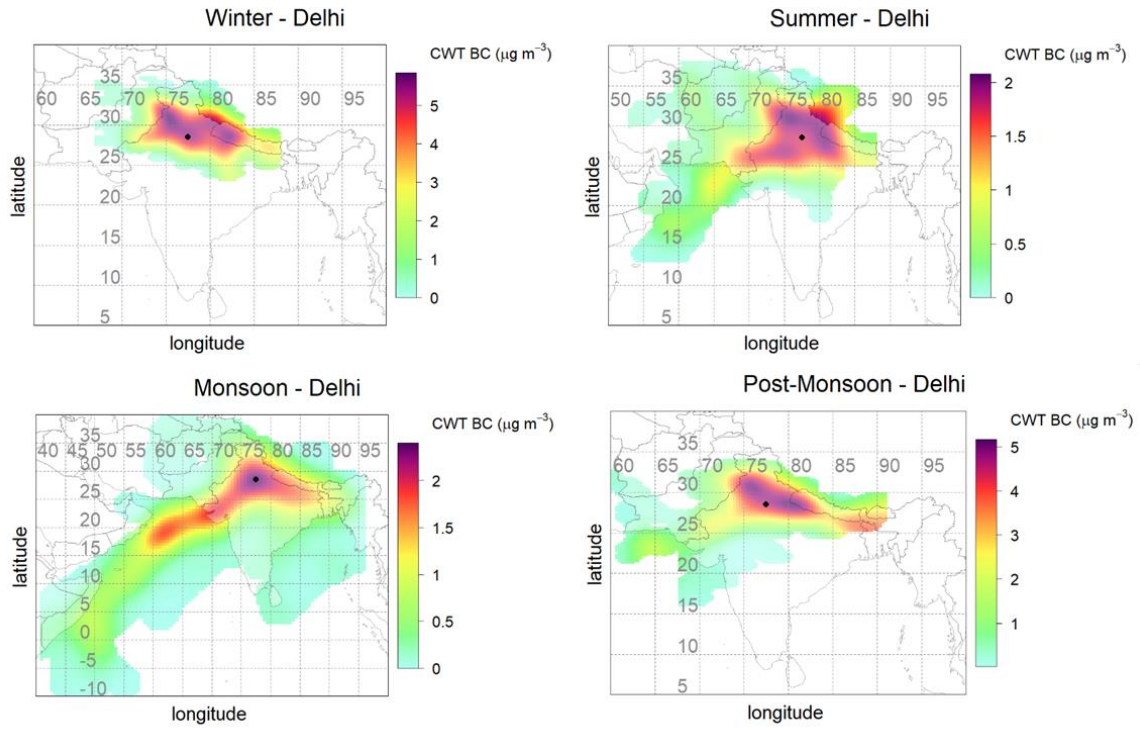


Fig 4.28: CWT analysis for BC mass concentrations ( $\mu\text{g m}^{-3}$ ) in Delhi

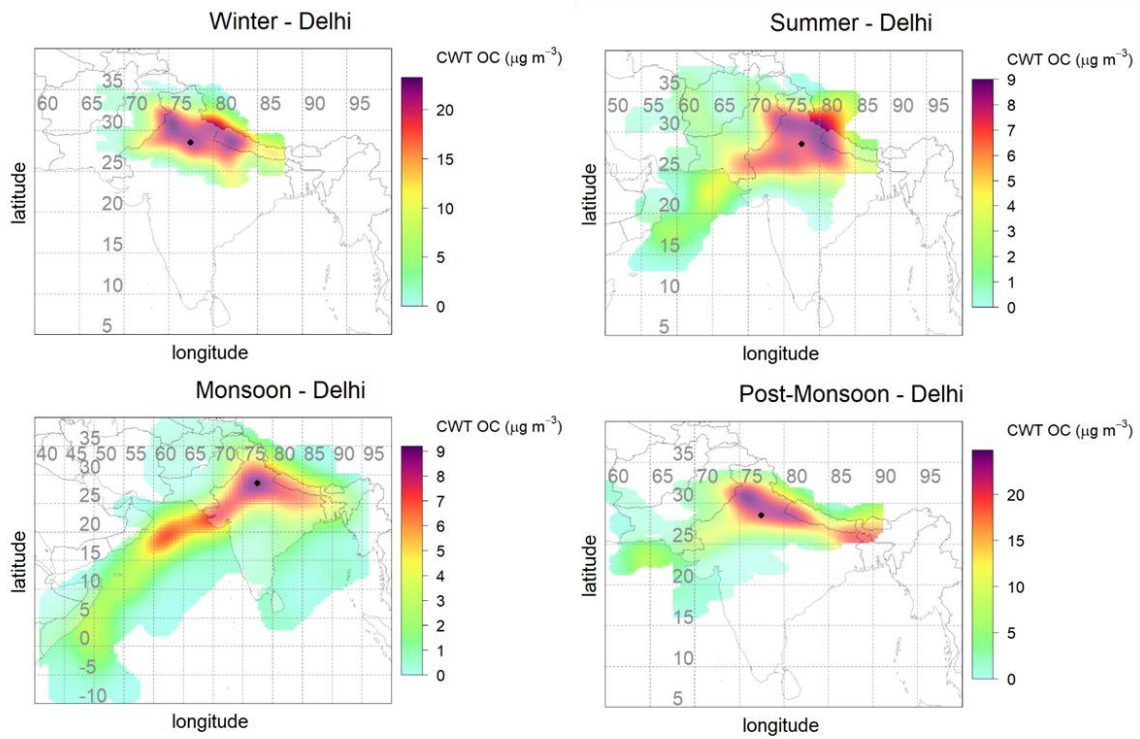


Fig 4.29: CWT analysis for OC mass concentrations ( $\mu\text{g m}^{-3}$ ) in Delhi

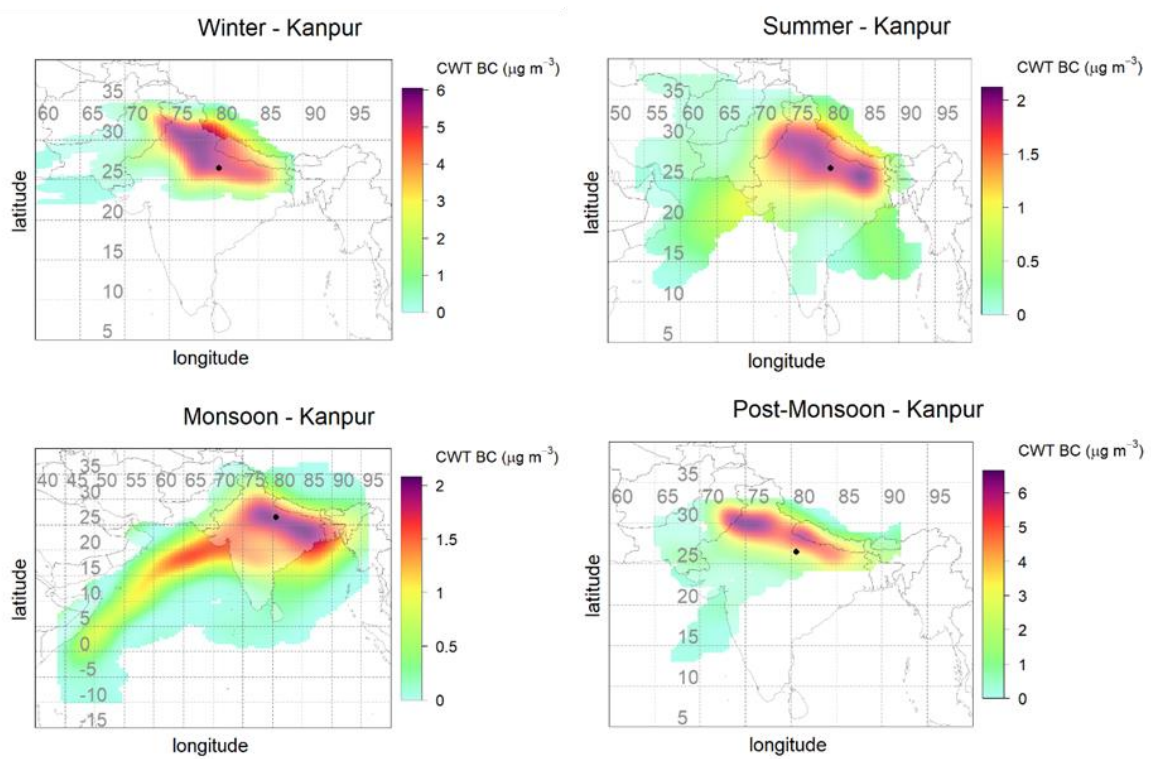


Fig 4.30: CWT analysis for BC mass concentrations ( $\mu\text{g m}^{-3}$ ) in Kanpur

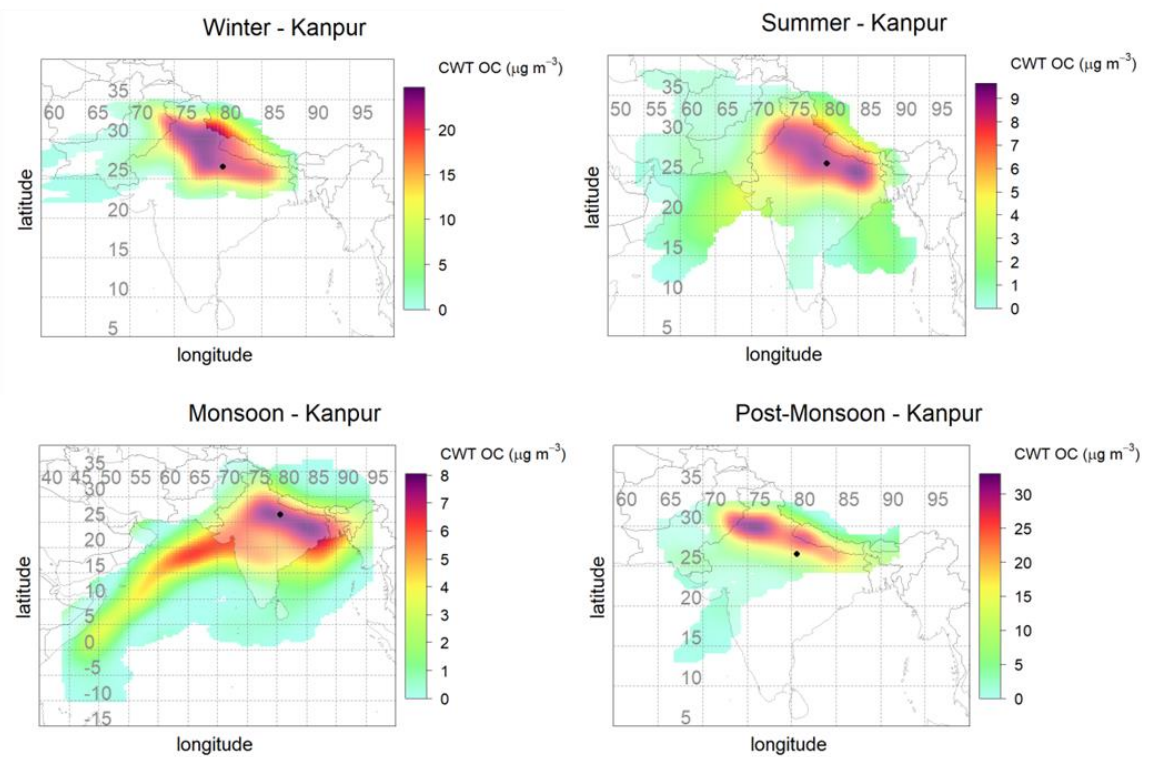


Fig 4.31: CWT analysis for OC mass concentrations ( $\mu\text{g m}^{-3}$ ) in Kanpur

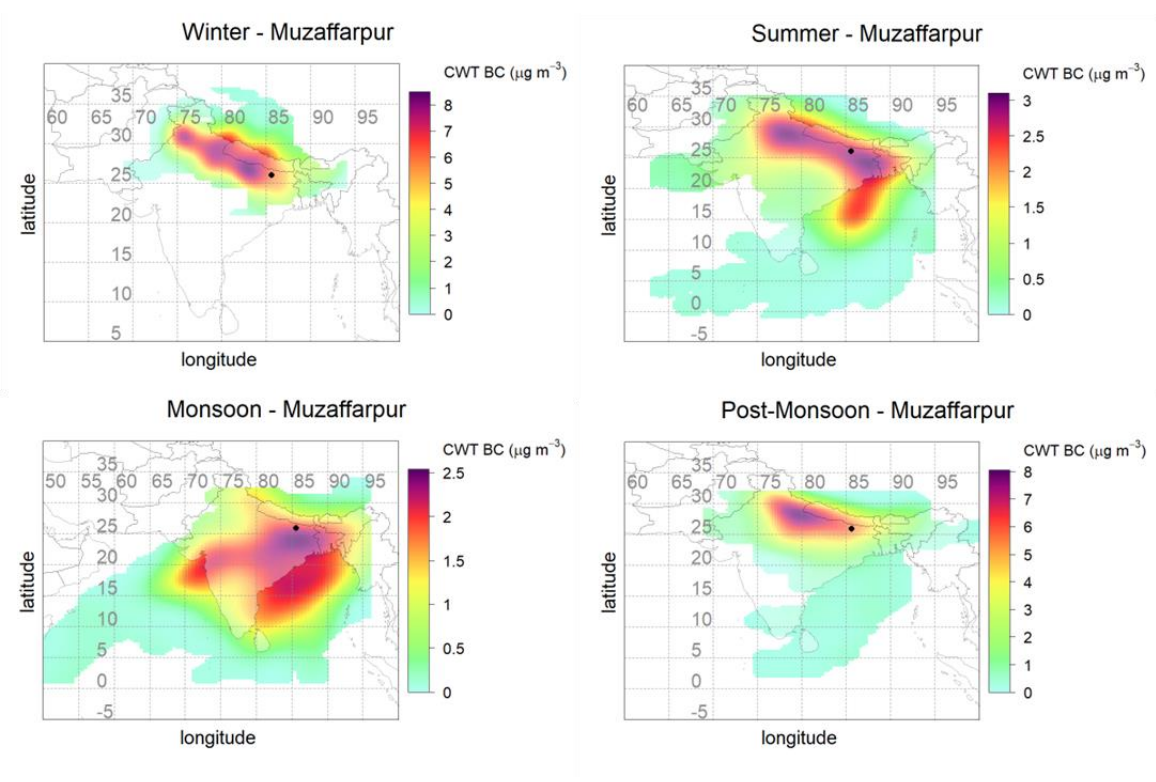


Fig 4.32: CWT analysis for BC mass concentrations ( $\mu\text{g m}^{-3}$ ) in Muzaffarpur

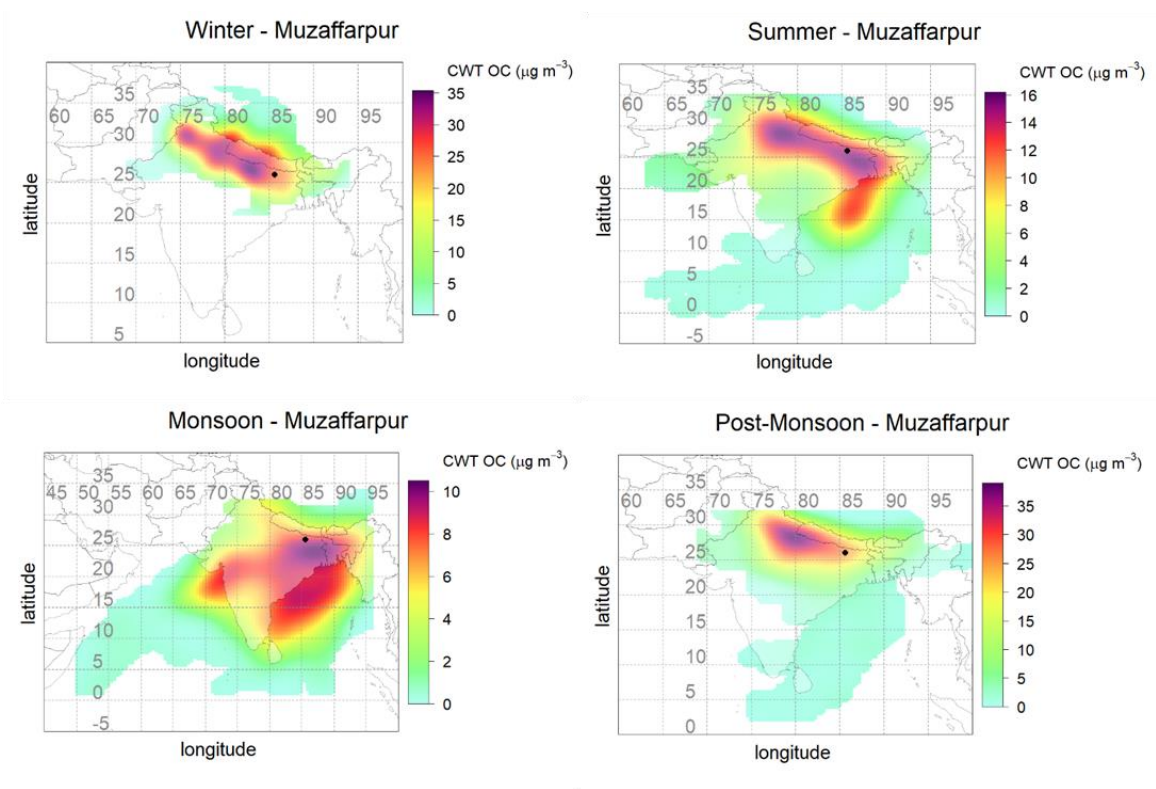


Fig 4.33: CWT analysis for OC mass concentrations ( $\mu\text{g m}^{-3}$ ) in Muzaffarpur



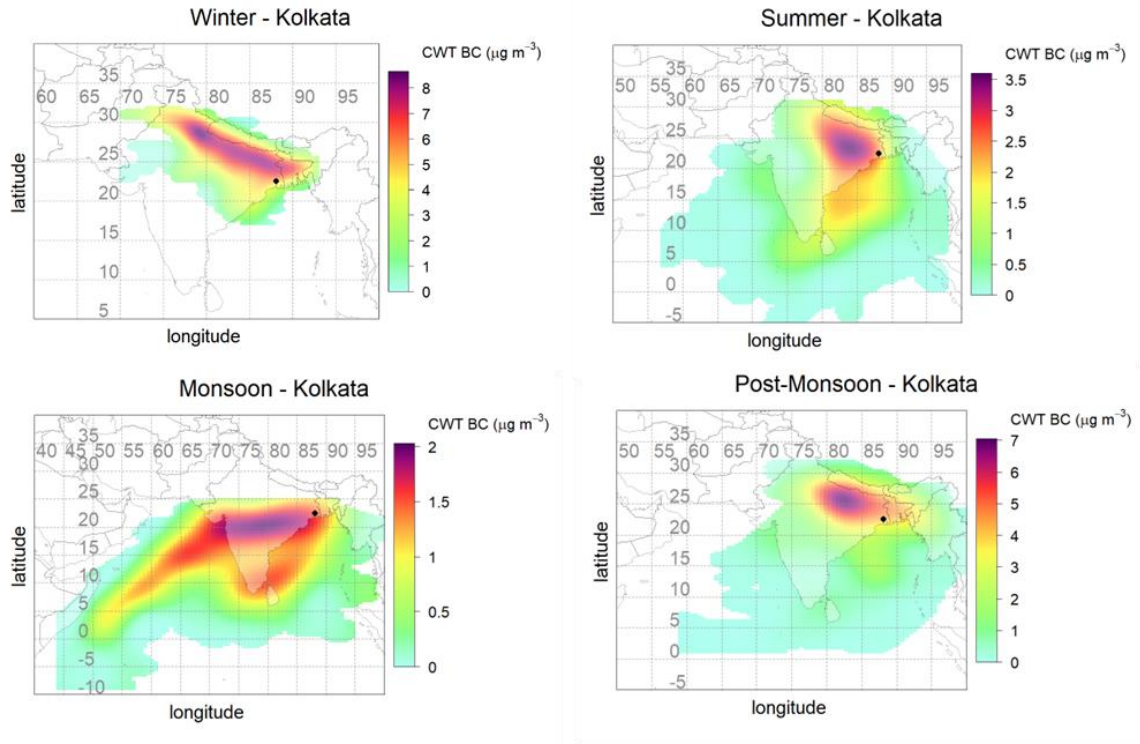


Fig 4.34: CWT analysis for BC mass concentrations ( $\mu\text{g m}^{-3}$ ) in Kolkata

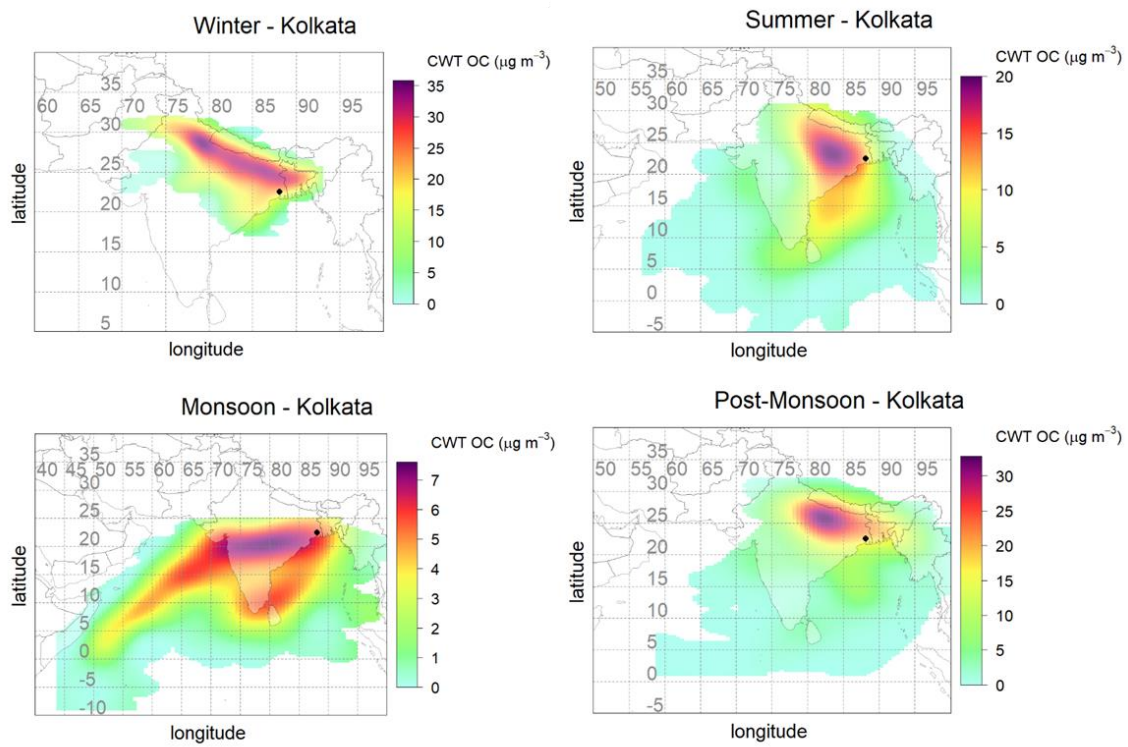


Fig 4.35: CWT analysis for OC mass concentrations ( $\mu\text{g m}^{-3}$ ) in Kolkata

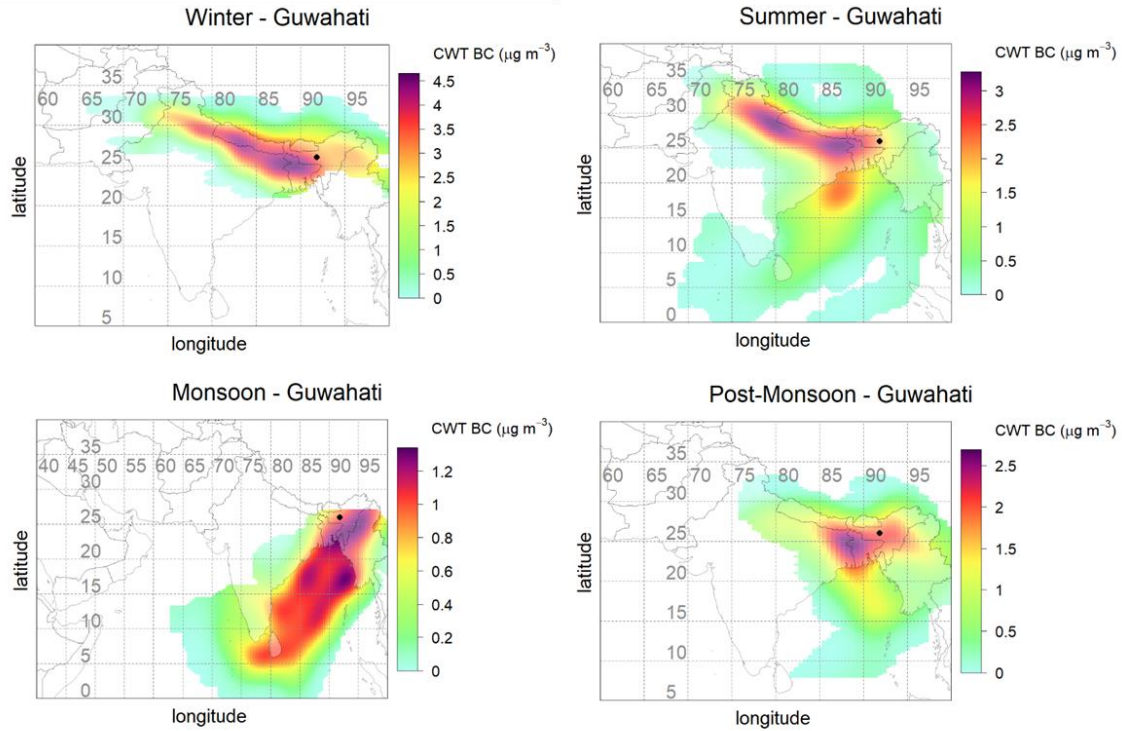


Fig 4.36: CWT analysis for BC mass concentrations ( $\mu\text{g m}^{-3}$ ) in Guwahati

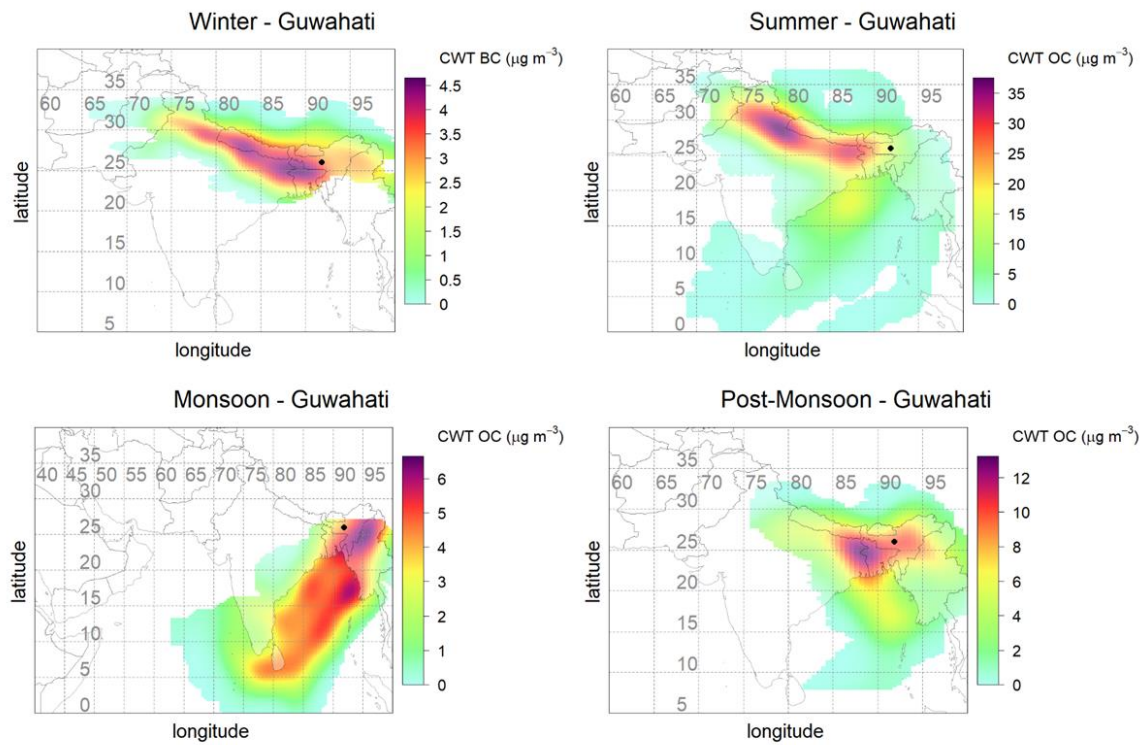


Fig 4.37: CWT analysis for OC mass concentrations ( $\mu\text{g m}^{-3}$ ) in Guwahati

## CHAPTER 5

### CONCLUSION

The BC and OC mass concentrations were analyzed for monthly, seasonally and interannual variations across 6 locations in IGP. The monthly mean BC and OC concentrations over IGP varied from 0.94 to 10.05  $\mu\text{gm}^{-3}$  and 3.49  $\mu\text{gm}^{-3}$  to 48.74  $\mu\text{gm}^{-3}$  respectively in different months. Highest monthly mean concentrations were observed in November, December and January months for both OC and BC for all locations except Guwahati which displayed different pattern throughout the analysis. Winter (DJF) > Post-Monsoon (ON) > Summer (MAM) > Monsoon (JJAS) for both type of aerosols. For Guwahati, maximum OC was observed in summers i.e., March. The Annual average for BC and OC over the study area ranged between 1.91 to 4.26  $\mu\text{gm}^{-3}$  and 9.38 to 19.61  $\mu\text{gm}^{-3}$  respectively. The OC/BC ratio variability was discerned for IGP and found varying between 3.56 and 11.11, with average ratio for entire IGP being  $4.42 \pm 0.98$ . Guwahati saw the highest mean across all seasons followed by Muzaffarpur, albeit with a larger variance. The order was: Guwahati > Muzaffarpur > Kolkata > Kanpur > Delhi > Hisar. For all locations the average OC/BC ratio is above and around 4 specifying dominance of diesel and gasoline vehicular emissions, biomass burning and coal combustion (power plants) as the major sources of carbonaceous aerosols throughout IGP. A strong positive correlation ( $>0.95$ ) with a significant level of  $p \leq 0.001$  is observed between OC and BC for all locations indicating common sources of emission. Overall, BC and OC have negative relationships with the meteorological conditions (RH, WS and AT) and low to moderate coefficients for the gaseous (air) pollutants. Clustering of air mass backward trajectories and CWT analysis revealed IGP as a major contributor to carbonaceous aerosols for all locations. Long-range transportation of aerosols from Myanmar; Bangladesh; Tibet; Yunnan China; Arabian Sea and Bay of Bengal was observed for most of the locations for monsoon season.

## CHAPTER 6

### LIMITATIONS

There are some limitations to this research. The BC and OC surface mass concentration data used for this study was taken from MERRA-2 aerosols products, which are reported to underestimate / overestimate the BC and OC concentrations. As reported by Prabhu et al., 2020, MERRA-2 aerosol products underestimated the carbonaceous species concentration at North-Western IGP (Beas region) by -53% and -60% MPE (Mean Percentage Error) for BC and OC respectively. While for Central IGP covering cities like Kanpur, Lumbini and Allahabad, MERRA-2 overestimated BC with an MPE of +18% and underestimated OC by an MPE of -34%. These disparities were primarily attributable to a lack of understanding of emissions and aging processes, particularly in the central-IGP. Error in BC models as observed, were lower than OC simulations, including/revising local emissions will aid in accurate and precise carbonaceous aerosol simulations over the IGP. Another study by Navinya et al., 2020, who evaluated the MERRA-2 data on PM<sub>2.5</sub> surface concentrations across 20 stations in India and thus concluded that the concentrations were underestimated by 34%. Yet another study done by Ramachandran et al., 2021, compared the MERRA-2 data with ground-based observations at Ahmedabad and Gurushikhar. A significant underestimation of BC concentration over Ahmedabad (2 to 5 times) was observed while it depicts the seasonal cycles perfectly. The simulations at the background region were quite well. For central and eastern China, the MERRA-2 persistently overestimated BC concentrations by a factor of 1.35 (Ma et al., 2021). According to Cao et al., 2021, in North-West, North-East, and Central South China, MERRA-2 underestimated BC concentration in most observations during 1980-2019. MERRA-derived aerosol products have also been found to underestimate carbonaceous aerosols in a few areas throughout the world, which could be attributable to biases in anthropogenic emission inventory estimates (Bali et al., 2021). The regional and global models severely underestimate BC mass concentrations over Asia (2-10 times) (Bond et al., 2013; Koch et al., 2009). The lack of proper/absence of aerosol emission inventories, notably due to region-specific fossil fuel and biofuel burning, was blamed for BC's underestimation (Bond et al., 2013).

Another limitation of this study is the lack of previous studies on aerosol loading in Guwahati. Guwahati has been found to be heavily loaded with carbonaceous species and shows a distinct behavior throughout the study. A comprehensive study on the characteristics of carbonaceous aerosols and their source identification is recommended.

## REFERENCES

- Ambade, B., Sankar, T. K., Panicker, A. S., Gautam, A. S., & Gautam, S. (2021). Characterization, seasonal variation, source apportionment and health risk assessment of black carbon over an urban region of East India. *Urban Climate*, 38. <https://doi.org/10.1016/j.uclim.2021.100896>
- Babu, S. S., & Moorthy, K. K. (2002). Aerosol black carbon over a tropical coastal station in India. *Geophysical Research Letters*, 29(23). <https://doi.org/10.1029/2002GL015662>
- Bali, K., Dey, S., & Ganguly, D. (2021). Diurnal patterns in ambient PM<sub>2.5</sub> exposure over India using MERRA-2 reanalysis data. *Atmospheric Environment*, 248. <https://doi.org/10.1016/j.atmosenv.2020.118180>
- Bangar, V., Mishra, A. K., Jangid, M., & Rajput, P. (2021). Elemental Characteristics and Source-Apportionment of PM<sub>2.5</sub> During the Post-monsoon Season in Delhi, India. *Frontiers in Sustainable Cities*, 3. <https://doi.org/10.3389/frsc.2021.648551>
- Bhuyan, P., Deka, P., Prakash, A., Balachandran, S., & Hoque, R. R. (2018). Chemical characterization and source apportionment of aerosol over mid Brahmaputra Valley, India. *Environmental Pollution*, 234. <https://doi.org/10.1016/j.envpol.2017.12.009>
- Bond, T. C., Doherty, S. J., Fahey, D. W., Forster, P. M., Berntsen, T., Deangelo, B. J., Flanner, M. G., Ghan, S., Kärcher, B., Koch, D., Kinne, S., Kondo, Y., Quinn, P. K., Sarofim, M. C., Schultz, M. G., Schulz, M., Venkataraman, C., Zhang, H., Zhang, S., ... Zender, C. S. (2013). Bounding the role of black carbon in the climate system: A scientific assessment. *Journal of Geophysical Research Atmospheres*, 118(11). <https://doi.org/10.1002/jgrd.50171>
- Buchard, V., Randles, C. A., da Silva, A. M., Darmenov, A., Colarco, P. R., Govindaraju, R., Ferrare, R., Hair, J., Beyersdorf, A. J., Ziemba, L. D., & Yu, A. H. (n.d.). *The MERRA-2 Aerosol Reanalysis, 1980 Onward. Part II: Evaluation and Case Studies*. <https://doi.org/10.1175/JCLI-D-16-0613.s1>
- Cao, S., Zhang, S., Gao, C., Yan, Y., Bao, J., Su, L., Liu, M., Peng, N., & Liu, M. (2021). A long-term analysis of atmospheric black carbon MERRA-2 concentration over China during 1980–2019. *Atmospheric Environment*, 264. <https://doi.org/10.1016/j.atmosenv.2021.118662>
- Cape, J. N., Coyle, M., & Dumitrean, P. (2012). The atmospheric lifetime of black carbon. *Atmospheric Environment*, 59. <https://doi.org/10.1016/j.atmosenv.2012.05.030>

- Chatterjee, A., Mukherjee, S., Dutta, M., Ghosh, A., Ghosh, S. K., & Roy, A. (2021). High rise in carbonaceous aerosols under very low anthropogenic emissions over eastern Himalaya, India: Impact of lockdown for COVID-19 outbreak. *Atmospheric Environment*, 244. <https://doi.org/10.1016/j.atmosenv.2020.117947>
- Chen, W., Tian, H., & Qin, K. (2019). Black carbon aerosol in the industrial city of xuzhou, china: Temporal characteristics and source appointment. *Aerosol and Air Quality Research*, 19(4). <https://doi.org/10.4209/aaqr.2018.07.0245>
- Devi, N. L., Kumar, A., & Yadav, I. C. (2020). PM<sub>10</sub> and PM<sub>2.5</sub> in Indo-Gangetic Plain (IGP) of India: Chemical characterization, source analysis, and transport pathways. *Urban Climate*, 33. <https://doi.org/10.1016/j.uclim.2020.100663>
- Haque, M. S., & Singh, R. B. (2017). Air pollution and human health in Kolkata, India: A case study. *Climate*, 5(4). <https://doi.org/10.3390/cli5040077>
- Hsu, Y. K., Holsen, T. M., & Hopke, P. K. (2003). Comparison of hybrid receptor models to locate PCB sources in Chicago. *Atmospheric Environment*, 37(4). [https://doi.org/10.1016/S1352-2310\(02\)00886-5](https://doi.org/10.1016/S1352-2310(02)00886-5)
- Kanakidou, M., Seinfeld, J. H., Pandis, S. N., Barnes, I., Dentener, F. J., Facchini, M. C., van Dingenen, R., Ervens, B., Nenes, A., Nielsen, C. J., Swietlicki, E., Putaud, J. P., Balkanski, Y., Fuzzi, S., Horth, J., Moortgat, G. K., Winterhalter, R., Myhre, C. E. L., Tsigaridis, K., ... Wilson, J. (2005). Organic aerosol and global climate modelling: A review. In *Atmospheric Chemistry and Physics* (Vol. 5, Issue 4). <https://doi.org/10.5194/acp-5-1053-2005>
- Kirchstetter, T. W., Novakov, T., & Hobbs, P. v. (2004). Evidence that the spectral dependence of light absorption by aerosols is affected by organic carbon. *Journal of Geophysical Research D: Atmospheres*, 109(21). <https://doi.org/10.1029/2004JD004999>
- Koch, D., Schulz, M., Kinne, S., McNaughton, C., Spackman, J. R., Balkanski, Y., Bauer, S., Berntsen, T., Bond, T. C., Boucher, O., Chin, M., Clarke, A., de Luca, N., Dentener, F., Diehl, T., Dubovik, O., Easter, R., Fahey, D. W., Feichter, J., ... Zhao, Y. (2009). Evaluation of black carbon estimations in global aerosol models. *Atmospheric Chemistry and Physics*, 9(22). <https://doi.org/10.5194/acp-9-9001-2009>

- Krishna, R. K., Panicker, A. S., Yusuf, A. M., & Ullah, B. G. (2019). On the contribution of particulate matter (PM<sub>2.5</sub>) to direct radiative forcing over two urban environments in India. *Aerosol and Air Quality Research*, 19(2). <https://doi.org/10.4209/aaqr.2018.04.0128>
- Li, C., Dai, Z., Liu, X., & Wu, P. (2020). Transport pathways and potential source region contributions of PM<sub>2.5</sub> in weifang: Seasonal variations. *Applied Sciences (Switzerland)*, 10(8). <https://doi.org/10.3390/APP10082835>
- Liu, P., Zhou, H., Chun, X., Wan, Z., Liu, T., Sun, B., Wang, J., & Zhang, W. (2022). Characteristics of fine carbonaceous aerosols in Wuhai, a resource-based city in Northern China: Insights from energy efficiency and population density. *Environmental Pollution*, 292. <https://doi.org/10.1016/j.envpol.2021.118368>
- Ma, X., Yan, P., Zhao, T., Jia, X., Jiao, J., Ma, Q., Wu, D., Shu, Z., Sun, X., & Habtemicheal, B. A. (2021). Article evaluations of surface PM<sub>10</sub> concentration and chemical compositions in merra-2 aerosol reanalysis over central and eastern china. *Remote Sensing*, 13(7). <https://doi.org/10.3390/rs13071317>
- McDonald, J. D., Eide, I., Seagrave, J. C., Zielinska, B., Whitney, K., Lawson, D. R., & Mauderly, J. L. (2004). Relationship between composition and toxicity of motor vehicle emission samples. *Environmental Health Perspectives*, 112(15). <https://doi.org/10.1289/ehp.6976>
- Meena, G. S., Mukherjee, S., Buchunde, P., Safai, P. D., Singla, V., Aslam, M. Y., Sonbawne, S. M., Made, R., Anand, V., Dani, K. K., & Pandithurai, G. (2021). Seasonal variability and source apportionment of black carbon over a rural high-altitude and an urban site in western India. *Atmospheric Pollution Research*, 12(2), 32–45. <https://doi.org/10.1016/j.apr.2020.10.006>
- Mor, S., Kumar, S., Singh, T., Dogra, S., Pandey, V., & Ravindra, K. (2021). Impact of COVID-19 lockdown on air quality in Chandigarh, India: Understanding the emission sources during controlled anthropogenic activities. *Chemosphere*, 263. <https://doi.org/10.1016/j.chemosphere.2020.127978>
- Nagpure, A. S., Gurjar, B. R., Kumar, V., & Kumar, P. (2016). Estimation of exhaust and non-exhaust gaseous, particulate matter and air toxics emissions from on-road vehicles in Delhi. *Atmospheric Environment*, 127. <https://doi.org/10.1016/j.atmosenv.2015.12.026>
- Navinya, C. D., Vinoj, V., & Pandey, S. K. (2020). Evaluation of PM<sub>2.5</sub> surface concentrations simulated by nasa's merra version 2 aerosol reanalysis over india and its relation to the air quality index. *Aerosol and Air Quality Research*, 20(6), 1329–1339. <https://doi.org/10.4209/aaqr.2019.12.0615>

- Pipal, A. S., Tiwari, S., Satsangi, P. G., Taneja, A., Bisht, D. S., Srivastava, A. K., & Srivastava, M. K. (2014). Sources and characteristics of carbonaceous aerosols at Agra “World heritage site” and Delhi “capital city of India.” *Environmental Science and Pollution Research*, 21(14), 8678–8691. <https://doi.org/10.1007/s11356-014-2768-0>
- Prabhu, V., Soni, A., Madhwal, S., Gupta, A., Sundriyal, S., Shridhar, V., Sreekanth, V., & Mahapatra, P. S. (2020). Black carbon and biomass burning associated high pollution episodes observed at Doon valley in the foothills of the Himalayas. *Atmospheric Research*, 243. <https://doi.org/10.1016/j.atmosres.2020.105001>
- Qi, M., Jiang, L., Liu, Y., Xiong, Q., Sun, C., Li, X., Zhao, W., & Yang, X. (2018). Analysis of the characteristics and sources of carbonaceous aerosols in PM<sub>2.5</sub> in the Beijing, Tianjin, and langfang region, China. *International Journal of Environmental Research and Public Health*, 15(7). <https://doi.org/10.3390/ijerph15071483>
- Qin, W., Zhang, Y., Chen, J., Yu, Q., Cheng, S., Li, W., Liu, X., & Tian, H. (2019). Variation, sources and historical trend of black carbon in Beijing, China based on ground observation and MERRA-2 reanalysis data. *Environmental Pollution*, 245, 853–863. <https://doi.org/10.1016/j.envpol.2018.11.063>
- Rajput, P., Sarin, M., Sharma, D., & Singh, D. (2014). Characteristics and emission budget of carbonaceous species from post-harvest agricultural-waste burning in source region of the Indo-Gangetic plain. *Tellus, Series B: Chemical and Physical Meteorology*, 66(1). <https://doi.org/10.3402/tellusb.v66.21026>
- Ram, K., & Sarin, M. M. (2015). Atmospheric carbonaceous aerosols from Indo-Gangetic Plain and Central Himalaya: Impact of anthropogenic sources. *Journal of Environmental Management*, 148. <https://doi.org/10.1016/j.jenvman.2014.08.015>
- Ram, K., Sarin, M. M., & Tripathi, S. N. (2010). A 1 year record of carbonaceous aerosols from an urban site in the Indo-Gangetic Plain: Characterization, sources, and temporal variability. *Journal of Geophysical Research Atmospheres*, 115(24). <https://doi.org/10.1029/2010JD014188>
- Ram, K., Tripathi, S. N., Sarin, M. M., & Bhattu, D. (2014). Primary and secondary aerosols from an urban site (Kanpur) in the Indo-Gangetic Plain: Impact on CCN, CN concentrations and optical properties. *Atmospheric Environment*, 89. <https://doi.org/10.1016/j.atmosenv.2014.02.009>



- Ramachandran, S., Rajesh, T. A., & Cherian, R. (2021). Black carbon aerosols over source vs. background region: Atmospheric boundary layer influence, potential source regions, and model comparison. *Atmospheric Research*, 256. <https://doi.org/10.1016/j.atmosres.2021.105573>
- Ramachandran, S., Rupakheti, M., & Lawrence, M. G. (2020). Black carbon dominates the aerosol absorption over the Indo-Gangetic Plain and the Himalayan foothills. *Environment International*, 142. <https://doi.org/10.1016/j.envint.2020.105814>
- Ramanathan, V., & Carmichael, G. (2008). Global and regional climate changes due to black carbon. In *Nature Geoscience* (Vol. 1, Issue 4). <https://doi.org/10.1038/ngeo156>
- Randles, C. A., da Silva, A. M., Buchard, V., Colarco, P. R., Darmenov, A., Govindaraju, R., Smirnov, A., Holben, B., Ferrare, R., Hair, J., Shinozuka, Y., & Flynn, C. J. (2017a). The MERRA-2 Aerosol Reanalysis, 1980 Onward. Part I: System Description and Data Assimilation Evaluation. *Journal of Climate*, 30(17).
- Randles, C. A., da Silva, A. M., Buchard, V., Colarco, P. R., Darmenov, A., Govindaraju, R., Smirnov, A., Holben, B., Ferrare, R., Hair, J., Shinozuka, Y., & Flynn, C. J. (2017b). The MERRA-2 aerosol reanalysis, 1980 onward. Part I: System description and data assimilation evaluation. *Journal of Climate*, 30(17). <https://doi.org/10.1175/JCLI-D-16-0609.1>
- Reizer, M., & Orza, J. A. G. (2018). Identification of PM<sub>10</sub> air pollution origins at a rural background site. *E3S Web of Conferences*, 28. <https://doi.org/10.1051/e3sconf/20182801031>
- Rengarajan, R., Sarin, M. M., & Sudheer, A. K. (2007). Carbonaceous and inorganic species in atmospheric aerosols during wintertime over urban and high-altitude sites in North India. *Journal of Geophysical Research Atmospheres*, 112(21). <https://doi.org/10.1029/2006JD008150>
- Saarikoski, S., Timonen, H., Saarnio, K., Aurela, M., Järvi, L., Keronen, P., Kerminen, V. M., & Hillamo, R. (2008). Sources of organic carbon in fine particulate matter in Northern European urban air. *Atmospheric Chemistry and Physics*, 8(20). <https://doi.org/10.5194/acp-8-6281-2008>
- Sembhi, H., Wooster, M., Zhang, T., Sharma, S., Singh, N., Agarwal, S., Boesch, H., Gupta, S., Misra, A., Tripathi, S. N., Mor, S., & Khaiwal, R. (2020). Post-monsoon air quality degradation across Northern India: Assessing the impact of policy-related shifts in timing and amount of crop residue burnt. *Environmental Research Letters*, 15(10). <https://doi.org/10.1088/1748-9326/aba714>

- Sharma, S. K., Mandal, T. K., Srivastava, M. K., Chatterjee, A., Jain, S., Saxena, M., Singh, B. P., Saraswati, Sharma, A., Adak, A., & K.Ghosh, S. (2016). Spatio-temporal variation in chemical characteristics of PM<sub>10</sub> over Indo Gangetic Plain of India. *Environmental Science and Pollution Research*, 23(18). <https://doi.org/10.1007/s11356-016-7025-2>
- Singh, A., Rastogi, N., Patel, A., Satish, R. v., & Singh, D. (2016). Size-segregated characteristics of carbonaceous aerosols over the North-Western Indo-Gangetic plain: Year round temporal behavior. *Aerosol and Air Quality Research*, 16(7), 1615–1624. <https://doi.org/10.4209/aaqr.2016.01.0023>
- Singh, D., Nanda, C., & Dahiya, M. (2022). State of air pollutants and related health risk over Haryana India as viewed from satellite platform in COVID-19 lockdown scenario. *Spatial Information Research*, 30(1). <https://doi.org/10.1007/s41324-021-00410-9>
- Singh, R., Kulshrestha, M. J., Kumar, B., & Chandra, S. (2016). Impact of anthropogenic emissions and open biomass burning on carbonaceous aerosols in urban and rural environments of Indo-Gangetic Plain. *Air Quality, Atmosphere and Health*, 9(7), 809–822. <https://doi.org/10.1007/s11869-015-0377-9>
- Sonwani, S., Saxena, P., & Shukla, A. (2021). Carbonaceous Aerosol Characterization and Their Relationship With Meteorological Parameters During Summer Monsoon and Winter Monsoon at an Industrial Region in Delhi, India. *Earth and Space Science*, 8(4). <https://doi.org/10.1029/2020EA001303>
- Srivastava, A. K., Bisht, D. S., Ram, K., Tiwari, S., & Srivastava, M. K. (2014). Characterization of carbonaceous aerosols over Delhi in Ganga basin: Seasonal variability and possible sources. *Environmental Science and Pollution Research*, 21(14), 8610–8619. <https://doi.org/10.1007/s11356-014-2660-y>
- Wang, Y. Q., Zhang, X. Y., & Draxler, R. R. (2009). TrajStat: GIS-based software that uses various trajectory statistical analysis methods to identify potential sources from long-term air pollution measurement data. *Environmental Modelling and Software*, 24(8). <https://doi.org/10.1016/j.envsoft.2009.01.004>
- Zhao, J., Liu, Y., Shan, M., Liang, S., Cui, C., Chen, L., Gao, S., Mao, J., Zhang, H., Sun, Y., Ma, Z., & Yu, S. (2021). Characteristics, potential regional sources and health risk of black carbon based on ground observation and MERRA-2 reanalysis data in a coastal city, China. *Atmospheric Research*, 256. <https://doi.org/10.1016/j.atmosres.2021.105563>

